

TRITA-EPP-82-08

INDUCTIVE ELECTRIC FIELDS IN THE
MAGNETOTAIL AND THEIR RELATION TO
AURORAL AND SUBSTORM PHENOMENA

R. J. Pellinen¹ and

W. J. Heikkila²

November 1982

Accepted for publication in
Space Science Reviews

- 1) Finnish Meteorological Institute
Department of Geomagnetism
SF-00101 Helsinki 10, Finland
- 2) Royal Institute of Technology
Department of Plasma Physics
S-10044 Stockholm, Sweden

Permanent address:
University of Texas at Dallas
Center for Space Sciences
Richardson, Texas 75080, USA

INDUCTIVE ELECTRIC FIELDS IN THE MAGNETOTAIL AND THEIR RELATION TO
AURORAL AND SUBSTORM PHENOMENA

R. J. Pellinen and W. J. Heikkila

ABSTRACT

The paper reviews the importance of inductive electric fields in explaining different magnetospheric and auroral phenomena during moderately and highly disturbed conditions. Quiet-time particle energization and temporal development of the tail structure during the substorm growth phase are explained by the presence of a large-scale electrostatic field directed from dawn to dusk over the magnetotail. Conservation of the first adiabatic invariant in the neutral sheet with a small value of the gradient in the magnetic field implies that the longitudinal energy increases at each crossing of the neutral sheet. At a certain moment, this may result in a rapid local growth of the current and in an instability that triggers the onset. During the growth phase energy is stored mainly in the magnetic field, since the energy density in the electric field is negligible compared to that of the magnetic field (ratio $1:10^7$). An analytical model is described in which the characteristic observations of a substorm onset are taken into account. One major feature is that the triggering is confined to a small local time sector. During moderate disturbances, the induction fields in the magnetotail are stronger by at least one order of magnitude than the average cross-tail field. Temporal development of the disturbed area results in X- and O-type neutral lines. Particles near to these neutral lines are energized to over 1 MeV energies within a few seconds, due to an effective combination of linear and betatron acceleration. The rotational property of the induction field promotes energization in a restricted area with dimensions equivalent to a few Earth's radii. The model also predicts the existence of highly localized cable-type field-aligned currents appearing on the eastern and western edges of the expanding auroral

bulge. It is shown that the predictions agree with satellite observations and with the data obtained from the two-dimensional instrument networks operated in Northern Europe during the International Magnetospheric Study (IMS, 1976-79).

1. INTRODUCTION.

Thirty years after the pioneering work of Chapman and Ferraro (1931) on the formation of the magnetosphere, Axford and Hines (1961) and Dungey (1961) proposed two different ideas for transferring solar wind particles, momentum, and energy into the magnetosphere to produce auroral phenomena. On the basis of ground based observations Axford and Hines concluded that magnetospheric plasma must circulate, implying that a magnetospheric electric field exists in the earth's frame of reference; they hypothesized that the solar wind drives magnetospheric convection by some type of viscous-like interaction. They had little idea as to the relevant process, but simply drew the name by analogy with hydrodynamics. In the same year Dungey (1961) suggested a different mechanism; he argued that the existence of a magnetic field B in the solar wind and in the magnetosphere would exert control over plasma transport processes. In particular, a southward interplanetary magnetic field (IMF) would create a magnetic neutral line with an X-type configuration of field lines completely around the magnetopause; an electric field along the dayside and nightside X-lines in the dawn-to-dusk sense would couple the solar wind flow with magnetospheric convection. Dungey called this process "reconnection of magnetic field lines". With either of the above processes (reconnection or viscous interaction) the resulting convection into the inner magnetosphere would energize the plasma particles to produce auroral effects (Axford, 1969). In 1961, when these two fundamental

works were published, most of the magnetosphere was still unexplored, measurements of its plasma properties and magnetic fields were almost non-existent, and there were no measurements at all of magnetospheric plasma flow or electric fields. We all owe a debt of gratitude to these authors (Axford, Dungey, and Hines) who displayed great understanding and imagination in their pioneering work.

These authors, and many persons since that time, based their work on magnetohydrodynamic (MHD) theory, first introduced by Alfvén (see Alfvén and Fälthammar, 1963). This is a one fluid theory (combining electrons and ions together) which treats the plasma as a perfect conductor. It is based on the conservation laws of particles, momentum, and energy; as such, it would seem to be necessarily correct. An alternative two-fluid formulation treats electrons and ions as separate but interacting fluids.

In MHD theory it is usual to eliminate the electric field \underline{E} by replacing it with $-\underline{V} \times \underline{B}$ (or a more complicated Ohm's law, where \underline{V} is the fluid velocity) and the current \underline{J} by $\underline{V} \times \underline{B}/\mu_0$. As Parker (1967) has noted, for some purposes such as calculation of plasma flow the electric field and current are "non-essential field quantities", and their elimination simplifies the problem: "only the field of principal interest, the magnetic field, remains. The dynamics of the geomagnetic field is reduced to a discussion of the balance of forces."

However, there is a catch: one must adopt an equation of state. The choice determines a model for the plasma. The physical content of the required approximation is that there should be sufficient locali-

zation of the particles in physical space. This is not possible if particles are able to move substantial distances in a short time. In a collisionless plasma, as in the case of the major part of the magnetosphere, this requirement may prove to be a crippling one. Thus fluid theory, though potentially of great practical use, relies heavily on the cunning of its user (see Krall and Trivelpiece, 1973, p. 88).

There is a second criticism of MHD theory. In all magnetospheric theories the existence of a large-scale electric field plays an essential role, associated with convection. It is commonly held that MHD theory properly includes the electric field, whatever its origin. This is not necessarily true. An electric field, unlike a magnetic field, has two sources. MHD lumps these into one, and thus the question of any possible relation between the two cannot even be addressed. For example, it is possible for the induction electric field (the cause) to produce charge separation (the effect). MHD theory can be used successfully to describe stationary processes where large-scale collective motions are guided by an existing conservative E-field, provided the length and time scales satisfy certain criteria (Krall and Trivelpiece, 1973, p. 97). Problems arise when transient effects have to be treated, requiring the tracing of charged particles in a region of non-conservative fields (see Heikkila, 1982, for one example). Substorm phenomena are typically transient, and hence the use of MHD theory to explain substorm features have met with some problems (see e.g. Heikkila, 1973 and 1974; Alfvén, 1976, 1977; Heikkila, 1978, 1982). As pointed out by Heikkila (1978, p. 123) "it is difficult to see how theories in which [the induction electric

field] is not included could be relevant to substorms."

In order to overcome such shortcomings, kinetic theory should be chosen as the basis for consideration of time-dependent magnetotail phenomena. In the plasma sheet it can be assumed that the particles to a high degree of approximation are collisionless, and interact only through the electromagnetic fields they produce. We can trace the motions of charged particles obeying the (relativistic) equation of motion presented by the Lorentz force in electromagnetic fields. However, we do run into a very serious problem in solving the complete Boltzmann equation, as is well known.

Therefore, even before applying kinetic theory it might be best to use basic laws (such as Newton's and Maxwell's relations) in an ad hoc fashion, guided as much as possible by observation, to get a clear idea of what is important for the theory. This is the view that has been adopted by us in a series of papers over the last five years. The present paper is largely a review of fourteen papers on magnetospheric and auroral phenomena published by the authors and collaborators during 1977-82. In these papers a simple model for the onset of substorms is formulated, and the predictions are tested mainly by means of ground observations made in Northern Europe during the International Magnetospheric Study (IMS, 1976-79). This model for localized substorm development in the magnetotail, based almost entirely on observations that were available in 1977, is formulated in a series of seven papers (Heikkila and Pellinen, 1977; Pellinen, 1978; Pellinen and Heikkila, 1978a; Pellinen, 1979a; Pellinen, 1979b; Heikkila et al, 1979; Heikkila, 1981). The theoretical justification

of the choice of a gauge condition for calculating induction electric fields is presented by Cragin and Heikkila (1981). Presubstorm development and triggering are described in four observational papers (Untiedt et al, 1978; Pellinen and Heikkila, 1978b; and Pellinen et al, 1982; Uspensky et al, 1982). Localized field-aligned currents appearing at substorm onset are treated in two papers (Opgenoorth et al., 1980; Baumjohann et al., 1981).

The presentation is organized in the following way. Section 2 covers the essential observations that must be explained. In Section 3 we summarize elementary theory, particularly on the electric field, trying to avoid the pitfalls of MHD. After that, in Section 4, we give our ideas of the theory of the quiescent auroral arcs, which go beyond the conventional views, for example as voiced in the Auroral Arcs conference in Alaska in 1980 (Akasofu and Kan, 1981). A particular concern is how auroral fading and blackening of the poleward sky before breakup can be explained; these are phenomena of what we call the trigger phase of magnetospheric substorms, discussed in Section 5. The actual onset is discussed in Section 6, where the induction field truly comes into its own as a medium to draw energy from the magnetic field. High energy particles can be produced by a two step process, essentially a discharge along a neutral line followed by betatron acceleration (Section 7). Section 8 outlines a scheme for accomplishing the current diversion to the ionosphere that has so often been postulated but never explained. Section 9 addresses the question of numerical modelling. The paper concludes with a discussion on some relevant, but still open, questions about our

understanding of the magnetospheric phenomena.

2. OBSERVATIONS

In order to understand the entire substorm mechanism, observations have to be made both in space and on the ground. During the IMS the possibilities to obtain extensive three-dimensional data sets were improved thanks to the two-dimensional instrument networks and the new satellites that were operated. Analysis is still in progress, but some new results can already be pointed out. Below we shall discuss these (and earlier) results as facts that must be explained by any comprehensive theory.

2.1 Ground-based Observations of Substorm Growth Phase

Observations made on the ground during the International Geophysical Year (IGY, 1957-58) revealed that auroral break-up, which signifies the onset of the expansion phase of a magnetospheric substorm, is a localized phenomenon occurring close to magnetic midnight. At earlier times auroral arcs move equatorwards with no significant disturbance in their structure and luminosity, but perhaps brightening somewhat. The auroral breakup begins with a local brightening of an arc, quite often an equatorward arc. This is followed by poleward expansion, and a westward travelling surge produced by energetic electrons, as shown in Figure 1 published long ago by Montbriand (1971). A little later there is also an eastward expansion, with evidence of proton precipitation (Montbriand, 1971; Fukunishi, 1975; Vallance Jones et al., 1982).

We think that it is significant that auroral breakup begins near midnight as a local phenomenon, and travels poleward. If it were

directly driven by the solar wind it should begin at the poleward edge (at the boundary between open and closed field lines) and travel inward, deeper into the magnetosphere.

There has been considerable discussion as to the existence of a growth phase, first proposed by McPherron (1970). If the substorm were an internal phenomenon, such a growth phase would seem to be mandatory. On the other hand, if the substorm were directly driven by the solar wind, as argued by Akasofu (1981), then a growth phase may not be necessary. Perhaps the best evidence for the existence of a growth phase comes from energetic electron (energy $W > 30$ keV) precipitation. The development of high-energy precipitation can be observed by using networks of riometers, and x-ray detectors carried by balloons at different points in the observational area. An excellent study was conducted by Pytte et al. (1976a) who advanced strong arguments for the existence of a substorm growth phase through the identification of phenomena which occur before and up to the onset of the expansion phase of the substorm. Their observations can be summarized as follows:

(1) Prebay precipitation appears first in the northern part of the auroral zone, and progresses gradually towards lower L-values; this progression is shown in Figure 2 for a substorm onset occurring over Ivalo, Finland, on 11 November, 1976 (Pellinen et al, 1982). The southward movement proceeds with a speed of roughly 100 to 300 m/s around local magnetic midnight.

(2) The region of high-energy precipitation is normally narrow in latitude, perhaps only of the order of 50 km, whereas it may extend

for at least 2000 km in the east-west direction along the auroral oval.

(3) At high L-values the precipitation ends well before bay onset. The precipitation lasts until bay onset at a lower L-value is reached, normally corresponding to the southern part of the auroral zone, and here merges with the subsequent bay-associated precipitation. Normally there is a drop in precipitation just before or at least at the onset of the associated negative magnetic bay; this is apparent in Fig. 2, especially at Kevo a few minutes before substorm onset at 2102 UT.

In this event, a quiet homogeneous arc and higher energy precipitation region equatorwards of the arc moved southwards during the growth phase, slowed down and stopped before the onset of the expansion phase at 2102 UT (Fig. 3), in complete agreement with Pytte et al. (1976a).

The interplanetary magnetic field (IMF) was monitored by IMP-8 for this substorm; the IMF turned southward at 2027 UT, remained southward until about 2039 UT, after which there was a brief northward excursion for 2 minutes, as shown at the top of Figure 3. Magnetometers around the northern hemisphere showed that a two-cell convection pattern was initiated shortly after 2027 UT, and well established by 2045 UT. The equivalent current pattern over Scandinavia and the auroral arc are shown in Figure 4. The current density of the westward electrojet (deduced from a two-dimensional network of magnetometers) moves equatorwards during the growth phase together with the quiet auroral arc, but displaced slightly equator-

wards from it. The half-width showed some tendency to decrease and the maximum current density to increase, while the total current remained relatively constant (see Fig. 7 of Pellinen et al, 1982).

Radar observations add much to substorm studies, especially with STARE (Scandinavian Twin Auroral Radar Experiment, Greenwald et al, 1978). Uspensky et al. (1982) conducted a study during a substorm growth phase on March 16, 1978, and found that during the time prior to a substorm onset the height-integrated Hall conductivity has a distinct jump across the auroral arc. In the event studied the conductivity decreased by a factor of 3-5 in going from the equatorward side of the arc to its poleward side. They found that the radar amplitude changed proportionally to changes in mean electron density and Hall conductivity. This occurs in regions where the electric field showed only minor changes. This observation is consistent with the features in the Nov. 11 events shown in Figures 2 to 4, where the high energy electron precipitation would produce higher conductivity south of the arc.

Thus, on the basis of observations, we believe that there is a growth phase lasting for some tens of minutes before the substorm onset; conditions are slowly evolving, and all physical features drift equatorwards slowly at a few kilometers per minute.

Because of the low latitude of these phenomena on these and other events we conclude that these features occur on closed magnetic field lines.

2.2 Trigger Phase of a Substorm

Something must happen locally either deep inside the plasma sheet

or on the flux tube reaching down to the ionosphere, to initiate the substorm expansion. The first indication of something unusual that we noticed is a slight fading of auroral luminosity occurring for about one or two minutes before the expansion. This was first observed in the all-sky photograph shown in Figure 5 while one of the authors (WJH) was visiting the Air Force Geophysics Laboratory in Bedford, Mass (Pellinen and Heikkila, 1978b). The general picture that we have developed is that the poleward sky clears (as already reported by Snyder and Akasofu, 1972), and the arc fades or becomes weaker in intensity close to the trigger area (Pellinen and Heikkila, 1978b); the arc then develops local ray structures. Optical fadings were reported in the papers of Untiedt et al. (1978), Opgenoorth et al. (1980) and Baumjohann et al. (1981). It is appropriate to call this interval just before onset the trigger phase of the substorm.

A summary of auroral fading based on extensive study of optical data was given by Pellinen and Heikkila (1978b):

- (a) Quiet auroral forms fade briefly in intensity for about 1 or 2 minutes, just before break-up initiated the expansion phase of a substorm. At the same time the poleward sky darkens, which is usually quite obvious on the original film. The fading is usually preceded by a brief intensification of auroral brightness. In some cases multiple onsets can be detected, with a sequence of short-duration fadings and intensifications prior to the final break-up.
- (b) The fading can be detected best in the electron aurora. There is some indication that the proton aurora fades in a similar

way.

- (c) The fading can occur under a variety of conditions: before and after midnight, during quiet and active periods, and on poleward or equatorward auroral arcs.
- (d) The subsequent increase in activity that initiates the expansion phase may take place on the arc that shows the deepest fade; or it may occur on another arc, often a new arc appearing either polewards or equatorwards of the fading arc (as in Fig. 5) where a new arc was formed south of the fading arc (which also brightened).
- (e) Frequently it is clear that an aurora fades on the spot; at other times there are indications that the fade travels ahead of the surge, either eastwards or westwards.
- (f) The geographical area in which fading is noted simultaneously, or nearly so, can be as small as a few hundred kilometers.

In the data presented by Pellinen et al. (1982) fading was observed in only the balloon X-rays (see Figure 6). In fact weakening of precipitation in higher energy ranges seems to be a commonly observed phenomena (e.g. Fytte et al., 1976a; Ullaland et al., 1981; T. Rosenberg, University of Maryland, private communication). Hence, in looking for changes in particle precipitation during this phase one should first look into the harder component fluxes, i.e., the electrons over 25 keV.

Fading of radar aurora has been observed to precede substorm onset (Pellinen and Heikkila, 1978b; Starkov et al, 1979). This seems natural if we accept the view presented by Uspensky et al. (1982) that behaviour of auroral backscatter during the substorm growth phase is mainly controlled by variations in ionospheric (Hall) conductivity in the backscatter region.

The multiple-onset substorm discussed by Baumjohann et al. (1981) (see also Section 9) gives examples of several subsequent auroral activations separated from each other by fadings. These auroral fadings were associated with a distinct decrease of equivalent current approximately in the same region (Fig. 7). The decrease of current strength must have been caused by a drop in the ionospheric conductivity, because the electric field recorded by the STARE was observed to remain approximately constant. These observations support the conclusion presented above, namely that before an auroral break-up the flux of energetic particles (which cause pre-break-up arcs, and diffuse aurora, riometer absorption, and enhanced ionospheric conductivity) decreases significantly before growing strongly during the onset.

There is still another feature that has not been reported before. Often there are some weak auroral patches or arcs poleward of the breakup arc; a movie film (made of all-sky films recorded in Finland on 27 and 30 January 1979) shown at the third IMS workshop at Skokloster, Sweden, September 3-7, 1979, demonstrated that these weak poleward patches were convecting rapidly southward toward the breakup arc just before the onset. Small details such as this (and fading) have been of great value for us in deciding on physical mechanisms.

2.3 Ground-based Observations of Onset-Related Field-Aligned Currents

The usual method of presenting currents from magnetometer data is in the form of total equivalent current vectors (TEC), derived by turning the horizontal magnetic disturbance vectors clockwise through 90° . The vertical component is usually indicated by different symbols for negative and positive variations, or by isolines.

The need to differentiate between quiet-time current-systems and

substorm-connected ones, as well as the need to recognize the characteristic of changes in an existing current-system, made the use of so-called differential equivalent current vectors (DEC) necessary. The basic idea of this method is the assumption that a current system observed at a time t_1 stays constant until a time t_2 , while an additional current system develops during the same time interval. The final result is naturally very much dependent on a reasonable choice of the times t_1 and t_2 ,

and ,hence, DEC-vectors have to be interpreted with care. In most cases other data (e.g. optical observations) allow restriction of the various possible causes of a certain pattern. The idea of splitting the total magnetic disturbance field was first introduced in the analysis of magnetic-latitude profiles by Kisabeth and Rostoker (1973) to study the small scale magnetic effects connected with auroral loops and surges. It was later applied by Untiedt et al. (1978) to data from a two-dimensional magnetometer array, and has shown its power in separating transient local phenomena from the more widespread global magnetic disturbances.

Opgenoorth et al. (1980) reported observations of a moderate substorm that occurred on 2 March 1978 with the onset at 2222:40 UT over the western part of Northern Scandinavia. DEC analysis was used to get an idea about the current system that was directly related to the break-up. The onset current system was switched on at the moment of auroral break-up and seemed to be fully developed at 2225:20 UT when the aurora reached its first maximum in northward expansion and increase of brightness. The resulting DEC-vectors in Fig. 8 a show in the western part a distinct U-

shaped equivalent current loop around the location of initial auroral intensification. The sense of rotation in this loop was counterclockwise with growing negative Z-variations towards its center. In the northeastern part of the picture there was another equivalent current loop with a clockwise sense of rotation. Correspondingly here the enclosed Z-variation was positive.

Considering the excellent temporal and spatial correlation between auroras and magnetic field variations as described above there must be a connection between the obviously local decrease of the intense discrete aurora to the east (mapped in Fig. 8a) and the main development of the clockwise equivalent current loop. Vice versa, there seems to exist a causal relationship between the counterclockwise equivalent current loop and the auroral breakup to the west.

The two oppositely directed equivalent-loops clearly coexisted during the whole 3-4 min. after the substorm onset. Thus it seems reasonable to consider both features as being connected with the auroral breakup and the ground signatures of the three-dimensional magnetospheric substorm onset current system.

Unfortunately the observation field of the STARE-radar does not reach far enough to the south to cover the entire area where the auroral breakup took place. However, in the recordings at 2225:20 UT (shown in Figure 9) there seems to be some evidence for a clockwise curvature in the irregularity drift-direction at the position where we observe the northern part of the counterclockwise equivalent current loop. Also, corresponding to the clockwise equivalent current loop there is a counterclockwise irregularity drift at the same location. This drift pattern would be produced by

downward current depositing positive charge to the east, and upward current leaving negative charge to the west, exactly as implied by the magnetometer data. This may explain the decrease in auroral luminosity to the east, since protons are not as efficient a means of excitation as electrons; if the downward current was carried by upward flowing ionospheric electrons the same conclusion holds.

The results by Opgenoorth et al (1980) show that the extent of the IMS-network of stations in Scandinavia is close to the scale size of substorm onset phenomena. This argument has been confirmed in other studies. Fig. 8b (and also Section 8 and 9 below) gives another example presented by Baumjohann et al. (1981). The same pattern of differential equivalent currents as presented by Opgenoorth et al. (1980) is repeated there. At 90 seconds after the onset at 2118:30 UT the aurora reached its first expansion peak (see the all-sky picture from Muonio in the lower right corner). The DEC vectors on the western Norwegian coast show a distinct counterclockwise U-shaped loop (negative Z growing towards the center is not exhibited) around the observed center of initial auroral intensification. The circular clockwise DEC loop began to form simultaneously with the U-shaped loop, but developed slower. Most of its development seems to have occurred between 90 s and 210 s after the onset (Fig. 8b). Thus, the substorm onset currents can be modelled as cable-type or filament Birkeland currents (Sections 8 and 9, see also Robert et al., 1982) where the current centers are separated some 500-1000 km from each other.

2.4 Ground-based Observations of Substorm Expansion

Substorm onset-related phenomena can be covered by networks in the Scandinavian sector. In order to study the full expansion development more extensive networks are needed. Hopefully some satellites, especially the Dynamics Explorer 1 launched in 1981, will give a more global view of the

expansion sequence.

From some earlier studies we get the following picture of the development of substorm expansive phase. Break-up begins with an explosive growth of auroral brightness and a rapid poleward movement of the auroral forms (see e.g. Akasofu, 1968). The disturbance spreads in all directions. A surge moves fairly quickly (few km/s) westwards as it expands (Akasofu et al, 1965). The eastward propagation often involves wavy structures called Ω bands (Akasofu, 1974). Pulsating patches on the morning side of the oval appear equatorwards of the Ω band. The expansion phase is followed by a recovery phase, during which the auroras calm down and return to their original quiet time condition.

In some recent studies the Scandinavian IMS data have been used to study substorm expansion in the evening sector (Yahnin et al., 1982; Opgenoorth et al., 1982). The following results are interesting for our further discussion.

At substorm onset auroral luminosity propagates with high speed along the preexisting growth-phase arc. In Yahnin et al. (1982) this structure, which is a precursor of the westward travelling surge (WTS), was named the "auroral horn." The altitude of the horn is not changing considerably from the growth-phase arc indicating that the brightening is mainly due to an enhancement in the particle flux, and not so much due to a much more effective energization of auroral particles.

The leading edge of the WTS is the center of upward field-aligned current tube. Auroral altitudes in this region are lower than in the surrounding area; The most luminous auroral structures appear in this region. Opgenoorth et al. (1982) have shown that the upward-flowing

Birkeland current propagates with the WTS keeping its cable-like form instead of forming an elongated current sheet expanding from the central meridian along with the surge.

2.5 Satellite Observations of Substorm Dynamics

Both single and multiple satellite observations have been used to form, piece by piece, a statistical picture of what goes on in the magnetotail before and at the onset of the expansion phase. Even if our understanding of the magnetotail dynamics is not yet complete, the following features have been fairly well established.

The start of the reduction of tail flux content coincides, within a few minutes, with the first signs of a low-latitude magnetic positive bay observed on the ground in the midnight sector (Nishida and Nagayama, 1973; Caan et al, 1973). Multiple onsets, too, have been found to be associated with a stepwise release of energy from the magnetotail (Pytte et al., 1976b; McPherron, 1979). Often the first signs (e.g. brief auroral activations) of an onset are only precursors of the substorm.

Many researchers believe that the onset is triggered within the near-earth plasma sheet (Pytte, 1976, for review). They may be biased by the fact that the observations made close to the geosynchronous orbit ($6.6 R_E$ from the earth) have been more numerous up to now than those recorded in the far tail (say $30 R_E$ or more from the earth). Furthermore, large substorms may be triggered closer to the earth than smaller ones. The main conclusion drawn from the various observations is that there seems to be a critical distance of $15 R_E$ down the tail separating the plasma sheet into two regions according to its behaviour during substorms. Earthwards of that boundary the plasma sheet thins before the onset, and recovers

rapidly during its expansion phase, while farther out the plasma sheet starts to thin at the expansion phase onset.

The thinning of the plasma sheet at a radial distance of $17 R_E$ is one of the best documented signs of the start of the expansion phase. Inside the thinned plasma sheet, plasma flows tailwards with a velocity of several hundred km/s (Hones et al., 1974). A few minutes after the onset of the substorm is observed on the ground, the magnetic field component B_z of the low latitude tail field turns from north to south (Nishida and Nagayama, 1973). Simultaneously the field closer to the earth stays northwards and increases sharply.

Impulsive bursts of energetic particles at the onset of the expansive phase of a substorm have been reported since 1965 (Anderson, 1965). Here we will not review the extensive literature on the subject (for a more detailed treatment see the review by Krimigis and Sarris, 1979), but will discuss only the publications of interest for the presentation that follows.

Fennell (1970) reported that bursts of energetic protons (>0.32 MeV) occurred at lunar distance in the magnetotail during intense magnetospheric substorms. His view was that the bursts appeared more frequently in the evening sector of the magnetotail than in the morning sector. Sarris et al. (1976a), Hones et al. (1976), and Carbary and Krimigis (1979) observed that intense proton fluxes usually have a component of flow towards the dusk side of the magnetotail as well as towards or away from the earth. Belian et al. (1981) characterized the energized protons flowing sunward near synchronous orbit as "drift echoes" and those flowing antisunward in the magnetotail as "impulsive" bursts. Electrons of about 50 keV display a

similar but opposite asymmetry to energetic protons (e.g. Montgomery, 1968; Meng, 1971), though higher-energy electrons (0.22 to 2.5 MeV) display no asymmetry whatever (Sarris et al. 1976a). All these particle fluxes were observed within the plasma sheet.

Several papers deal with the location and size of the source region. Carbary and Krimigis (1979) found that the acceleration region is localized and small, and that the effects will be seen only if the observing spacecraft happens to be magnetically connected to such a region. Sarris et al (1976b) concluded from multi-spacecraft proton observations that the length of the source region along the x axis was 300 to 2,400 km and that it moved at speeds of 30 to 80 km/s or more along the tail. The location of the source was beyond $33 R_E$ in the magnetotail, and the source produced energies over 1.85 MeV in a localized region.

In the above examples no persuasive evidence for an X-type neutral line was found in association with the source. This contradicts the observations reported by Terasawa and Nishida (1976), who concluded that relativistic electron bursts (0.3...1.0 MeV) probably occur at the time of the southward turn of the local B_z , i. e. near a magnetic neutral line in the magnetotail.

The association of the local neutral-line structure with particle bursts has partly satisfied researchers who try to explain all particle energization during auroral substorm by "enhanced reconnection." Terasawa and Nishida (1976) point out that the conventional explanation of acceleration along the neutral line is in trouble unless there is an induction field of 80 mV/m along the X-line over a distance of $1R_E$. This is too high in magnitude for typical magnetotail conditions, as pointed out by Pellinen

and Heikkila (1978a).

Kirsch et al. (1977) report large transient anisotropic fluxes of high-energy particles along the magnetotail ($W_p > 0.39$ MeV, $W_e > 0.22$ MeV). The anisotropies were 30:1 for protons and 5:1 for electrons when the electrons propagated tailwards and the protons earthwards. The local magnetic field changed by about 15 nT during the one minute in which the enhanced fluxes were observed. After a detailed analysis they conclude that this provides indirect evidence for a short-duration DC electric field or a localized inductive electric field which accelerates protons and electrons in opposite directions by up to 1 MeV in 20-40 seconds.

Kirsch et al. (1977) end their paper with a summary of the conditions for theoretical models of transient electric fields in the magnetotail:

- "(a) Electrons and protons must be given hundreds of keV of energy in a few seconds,
- (b) The process must allow for oppositely directed proton and electron anisotropies."

In a more extensive study of Kirsch et al. (1981) the existence of flux anisotropies was confirmed. From the temporal delays between the appearance of protons and particles in different energy ranges it was concluded that the acceleration mechanism is charge dependent and capable of energizing particles up to ~ 1 MeV/charge.

Actually Kirsch et al.'s observations (1977) could be expected in view of the ground observations reported by several authors between 1969 and 1975. Even though the energy ranges are quite different, separation in

the proton and electron precipitation regions has been observed during the expansive phase of substorms. Akasofu et al. (1969) and Moutbriand (1971) found that $H\beta$ emission is absent in the WTS (westward travelling surge) that appears on the evening side after auroral break-up. Oguti (1973), Fukunishi (1975), and Vallance Jones et al. (1982) demonstrated that, in the morning sector, both the diffuse (electron) aurora and the proton aurora overlap during quiet times, but the proton aurora lies polewards of the electron aurora during a substorm. According to Fukunishi, there is a mechanism accelerating electrons in the pre-midnight region and protons in the post-midnight region along the geomagnetic field lines down to the ionosphere. Equatorwards of these regions are areas of diffuse proton (dusk) and electron (dawn) precipitation. The relationship of these regions with field-aligned currents during onsets will be discussed in Section 8.

3. BASIC THEORY

3.1 Electric Fields

All vector fields in three dimensions are uniquely defined if their divergence and curl are specified, and if these as well as the vector itself vanish at infinity; this is known as Helmholtz' theorem. Consider the vector field \underline{V} (x, y, z) such that

$$\nabla \cdot \underline{V} = s \quad (3.1)$$

$$\nabla \times \underline{V} = \underline{C} \quad (3.2)$$

The inhomogenous terms on the right hand sides are mathematically known as the sources of the vector field \underline{V} ; if both sources are zero everywhere the vector field itself vanishes.

Thus, the magnetic field has only one source, since $\nabla \cdot \underline{B} = 0$; the source is a current density defining the curl of \underline{B} . However, the electric field has two types of sources. One is charge distribution, as specified by Gauss's law $\nabla \cdot \underline{E} = \rho/\epsilon_0$. The other source is a change in the magnetic field given by Faraday's law, $\nabla \times \underline{E} = -\partial \underline{B}/\partial t$. Both the sources of the electric field can be independent quantities; in fact, one can take the view that all the physics is contained in the properties of these sources. Thus, it makes good sense both mathematically and physically to divide the electric field into two parts,

$$\underline{E} = \underline{E}^{cs} + \underline{E}^{ind} \quad (3.3)$$

with the definitions

$$\nabla \cdot \underline{E}^{cs} = \rho/c_0 \quad (3.4)$$

$$\nabla \times \underline{E}^{cs} = 0 \quad (3.5)$$

which is the usual definition of the electrostatic field, and

$$\nabla \cdot \underline{E}^{ind} = 0 \quad (3.6)$$

$$\nabla \times \underline{E}^{ind} = -\partial \underline{B}/\partial t \quad (3.7)$$

which is the induction electric field, without any contribution by charge separation.

As stated already in Section 1, it is our view that a serious shortcoming of MHD theory is that these two types of electric field are lumped into one, thereby denying any discussion of the mathematically and physically distinct sources. When there is no dissipation perhaps this is excusable, but when there is dissipation, however small, one must look for cause and effect relationships to understand the physics.

One can also discuss the fields in terms of potential functions, the scalar potential ϕ and the vector potential \underline{A} . In order to do that one must choose a gauge condition. The choice of the Lorentz gauge is particularly useful for formal calculations since then the potential functions are Lorentz invariant. However, in any given frame of reference the Coulomb gauge (defined by $\nabla \cdot \underline{A} = 0$) divides the field into the two parts, equations 3.4 to 3.7.

This gauge is not Lorentz invariant; the reason is that the charge distribution depends on the frame of reference, even at low velocities. Hence one must be very clear as to the proper choice of frame of reference. With the Coulomb gauge we have

$$\underline{E}^{cs} = -\nabla\phi \tag{3.8}$$

$$\underline{E}^{ind} = -\partial\underline{A}/\partial t \tag{3.9}$$

where

$$\underline{A} = \frac{\mu_0}{4\pi} \iiint \left[\frac{\underline{J}_T}{r} \right] dt \tag{3.10}$$

and

$$\phi = \frac{1}{4\pi\epsilon_0} \iiint \left[\frac{\rho}{r} \right] dt$$

where the square bracket indicates retarded solutions, and where \underline{J}_T is the solenoidal part of the current with $\nabla \cdot \underline{J}_T = 0$; for most purposes this is the significant part since the irrotational part governed by eq. 3.4 is at least six orders of magnitude smaller.

3.2 Response of a Plasma to an Induction Field

The response of a real plasma to an induction field in three dimensions has not been discussed extensively. Here we shall review the main results of the papers by Heikkila and Pellinen (1977), Pellinen (1979a), Heikkila et al. (1979), and Cragin and Heikkila (1981).

If charged particles could be totally disregarded as contributing to the electric field, the inductive electric field \underline{E}^{ind} could be calculated from the change of the current density distribution \underline{J} by using equation 3.9

together with the definition of the vector potential \underline{A} (eq. 3.10)

When charged particles (ions and electrons) are introduced into the system, their differential motions may create a charge polarization field, which is irrotational given by equation 3.8. When added to the "pure" induction field we have for the total field

$$\underline{E} = -\frac{\partial \underline{A}}{\partial t} - \nabla \phi \quad (3.11)$$

The potential ϕ , and thus the real electric field \underline{E} , are difficult to calculate because

- (a) The plasma responds on many different time scales (electron plasma period, electron gyro period, electron bounce period, the corresponding ion periods, Alfvén wave resonance times, etc.)
- (b) The potential depends very sensitively on the actual differential displacements of positive and negative particles. In the plasma sheet, a relative charge imbalance of 10^{-10} over any substantial part of its volume would be enough to generate electric fields of a strength comparable to the pure inductive field (equation 3.9).

Regardless of the complexities involved in calculating the real electric field, we can distinguish the following important features:

- (a) Polarized and induced electric fields are topologically different; an electrostatic field has a vanishing line integral around every closed contour, so it cannot effect the electromotive force of the induced electric field, i.e.

$$\oint \underline{E} \cdot d\underline{l} = \oint (\underline{E}^{\text{ind}} + \underline{E}^{\text{cs}}) \cdot d\underline{l} = \oint \underline{E}^{\text{ind}} \cdot d\underline{l} + \oint \underline{E}^{\text{cs}} \cdot d\underline{l} = -\frac{d\phi^M}{dt} + 0 \quad (3.12)$$

where ϕ^M is the total magnetic flux enclosed by the contour.

Whatever the distribution of the secondary field \underline{E}^{CS} is, the resultant field must remain finite and large enough to make the line integral finite and equal to $-\frac{d\phi^M}{dt}$.

- (b) There will be an induction electric field in the plasma wherever the magnetic field changes; its source is not entirely local, but is weighted by the inverse dependence on distance in the definition for \underline{A} . With the complex geometry of any real magnetic field, this induction electric field will in general have components both perpendicular and parallel to the magnetic field at every point in space.
- (c) The effect of E_{\parallel}^{ind} must be to polarize the plasma along the magnetic field, so as to reduce the total parallel field. Thus, to say that E_{\parallel} is zero (or small) is not to say that everything is quiescent. The plasma will continually adjust its charge density in response to the changing induction electric field. One could think of this situation as dynamic equilibrium, and not static. The charge will be mainly carried by the electrons because of their mobility, but even electron mobility is not infinite. Transit time effects, and various instabilities, are bound to occur.
- (d) If the polarization of charges leads to suppression of the magnetic-field aligned electric field component E_{\parallel} , the requirement on the line integral around an arbitrary contour mentioned above in point (a) implies that the transverse component E_{\perp} is enhanced instead.
- (e) When the net E_{\parallel} becomes small ($E_{\parallel} = E_{\parallel}^{ind} + E_{\parallel}^{CS} \rightarrow 0$) the transverse

electric field $E_{\perp} = E_{\perp}^{\text{ind}} + E_{\perp}^{\text{CS}}$ in the ionosphere and in the magnetotail may be in opposite senses, to provide a net circulation, in agreement with Eq. 3.12. For example, when $d\phi^M/dt < 0$ we might have a westward electric field on the night side at low altitudes (in apparent agreement with a dawn-dusk magnetotail electric field), while at greater distances in the magnetotail along the same magnetic field lines there would be a dusk-dawn electric field. Even if some unknown electrostatic field of external origin (such as the cross-tail field) is added, the transverse electric field can vary in both magnitude and direction along magnetic lines. Thus, with an induction electric field we cannot map electric fields from one region in the magnetotail to another.

Although the term "induced electric field" appears in many articles on magnetospheric physics, the fact that it has a curl and its relation to irrotational fields has not been explicitly noted in the magnetospheric literature previous to the article by Heikkila and Pellinen (1977).

3.3 Energy Transfer

The energy of charged particles can be increased only by means of electric fields, d.c. or a.c.; this energy can be redistributed among the particles by collisions or wave-particle interactions. (In the magnetosphere the former mechanism is not important.) The specific mechanisms that dominate the energization of particles may be different in different phases of auroral development. In any phase, Poynting's theorem can be used to elucidate the exchange of energy between the electromagnetic field

and the kinetic energy of particles (Heikkila and Pellinen, 1977; Heikkila et al., 1979; Semenov and Sergeev, 1981).

$$\begin{aligned} \int_V \underline{E} \cdot \underline{J} d\tau &= -\int_V \left(\frac{B}{\mu_0} \cdot \frac{\partial B}{\partial t} + \epsilon_0 \underline{E} \cdot \frac{\partial \underline{E}}{\partial t} \right) d\tau - \oint_S \left(\underline{E} \times \frac{B}{\mu_0} \right) \cdot d\underline{s} \\ &= -\int_V \left(\frac{\partial}{\partial t} \cdot \frac{B^2}{2\mu_0} + \frac{\partial}{\partial t} \cdot \frac{\epsilon_0 E^2}{2} \right) d\tau - \oint_S \left(\underline{E} \times \frac{B}{\mu_0} \right) \cdot d\underline{s} \end{aligned} \quad (3.13)$$

The left hand term indicates the total rate of transfer of energy given to the charged particles by the electric field. (The work done on a charged particle is $q\underline{E} \cdot \underline{v}$, and the summation $\sum q\underline{v}$ over all particles is, by definition, the electric current.) This energy can come from (or go to, depending on the sign) the terms on the right hand side. Those describe, respectively, the rate of change of magnetic energy, the rate of change of electric energy and the Poynting flux through the bounding surface. (As usual, the surface unit vector is positive outwards.)

While it is only the electric field that can energize the charged particles the energy density residing in the electric field is negligible compared to that in the magnetic field. For example, a magnetic field of 10 nT has an energy density of $4 \times 10^{-11} \text{Jm}^{-3}$ ($=200 \text{ m}^2\text{Vm}^{-3}$) while an electric field of 1 mVm^{-1} has an energy density of only $4 \times 10^{-13} \text{Jm}^{-3}$ ($=20 \text{ eVm}^{-3}$). Thus the induction electric field essentially acts as an intermediary in the transfer of energy. We should also note that the first two terms on the right hand side in (3.13) also include the energy residing in waves. For any wave fields, except in the ULF range, the rms amplitudes so far observed (Shawhan, 1979) or reasonably expected to exist are small enough for the contribution to the energy density to be negligible.

At quiet times and during most of the growth phase of a substorm, the electric field is essentially static in nature, and we can neglect the time dependence. Hence only the Poynting flux term in Eq. (3.13) is effective

during quiet periods, which implies that the energy for the auroral particles enters the magnetosphere from outside.

During storm conditions the time dependent terms in Eq. 3.13 differ from zero. The source term $-\partial B/\partial t$ gives the induced electric field by Faraday's law. Even in moderate substorms, the strength of the induced electric field sometimes exceeds the average strength of the cross-tail electrostatic field by more than a power of ten (Pallineu, 1978, 1979a). Thus we can safely neglect the effect of Poynting's flux under the conditions prevailing during a substorm.

4. ENERGIZATION OF AURORAL PARTICLES TO PRODUCE QUIESCENT AURORAL FORMS

Auroral phenomena can be divided into two main categories: quiet-time auroral arcs, and active auroral forms of the type encountered during a substorm. By quiet-time aurora we mean the homogeneous arc on the evening and night side of the auroral oval, and the diffuse glow appearing equatorwards of it. These forms move equatorwards in the course of the evening and, depending (at least partly) on the IMF conditions (Coroniti and Kennel, 1972), the auroras occasionally undergo a growth phase which ends in auroral break-up.

There now seems little doubt that a component of the electric field parallel to the magnetic field lines occurs above discrete auroral arcs (see Akasofu & Kan, 1981). In a plasma this E_{\parallel} is dependent upon a strong upward current. This has led to the commonly accepted view that "The aurora results from an electrical discharge which is powered by the solar wind-magnetosphere dynamo" (Akasofu, 1981). In what appears to be an alternative statement, Kan (1982) has said that "The discrete auroras are manifestations of the imperfect coupling state due to enhanced

magnetosphere- ionosphere interactions."

However, a number of difficulties exist with this rather simplistic view. We list a few as follows:

1. What causes the field aligned current in the first place, that seems to be a necessary condition for the creation of E_{\parallel} ?
2. How can electron and positive ion precipitation sometimes occur in the same location at the same time, with both showing signs of field aligned acceleration? (Multqvist et al., 1971; Bryant et al., 1977)
3. How can field alignment occur over a very large energy range, sometimes with no enhancement near the characteristic peak in the energy spectrum (Whalen and Daly, 1979; Bryant, 1981)
4. How can there be a decrease in the flux of precipitating electrons over a wide energy range (1 to 50 keV), just before auroral breakup, to cause auroral fading and other concurrent phenomena (Pellinen and Heikkila, 1978b)

We suggest that plasma sheet processes play an essential role in the formation of auroral arcs. Not until we understand these can we claim to have a united view of the creation of auroral arcs.

The first point to notice is that there is dissipation of electromagnetic energy in the plasma sheet at all times. The magnetotail structure is maintained by a cross-tail current approximately 30 mA/m. Both observations of particle drift motions on closed magnetic field lines (De Forest and McIlwain, 1971; McIlwain, 1974) and direct electric field measurements on GEOS-1 and ISEE-1 (Mozer et al, 1978; Pedersen and Grard, 1978) show that the average potential drop over

the plasma sheet is about 50 kV (the extremes are 5 kV and 200 kV). With typical dimensions of the plasma sheet these values of current and voltage correspond to a total power of about 10^{12} W in the plasma sheet (Heikkila et al., 1979).

This dissipation in the collisionless plasma in the magnetotail is in the form of particle energization. The number of particles supplied to maintain the global quiet-time auroral precipitation has been estimated by Hill (1974) to be about 10^{26} s⁻¹. With 10^{26} particles to share 10^{12} W, an average energization of the order 25 keV per particle is implied. This corresponds to a motion about halfway across the magnetotail, to get this much energy from the electric field.

With the assumption that plasma sheet particles are essentially collisionless it follows that orbit theory can be used, with conservation of the adiabatic invariants, at least to first order. When the first invariant is conserved, the mirror point of a particle which gains energy will be lowered (in terms of geocentric distance), as can be shown very easily (this invariant is the transverse energy divided by the magnetic field strength). Assume that the particle at two different times has energies W^1 and W^2 , with

$$t^2 > t^1$$

$$W^2 > W^1$$

At the mirror points this energy is entirely in the transverse component, by definition, so that

$$W_1^2 > W_1^1 \text{ at mirror points}$$

Then conservation of the invariant implies that

$$W_1^2 / B_m^2 = W_1^1 / B_m^1$$

Thus the magnetic field B_m at the mirror point must increase in accordance with the relation

$$B_m^2 = \frac{W_1^2}{W_1^1} B_m^1$$

The geomagnetic field strength at constant geocentric distance decreases with decreasing latitude so that the mirror point will be lowered quite rapidly with plasma convection toward lower L-shells (Dungey, 1963).

This statement is true for any energization process whatever, as long as the first invariant is conserved in that process, even for betatron acceleration despite the fact the energization is mostly transverse.

This would seem to be almost a trivial fact, yet its significance has been overlooked. To quote one single example, Swift (1981) in a review of mechanisms for auroral precipitation concluded that "The diffuse aurora, likely caused by proton and electron precipitation, is the result of pitch angle scattering by electrostatic cyclotron waves." Since (1) there is particle energization in the magnetotail at all times; (2) there are particles with mirror points already at low altitudes; and (3) these mirror points must come down by any energization process if the first invariant is conserved, there will always be precipitation. These definite statements are consistent with the fact that auroras occur at all times, even in very quiet times (see Meng, 1981).

Of course, if, in addition, there is pitch angle scattering this will enhance any precipitation. However, pitch angle scattering is not necessary to cause precipitation.

In the past, energization of plasma sheet particles has generally been taken to mean adiabatic compression, using the concept of moving magnetic field lines (Azford, 1969). Particles with 90° pitch angles in the equatorial plane are thought to be compressed as they move inward; this is commonly called betatron acceleration. Particles which have a large component of velocity along magnetic field lines undergo longitudinal compression, thought to be associated with conservation of the second invariant; this is the so-called Fermi acceleration process.

An alternative way (and the more fundamental) is to do orbit calculations on individual particles. Collisionless particles in the plasma sheet undergo the following three large-scale (guiding center) drift movements (e.g. Hines, 1963; Northop, 1963; Roederer, 1970; Pellinen, 1979b; Heikkila, 1981).

Electric drift,
$$\frac{v}{c} = \frac{\underline{E} \times \underline{B}}{B^2} \quad (4.1)$$

where \underline{E} is the dawn-to dusk transverse electric field, and \underline{B} the local magnetic-field vector.

Gradient drift,
$$\frac{v}{c} = \frac{W \sin^2 \alpha (\underline{B} \times \nabla B)}{qB^3} \quad (4.2)$$

where W is the kinetic energy of the particle, α the pitch angle, and q the particle charge. The transverse kinetic energy is $W_{\perp} = W \sin^2 \alpha$.

Curvature drift,
$$\frac{v}{c} = \frac{2W \cos^2 \alpha (\underline{B} \times \underline{R})}{qB^2 R^2} \quad (4.3)$$

where \underline{R} is the radius of curvature from the field line to the centre of curvature. The longitudinal kinetic energy is $W_{\parallel} = W \cos^2 \alpha$.

The total drift velocity is $\underline{v} = \underline{v}_E + \underline{v}_G + \underline{v}_C$ (4.4)

Since \underline{v}_G is perpendicular to \underline{E} , the energy of charged particles cannot be changed directly by their movement in the direction of \underline{v}_E .

Gradient and curvature drifts depend on the charge, energy, and pitch angle of the particles. Positive particles in the magnetosphere drift westwards, negative particles eastwards. In the magnetotail these motions carry a westward current; as this is in the direction of the electric field, there must be a net transfer of energy specified by $\underline{E} \cdot \underline{J}$, which was evaluated above.

Hines (1963) has considered the equivalence of the two methods, the fluid treatment and the orbit theory. He finds good consistency with regards to betatron acceleration, although the apparent physical interpretation is quite different in the two approaches. As one example, with MHD only \underline{v}_E is important, whereas in the particle approach \underline{v}_G is the relevant quantity. This alone should be a warning on the use of MHD theory. On Fermi acceleration, he has concluded that although the second invariant may be preserved in longitudinal compression on a differential scale, this might not be true on an integral scale. A similar situation exists with infinitesimal and finite rotations in mechanics. In any case, as he recalls, MHD theory is only approximate, and it must be based on particle orbit theory.

It is the net drift over one bounce period that is important, not curvature drift or gradient drift by itself. In certain types of field geometry it is possible to have zero integrated drift, since curvature drift at the equatorial crossing is opposed by gradient drift as the particles go into stronger magnetic field in the lobes (Stern

and Palmadesso, 1975; Cowley, 1978). The geometries used by these authors were basically one-dimensional with no gradient toward the earth, and hence the results obtained have only academic interest to the production of auroras. With no dependence along the x-direction, there can be no compression, and hence no energization, to use the fluid approach. With orbit theory, the existence of integral drift motions in the magnetosphere can be demonstrated by the ring current which is mainly produced by gradient and curvature drifting of particles around 50 keV. What goes on in the plasma sheet is just a simple extension of the ring current processes. Even in a dipole field, curvature drift is more important for particles mirroring at low altitudes; when the magnetic field has a tail-like geometry, curvature drift should be enhanced even more.

The magnetic gradient ∇B is the dominant factor in the near magnetotail where R is large, and hence the curvature drift negligible. Particles with large pitch angles ($\sin^2 \alpha \approx 1$) gain energy most effectively in this region. Thus the equatorward part of the quiet-time auroral oval is covered by a diffuse aurora, noting that betatron acceleration is accompanied by precipitation. Particles that produce high latitude arcs have small equatorial pitch angles in the distant plasma sheet. These particles must therefore be accelerated by curvature drift in the far tail, where R is small, ∇B negligible, and $\cos^2 \alpha$ is large.

Thus it is entirely natural that there should be two different kinds of auroras, discrete arcs and the diffuse glow, because of the two terms in the drift velocity to cause energization, \underline{v}_C and \underline{v}_G , as

already stated by Heikkila (1974, p. 2499).

If we assume that the energization process by curvature drift is adiabatic (i.e. the magnetic moment remains constant in the guiding center system of the particle), the increase in the total kinetic energy of the particle has to go directly to its longitudinal component W_{\parallel} (see Heikkila, 1981). Particles that are trapped on closed field lines will pass the acceleration region several times on each bounce, and each time they receive more longitudinal energy and their pitch angles decrease; the mirror points of the particles descend rapidly. Hence curvature drift in the presence of the transverse electric field provides a mechanism that feeds particles continuously and rapidly into the loss cone.

It is also interesting to note that a purely transverse electric field can cause longitudinal (or parallel) acceleration. The main difference between energization by magnetic-field-aligned electric fields and transverse energization by curvature drift is that the former produces clear electron and proton anisotropies, while the latter does not.

Since we are mainly interested in the effects to be seen on sharp auroral arcs, we should study the curvature energization in greater detail. The radius of an arbitrary smooth curve,

$$\frac{R}{R^2} = (\underline{t} \cdot \nabla) \underline{t}, \quad (4.5)$$

where \underline{t} is a unit vector tangent to the curve. Here we can set \underline{t} as \underline{B}/B , and using standard vector-analysis equations we obtain

$$\begin{aligned} \frac{R}{R^2} &= \left(\frac{\underline{B}}{B} \cdot \nabla \right) \frac{\underline{B}}{B} = -\frac{\underline{B}}{B} \times \left(\nabla \times \frac{\underline{B}}{B} \right) \\ &= -\frac{\underline{B}}{B} \times \left[\frac{1}{B} \nabla \times \underline{B} - \underline{B} \times \nabla \left(\frac{1}{B} \right) \right] = -\frac{1}{B} \underline{B} \times (\nabla \times \underline{B}) + \frac{1}{B} (\nabla B)_{\perp} \end{aligned} \quad (4.6)$$

$$\text{Thus, } \underline{v}_C = \frac{2W \cos^2 \alpha}{qB^2} \left[\frac{B \times \{(\nabla \times B) \times B\}}{B^2} + \frac{B \times (\nabla B)_\perp}{B} \right] \quad (4.7)$$

As stated above ∇B is negligible in the far-tail neutral sheet, so we can drop the second term in equation (4.7). As the local currents in the far tail affect B , we can write $\nabla \times B = \mu_0 \underline{J}$, where \underline{J} is the resultant of the local currents. Hence

$$\begin{aligned} \underline{v}_C &= \frac{2W \mu_0}{qB^2} \left[\frac{B}{B} \times (\mu_0 \underline{J} \times \frac{B}{B}) \right] \\ &= \frac{2\mu_0 W \mu_0}{qB^2} \left[\underline{J} - \underline{J}_\parallel \right] = \frac{2\mu_0 W \mu_0}{qB^2} \underline{J}_\perp, \end{aligned} \quad (4.8)$$

where \underline{J}_\perp is the current transverse to B , i.e., the cross-tail current. Equation (4.8) shows that the curvature drift is directly proportional to the local cross-tail current density, so it can be written in the form

$$\underline{J}_C = \sum_i n_i q_i \underline{v}_{Ci} = \sum_i n_i W_{\perp i} \left(\frac{B^2}{2\mu_0} \right)^{-1} \underline{J}_\perp, \quad (4.9)$$

where the summation i is over all the different types of particles. From Eq. (4.9) it can be seen that $\underline{J}_C = \underline{J}_\perp$ if the longitudinal energy density is in balance with the energy density of the local magnetic field. If the particle currents are equal to or less than \underline{J}_\perp the system remains stable. If the particle currents exceed \underline{J}_\perp (i.e., the longitudinal energy density of the plasma exceeds the magnetic energy density) a current-type instability, called Firehose instability, sets in (e.g. Schmidt, 1966, p. 249).

A quiet auroral arc has, typically, a narrow sheet structure which extends over a wide longitudinal sector. To explain the auroral arc structure Heikkila (1981) modified the model presented above by introducing a filamentary current, or current sheet pinch (Fig. 10) in the

magnetotail.

This model would appear to satisfy the objections to the simplistic model given earlier, that of providing an upward field-aligned current, given such a current filament, and noting the lowering of mirror points with energization. A filamentary nature of the cross-tail current would appear to be more likely assumption than a perfectly smooth sheet; this has been pointed out by Alfvén (1931), who has given numerous examples in other plasmas.

Starting from a non-uniform distribution of cross-tail current Heikkilä inferred that the energization by curvature drift is enhanced where the current density is locally increased. This leads to a latitudinal profile of particle energy which is similar to an inverted V. Hence a particle energy profile measured by a satellite gives information of the profile of the cross-tail current in the equatorial plane.

In addition, therefore, according to our view, the final energy of the precipitated particle would be

$$W^F = g W^I + e\Delta\phi \quad (4.10)$$

where the first term represents the gain in energy produced by plasma sheet processes (W^I represents the initial particle energy and $g (> 1)$ is a factor to be defined by the plasma sheet processes, mainly curvature drift), while the second term shows the gain in energy by a parallel electric field above the auroral form.

We can now see that it also satisfies the second and third objections at the beginning of this section, since it is the pitch angle of the particle that is important, not the total energy or sign of the charge. In the next section we explore the possibilities for producing auroral fading.

5. TRIGGER PHASE

A new distinct observation related to substorm onset is that of auroral fading (Section 2) which occurs at the moment when the equatorward movement of the aurora has stopped, a few minutes before the impulsive growth of auroral luminosity at breakup. Some other ionospheric parameters also fluctuate rapidly before substorm onset. Hence, the interval between substorm growth and expansion phases when the rapid variations occur has been called "trigger phase" by Pellinen et al. (1982).

To understand the development of the trigger phase, we need to examine the neutral sheet current and, especially, the growth of J_C due to the transverse energization in more detail. The rate of particle energization by the cross-tail field can be given as (see Eq. 4.8)

$$\frac{dW}{dt} = q\underline{E} \cdot \underline{v}_C = \frac{2\mu_0 W_{II}}{B^2} (\underline{E} \cdot \underline{J}_I) \quad (5.1)$$

In the magnetotail $\underline{E} \cdot \underline{J}_I > 0$, which means that particles gain energy. All the energy gained in adiabatic acceleration by the transverse electric field goes directly to the longitudinal component (Section 4). Hence, in the left-hand term of Eq. (5.1) $\frac{dW}{dt} = \frac{dW_{II}}{dt}$, which means that the energy growth is exponential in time if $(\underline{E} \cdot \underline{J}_I)/B^2$ stays constant. In practice this term responds to the changes in J_C by induced electric fields, polarization currents and changes in B, so the growth may be damped effectively at the start, thus permitting the relatively slow growth phase development observed (Pellinen, 1979b; Heikkila, 1981).

During early times of the substorm growth phase the increase of the cross-tail current and the related thinning of the plasma sheet will be approximately linear, but after a certain moment the increase of the cross-tail current becomes locally non-linear. During the linear growth and the

early phase of the non-linear growth enhanced particle precipitation into the ionosphere can be observed which results in a momentary increase in the D-layer absorption, ionospheric conductivity, and auroral brightness in a narrow latitudinal region (Section 2).

As pointed out in Section 4 we believe that the neutral sheet current is filamentary, with individual filaments being connected to auroral arcs as shown in Figure 10. When this current is pinched, becoming enhanced locally, there will be an induction electric field. The mechanism operates in the following way: Close to substorm onset W_{II} in Eq. (5.1) grows non-linearly. According to Eq. (4.3) this leads to non-linear growth in \underline{v}_C and, hence, in \underline{J}_C (Eq. 4.9). The non-linearly growing particle drift currents lead to an effective current pinching and to a growing induced electric field which can be most easily calculated by using the Coulomb gauge, according to equations 3.9 and 3.10. These equations show, because of the negative sign in Eq. 3.9, that this induced electric field will oppose the current variations, in conformity with Lenz's law. Thus a local increase in the current density will induce an electric field which is in the sense from dusk to dawn, opposing the cross-tail electrostatic field, thus weakening it. This will result in less efficient energization, and consequently less precipitation, at all energies, and for both signs of charge. Of course for the ions transit time effects will be more important than for the lighter electrons.

At lower energies the second term of equation 4.10 is more important, due to the parallel electric field, and so there may not be much fading in auroral luminosity, in keeping with the observations. At the higher energies, this second term is not so important and thus there should be

more of a decrease at those higher particle energies. This is clearly supported by the observations, as discussed in Section 2 and shown in Figure 6.

When the cross-tail current density is increasing in one region it must be decreasing in some other region, since the current is described by $\nabla \cdot \underline{J} = 0$. It is appropriate to call this a current meander. This feature is shown in Figure 10, which indicates that in the region of decreasing current density the induction electric field will enhance the cross-tail electrostatic field. Therefore, in this region the plasma convection should proceed faster than elsewhere. This explains the southward rush of the weak auroral patches poleward of the breakup arc that were shown in the film at the Workshop discussed in Section 2.

As soon as the induced electric field dominates the cross-tail electric field in a localized region of the neutral sheet the mechanism described by Heikkilä and Pellinen (1977) and Pellinen (1979a) may result in the onset of the actual substorm phenomena.

Pellinen et al. (1982) presented some observations that supported an idea of a two-stage trigger phase. During the first stage of the trigger phase (Figs 3,6) the southward drift of aurora still persisted and the X-ray counting rate reached maximum, while the electrojet half-width (observed by a meridional chain of ground-based magnetometers) was reduced with increasing current density. However, the total amount of integrated equivalent polar electrojet (PEJ) current was decreasing, and no dramatic auroral fading effects could be resolved during this stage.

According to the theory presented above we interpret these observations as an indication of the non-linear increase in the cross-tail current density following the nearly linear increase during the growth phase. The transition between these two phases should occur as a natural development

of purely internal magnetospheric processes. As a result the total electric field in the source region of the precipitating particles decreases but still remains westward, the precipitation becomes somewhat harder and the area of particle precipitation in the ionosphere shrinks in the north-south direction (pinching).

During the second stage the aurora stopped and brightened (Fig. 3). Auroral fading was expected at this moment but it was observed only in balloon X-rays. This is in agreement with the interpretation of Eq. 4.10 presented above. The start of substorm onset was signalled by the growing trend in the electrojet parameters during this second stage. The final triggering may have been influenced by the northward turning of the IMF as will be discussed later.

6. MODEL FOR SUBSTORM ONSET

Observations made on the ground show that the substorm starts in a limited region close to magnetic midnight and generally not at high latitudes. The disturbance then expands poleward and equatorward, to the west and to the east. From this we can deduce that these ionospheric features must be connected to the plasma sheet, however distorted the mapping may be.

In fact, a great variety of evidence indicates that the region of the magnetotail involved initially is from 10 to 30 earth radii in distance from the earth, certainly on closed field lines at non-substorm times.

From the ground level observations we can deduce, and satellite observations agree, that there are local fluctuations in the magnetic field in the plasma sheet (Rostoker and Camidge, 1971). Local variations in the tail field must be created by variations in the local currents.

Therefore, our model of substorm onset is based on a model of current perturbations.

We make the following four assumptions:

- (1) There are local variations in the cross-tail current \underline{J}_{NS} ;
- (2) The current perturbation grows in intensity, and spreads;
- (3) To a high degree of accuracy $\text{div } \underline{J}_{NS} = 0$;
- (4) We assume that $\delta J_z = 0$, and therefore $\delta I_x = -\delta I_y$.

The first three assumptions hardly need any further comment than what has already been given. The first two make this an ad hoc model, but surely these are based on solid fact.

The fourth assumption is really our only true assumption, and we will now attempt to explain it. We do assume it because in our view it is the energized plasma that initiates the whole process. Sooner or later the plasma must leave the plasma sheet, carrying its energy with it. One possible escape route is around the earth, following the normal convection pattern as outlined by Axford and Hines (1961), and Brice (1967). If it can do that, then there would be no substorm; undoubtedly, this is a normal course of events most of the time. However, at certain times, perhaps due to variations in external conditions, or an especially high value of the magnetotail electric field or the plasma density, such a normal escape route for the energized plasma may not be rapid enough. We hypothesize that the energized plasma will pile up deep in the plasma sheet. It can not go into the high latitude lobes, because the magnetic field is strong there also, and $\underline{E} \times \underline{B}$ drift is inward. Surely it will go in the direction of the least electromagnetic pressure that is confining it, namely outward in the equatorial plane of the neutral sheet.

Such an escape could be accomplished by an outward current meander in the plane of the neutral sheet, as depicted in Figure 11 on the right for a specific model that will be discussed shortly. It is not necessary to have any variation perpendicular to this plane to accomplish such an escape. In fact, any variation in the z-direction would induce an electric field opposing that current perturbation. If such a current perturbation in the z-direction (and the consequent induction field) were of one sign only (as for a flapping motion of the magnetotail), then the breakup auroras should exhibit differences between the northern and the southern auroral zones. All evidence argues for very similar conjugate point effects, suggesting that any E_z^i is small initially. On the other hand, any broadening of the current sheet (with both $+\delta J_z$ and $-\delta J_z$ on opposite sides of the neutral sheet) is not very likely, as it would mean that the plasma would have to go toward the higher magnetic field strength in the lobes, which we ruled out earlier.

Therefore, our model is based on one single assumption that is not based on observations; it is, however, supported by fundamental physical reasoning.

In Figure 11 we also show an opposite meander, on the left hand side. We call these negative and positive meanders. The reason we include this positive meander is based on Newton's third law of motion, which deals with action and reaction. The plasma that is taking part in the negative meander will move outward, away from earth, as will be shown later; this action must be accompanied by a reaction, namely an inward motion of the plasma that is earthward of the escaping plasma. For simplicity, in our calculations we have shown this inward meander as being of the same strength, since its total effects are small in any case. It is the nega-

tive meander to the right in Figure 11 that is most effective.

We have done calculations on this model, chosen because its solution is entirely analytical (Pellinen, 1978, 1979a) There are six input parameters of the model calculations: two depicting the size of the disturbed area; $j(t)$ the temporal current density in the middle of the disturbance; $\frac{\delta j}{\delta t}$, the rate of current decrease in the same area; and two parameters for the expansion speeds of the disturbance.

Let us first look at the magnetic field produced by the current meanders. After a certain time interval the intensifying and spreading current perturbation produces a magnetic field as shown in Figure 12, for the exact middle of the disturbance at $y=0$. In Figure 12a the x-component is shown; near $x=0$ the component has the opposite polarity to the tail field, and thus the combination becomes weaker. On the other hand, the z-component reverses in sign along the x-axis.

For an explicit study of the effects of the disturbance in the magnetotail it must be superposed on an appropriate tail-field model. Unfortunately, all the existing models have been developed for quiet-time conditions, so they do not represent the pre-onset condition of the plasma sheet correctly. We have used the analytical model of Beard et al. (1970) which includes a thin neutral sheet current with a strength decreasing slowly with distance down the tail (at the top in Fig. 13).

Fig. 13 shows the tail structure development in the midnight meridian plane during 25 seconds following the onset of the substorm. The center of the disturbance is at $X=-30R_E$. The graph clearly shows the projections of the X- and O-type neutral lines. The O-type neutral line appears near the regions of enhanced current density, the X-type line in the region of

decreased current density. Fig. 14 shows the shapes of the neutral lines at 15 seconds after the onset in the x-y plane. It can be compared to the diagrams presented by Vasyliunas (1976) for a similar type of development, even though the physical bases of these two diagrams are totally different.

The temporal and spatial development of the current system creates an induced electric-field structure that even penetrates areas in which the magnetic field disturbance is negligible, assuming inadequate response by the plasma to shield the violent disruption. This is because E^i behaves asymptotically like $1/r^2$, while the B values decrease like $1/r^3$. This fact also enables an electric field to be projected on undisturbed magnetic field lines in the tail lobes. At reasonable values of the parameters (Pellinen, 1978), we obtain induced electric field strengths of several mV/m within and around the disturbance (Fig. 15). The static electric field values appearing in the plasma sheet average 0.15 mV/m, which means that they are negligible compared to the induction field close to the disturbance bubble at the onset of the substorm.

7. PRODUCTION OF HIGH-ENERGY PARTICLES

The above calculations assume no response by the plasma. This is completely unreal, and now we begin to see what that response might be. We first consider the bursts of particles which are observed to occur shortly after the onset of the expansion phase. The number of particles that are involved is low enough that they do not affect the gross structure of the plasma sheet.

Immediately after onset, before any new neutral line is formed, there is already an induction electric field, caused by the initial current meander, or alternatively by the changing magnetic field. Since we assumed

that $\delta J_z=0$, equation 3.10 shows that the induction electric field also has no Z component, having only x and y components everywhere. In the plane of the neutral sheet the induction electric field is everywhere perpendicular to the magnetic field. However, above and below that plane where the magnetic field is tipped over because of the tail-like structure, this field has components both perpendicular and parallel to the magnetic field, as shown in Figure 16. The immediate and obvious plasma response must be to produce charge separation by means of a field aligned current (as discussed in Section 3 and later in Section 8), and thus to reduce the total electric field parallel to the magnetic field. In so doing, the plasma must enhance the perpendicular component (see Section 3). Thus, if anything, the total electric field in the x -direction shown in Figure 15 in the plane of the neutral sheet will be enhanced (not reduced) by the action of the plasma.

In our conversations we have often met with the objection to our reasoning that the electric field produced by induction will be modified by the plasma. We totally agree with this comment; however, it seems to be further assumed that the electric field must be decreased by the conducting plasma. The arguments presented above show that in fact it may be enhanced in certain regions.

At a certain time a new neutral line is formed (see Figure 13 and 14), an X-type in the region of decreasing current, connected to a O-line in the region of increasing current. Both types of neutral lines are formed in the presence of an induction electric field in the plane of the neutral sheet, with the x -component enhanced by the plasma as the y -component is reduced.

At the X-line this electric field will be of the same sense as assumed

in reconnection or merging theories (Vasyliunas, 1975; Sonnerup, 1979). Fluid (or MHD). concepts lead to the formation of magnetic and electric field structures as discussed above, but it is a few individual particles that will be energized to high energies, which cannot be discussed by MHD theory.

The interaction between charged particles and electromagnetic fields can be expressed by the relativistic equation of motion, which consists of separate electric- and magnetic-field terms. The electric field must be the immediate cause of particle energization, because the magnetic force $q\mathbf{v} \times \mathbf{B}$ does not affect the speed of the particle. To change its energy a particle must have a velocity component parallel to the electric field. The rate of energy change can be estimated from the following:

$$dW = \underline{F} \cdot d\underline{s} \quad (7.1)$$

where \underline{F} is the electric Lorentz force acting on the particle, and $d\underline{s}$ is an infinitesimal distance along the trajectory of the particle. To study particle energization, we must know the movement of a given particle and the time-dependent electromagnetic field at each point on its trajectory.

As guiding-center approximation may be non-valid in some regions of the tail, the only way to treat the movement of the particle is to use the equation of motion in calculating $d\underline{s}$ in Equation (7.1). In fact this is the only way to treat the effects of induction fields because the energy of the particle changes during each gyration at any one location

owing to the non-vanishing value of $\oint \underline{E} \cdot d\underline{s}$.

Since the cross-tail electric potential field has an upper-limit of around 100 keV in the plasma sheet in particle energization, owing to its conservative

The dependence of the mechanism on the neutral line-region also demonstrates how selective acceleration can be achieved rather than an equitable distribution of the available energy among the whole particle population.

In the model simulations made by Pellinen and Heikkila (1978a) 1 keV electrons and 10 keV protons (90° pitch angle) were launched at different locations in the neutral sheet. In the launching grid those points were selected from which the particles were most effectively energized. It turned out that regions close to the X- and O-type neutral lines were the best, thanks to the two-step energization process described earlier in this paper. In Fig. 17 we show a few representative particle trajectories within the neutral line. The diagram shows that

1. Energetic proton bursts appear mainly on the dusk side outside the loop. The protons launched near the O-type neutral line seem to stay inside the bubble.
2. Energetic electrons appear both on the dawn and the dusk sides of the bubble and drift out from the bubble close to the O line.
3. Gyrobetatron acceleration can give the electrons an energy gain of 80 keV, while corresponding acceleration on a straight line from launch point to end point would give only 5 keV. This confirms the importance of the exact trajectory.

On comparing our results with the observations presented above (Section 2), we find they agree amazing well. We have done calculations for about 200 particles whose pitch angle were 90° . When the field lines are enclosed in a loop about the O-line the particles cannot escape along them, so even particles with smaller pitch angles remain inside the loop for some time before they can drift out. Hence the magnetic loop structure together

nature, an induction field energizes particles more effectively. For one thing, an induction field is larger and thus permits higher acceleration (e.g. along the neutral line, see Terasawa and Nishida, 1976). However, it has its limitations because super-Alfvénic drifts are unlikely in the magnetotail, so there is an upper limit on the electric field which is probably smaller than 10 mV/m (for details see Pellinen and Heikkilä, 1978a). Another and more important feature of induction fields is their ability to energize charged particles locally by betatron acceleration. This, too, has its limitations. The ratio of the final to the initial energy is directly proportional to the ratio of the final to the initial magnetic field strength. Hence the biggest relative energy increases are again achievable only near a magnetic neutral line, where the initial field is very small. Expressed in the language of orbit theory, the limitation is due to the dependence on the magnetic moment of the particle (for relativistic particles the relevant quantity is the flux enclosed by the gyro orbit). Only particles with a substantial magnetic moment at low values of $|B|$ (i.e. particles that already have a fairly high energy) can be efficiently energized. In particular, betatron acceleration is ineffective on cold plasma particles.

Near a neutral line the difficulty of energizing cold plasma particles can be overcome by a two-step process in which linear, non-adiabatic acceleration along the neutral line provides adequate momentum so that, when the particle leaves the neutral line and enters a gyro orbit in the surrounding magnetic field, it has a sufficient magnetic moment to benefit from the betatron acceleration. As shown by Pellinen and Heikkilä (1978a), for reasonable values of the magnetic-field changes during a substorm, initially zero-energy particles can be energized to MeV energies.

with the rotational property of the induction electric field (which is not generally taken into account by other authors dealing with the subject) may provide an explanation for the localized appearance of energetic particle bursts observed in the magnetotail during substorm.

The values in Fig. 17 were obtained during relatively small tail-field changes, 10 nT/min. In order to stress that the energy gain is dependent on the assumed rate of change of the magnetic field we show in Fig. 18 one case of electron energization with the very large rate of $-\frac{\partial B}{\partial t}$, 2.5 nT/s, a value actually observed on at least one occasion (Kirsch et al. 1977, reporting data obtained by W. F. Ness). Here the electron energy reached 1 MeV in about 3 s. Since this example nicely demonstrates how the energizing mechanism actually works let us analyze the development in more detail. In the initial linear acceleration along the neutral line the energy rose to 50 keV at point A. During the subsequent betatron process AB the energy steadily increased on each gyration, and the relativistic invariant $\gamma\mu$ was constant (see Roederer, 1970, p. 21). over the portion BC the drift velocity was so high, about 10% of the total, that allowance must be made for it, as is shown by the dashed line, since the magnetic moment is evaluated in the drifting coordinate system. Between C and D the energy increases at a much slower rate; this is due to a combination of two opposing factors. The electron drift here is in the direction of the electric field, with a resultant loss in energy amounting to 120 keV by the drift betatron process. At the same time the electron gains 278 keV due to its gyrational motion, about 0.4-keV average over 706 gyrations, leaving a net gain of 158 keV as shown in Fig. 18. The total path over CD alone is 65 R_E , within the confines of a region with dimensions of about 1 R_E . This particular

result demonstrates clearly the capabilities of a rotational electric field, which are quite different from those of an electrostatic field. After point D the electron again gains energy from both the drift and the gyrotational motions.

To study field-aligned acceleration, particles were launched slightly above the neutral sheet (where $E_n \neq 0$) in the regions where the field lines were connected to the earth. The picture of precipitation at the substorm onset bore out Fukunishi's (1975) finding (Fig. 19). In a typical substorm, the estimated area of electron precipitation exceeding 5 keV at the ionospheric level on the evening side is about $400 \times 200 \text{ km}^2$, which would almost fill an all-sky photograph (diameter around 500 km). This agrees well with observations of auroral break-up.

8. THREE-DIMENSIONAL CURRENTS ASSOCIATED WITH SUBSTORM ONSET

The actual onset of auroral breakup and the expansion phase of the substorm, including the development of field-aligned currents, must involve the response of the plasma in the plasma sheet, and also in the ionosphere. They are extremely difficult to analyze in detail, and we will discuss them here only in outline. However, when cause and effect relationships are properly noted, we believe that understanding the sequence of events is not difficult in principle.

It is our hypothesis that substorm phenomena stem from the escape of energized plasma from closed field lines in the plasma sheet, away from the earth. That such an escape might be possible is shown by a careful consideration of the virial theorem; it says that an energized plasma cannot be held together by electromagnetic fields of its own

making. We believe that this escape will at first involve an outward current meander, most likely associated with an ion-tearing instability (Schindler, 1974; Galeev, 1979). It certainly is not reconnection since there is no neutral line at this time. This current meander will induce an electric field, always opposing the current perturbation, so that with an outward meander the induction electric field will be from dusk to dawn. Because there is an electrostatic field in the opposite sense, a weak meander is not sufficient; this is consistent with the finding of Galeev and Zelenyi (1976) that the cross-tail field stabilizes the instability. However, with sufficiently strong meander the induction electric field is overwhelming, and $\underline{E} \times \underline{B}$ flow is outward, still on closed field lines. An intensifying and spreading current perturbation is involved. Such an explosive development has been considered by others, e.g. Galeev et al. (1978).

Next we will consider the generation of field aligned currents. There are two different Birkeland current systems, the large-scale Birkeland current sheets and the auroral current filaments observed most clearly at the onset of a substorm. The treatment of field-aligned currents in the literature is often confusing because, in many cases, large-scale currents have not been separated from storm currents. These currents are quite different in origin and production mechanisms, and the physical and numerical models developed to study their ionospheric

effects should take into account the differences in their scales, strengths, and dynamic properties.

We will not discuss the production mechanism of large-scale steady-state Birkeland current sheets. Several studies, both theoretical and experimental, have been made of these currents during 1970's (see e.g. Potemra 1979 for review).

The substorm current system is often attributed to a short circuiting of the current in the neutral sheet through the ionosphere along magnetic field lines (e.g. Boström, 1964; Clauer and McPherron, 1974). The mechanism responsible for the disruption of the tail current has not been treated adequately in the literature. A simple short-circuiting is too narrow a concept, because the particles on the magnetic field lines do experience an upward force, namely the mirror force $-\mu VB$. Therefore, divergent magnetic field lines in a conducting plasma cannot be regarded as infinite conductors. A force must be involved to get the current carriers down the field lines. Pellinen (1979a) discussed our mechanism qualitatively, presenting a description of the whole three-dimensional current system associated with substorm onset.

According to the model presented in Section 6 there are parallel induced electric field components (E_{\parallel}^i) along magnetic field lines outside the neutral sheet. This E_{\parallel}^i accelerates electrons and ions along the field lines (Section 7). Thus a net current (the effect) due to the meandering currents in the neutral sheet (the cause) can be observed along the field lines (Fig. 16).

The temporal development of the electric field at any arbitrary

field point leads to polarization currents which tend to prevent changes of \underline{E} in the plasma. The macroscopic behaviour of the plasma cloud perpendicular to \underline{B} is similar to the reaction of dielectric media, while the effect parallel to \underline{B} depends on inertial forces (i.e. the inertia of the plasma particles).

In front of and on the sides of the expanding current disturbance, where $\underline{E} \perp \underline{B}$, polarization currents may flow in regions where \underline{B} is almost unchanged. These currents are directed along $\partial \underline{E} / \partial t$ which means, e.g., that the polarization current \underline{J}_y^P opposes the crosstail current J_z (Fig. 16) on the outer edge of the disturbance. Hence, the net effect of these two currents is a "current disruption". In other words, field-aligned currents must continue to flow to deliver charges to reduce E_{\parallel} , but these charges are negated by the opposite charges accumulated by \underline{J}_y^P .

To summarize, the effect of the parallel component of the induction electric field will be to accelerate particles in a cyclic pattern. At high latitudes there will be electron precipitation to the west, associated with the westward travelling surge (WTS), and a little later proton precipitation to the east. The effect of the secondary positive current meander (a consequence of Newton's third law) is to produce a proton flux on the equatorward side of the WTS, and electron precipitation to the east.

The energized electrons seem to be the natural current carriers of the upward current. However, ion inertia is too great for the ions to carry the downward current entirely, especially at first. In order to fulfil the requirement of current continuity right from the beginning of

substorm the ionosphere has to respond by sending up some electrons. In many cases even cold electrons may be adequate, as results of Klumpar (1979) suggest. The consequences of this hypothesis will be discussed in Section 10.

9. NUMERICAL MODELLING OF THE IONOSPHERIC PART OF THE SUBSTORM CURRENT SYSTEM

Opgenoorth et al. (1980) argued that the main magnetic ground perturbations observed at the substorm onset seemed to be produced by ionospheric Hall-currents, driven by ionospheric electric fields due to net charge distributions accumulated by field-aligned currents. They presented some STARE data that supported their observations but they did not model the substorm current wedge to see what type of horizontal currents connected the cable-type field-aligned currents in the ionospheric E-layer. The modelling work was done by Baumjohann et al. (1981) for another event with similar characteristics. In a more recent paper the expansion of the western part of the current system was modelled by Opgenoorth et al. (1982).

The event analyzed by Baumjohann et al. (1981) occurred on 15 February 1977 when three consecutive localized auroral activations were observed between 2100 and 2130 UT, i.e. around magnetic midnight, over Scandinavia. Combined magnetic and STARE data were used to deduce that each of these activations occurred south of the Harang discontinuity (Harang, 1946) in a region of north-westward electric field.

Fig. 20 presents data of the second auroral activation. It shows the two-dimensional distribution of the ground magnetic and ionospheric electric fields and auroral structures before (2118 UT) and during the initial brightening (2119 UT), and during the maximum development of the sudden auroral activation (2120:30 UT). The data presented in the 2119 UT and 2120:30 UT panels were used for the numerical modeling. Below we will review the essential parts of their work.

For the numerical modeling the ionosphere was divided into small cells, each measuring 50 x 50 km. For each cell the height-integrated Hall and Pedersen conductivities and the electric field were given, and the height-integrated ionospheric current was computed according to the Ohm's law. The current flowing nearly vertically along the field line out of each cell was determined from the divergence of the horizontal currents in order to preserve current continuity everywhere in the three-dimensional system.

The model electric field data was derived from the measured STARE data as follows: the quiet-time electric field at 2118 UT (cf. Fig. 20) was extrapolated to the south, east and west. A southward polarization electric field was then added in the region covered by active aurora to fit the electric field measurements made in the STARE observation area at 2119:00 and 2120:30 UT (see Fig. 20), and was likewise extrapolated to the south, east and west. Since the magnetic field observed at 2118 UT was very weak, it was assumed that the height-integrated conductivities outside the active regions were close to zero. Optical auroral data were used to deduce the conductivity profiles (details given in Baumjohann et al., 1981). By varying the extrapolations of the southward polari-

zation electric field and the height-integrated Hall and Pedersen conductivities in the active regions, the current systems were fitted to the magnetic fields observed at 2119:00 and 2120:30 UT (cf. Fig. 20) by trial and error. Here we will reproduce the calculations at 2119:00. The spatial distributions of the height-integrated Hall and Pedersen conductivities, total ionospheric electric fields, height-integrated ionospheric current densities, and field-aligned current intensities are given in Fig. 21. Also shown are the spatial distributions of the ground-equivalent current vectors attributable to the field-aligned currents (Fig. 21c) and the total three-dimensional currents (Fig. 21f). As can be seen in comparing Fig. 21f with the respective panel in Fig. 20, the model current systems reproduce all the essential features in the observed data. The remaining differences can probably be attributed to some outstanding ambiguities in the extrapolation of the electric field outside the STARE observation area, possibly to the assumed conductivity distributions, and to the hypothesis that the height-integrated conductivities are zero outside the regions covered by active aurora.

The results led to the following conclusions. The model ionospheric currents (Fig. 21c) are directed mainly westward and are concentrated in the western half of the active region, where also the highest conductivities are found. The current densities of 600 to 700 μAm^{-1} are comparable to those reported by Sulzbacher et al. (1980) and Baumjohann and Kamide (1980) for the Hall-current westward electrojet. Most of the current, i.e., the westward component, is closed by very localized and intense upward field-aligned currents at the western edge (about 7 μAm^{-2} , probably carried by energetic electrons; e.g. Akasofu et al., 1969; and

Kamide and Rostoker, 1977) and less intense (about $2 \mu\text{Am}^{-2}$) and more widespread downward field-aligned current in the eastern third of the break-up region (see Fig. 21d). Only about 25% of it flows northwards and is closed by the field-aligned sheet currents at the southern and northern boundaries of the active region. Thus, the model ionospheric current is not an ideal Cowling current in which no field-aligned currents flow at the northern and southern boundaries, but it is consistent with the more realistic case discussed by Coroniti and Kennel (1972), in which the northern and southern field-aligned sheet currents cannot exceed a critical level (about $2 \mu\text{Am}^{-2}$ in this model). The temporal development matches that of the conductivities and polarization electric field; a north-west expansion mainly of ionospheric currents and upward field-aligned currents.

The numerical values of the model current systems are valid only for the second break-up, but a comparison with the data from the other two activations shows that the general features are in agreement with the data treated here.

In conclusion, the model current system presented by Baumjohann et al. (1981) is in general agreement with the classical concept of the substorm current wedge (e.g. Akasofu and Meng, 1969; McPherron et al., 1973). Thanks to the higher and two-dimensional spatial resolution of the magnetic data and the utilization of the STARE electric field data the following facts can be added to this concept. The ionospheric current connecting the two field-aligned current regions is mainly of Cowling type; the current wedge is restricted not only latitudinally but also longitudinally, at least during the initial moments; the upward

field-aligned current is concentrated at the western edge of the active region and its density is higher than the widespread downward field-aligned currents. These results are in agreement with the field-aligned current circuit presented in Section 8.

Opgenoorth et al. (1982) studied the expansion of the western edge of the current wedge. They found that the cable-type structure of the upward flowing field-aligned current is preserved and propagates within the leading edge of the westward travelling surge. Fig. 22 shows the result of their model calculation. The trailing edge of the WTS is surrounded by ionospheric Hall currents while a Cowling-type current channel (where the westward electrojet is a combination of Hall and Pedersen currents) follows in the wake of the WTS. The result is in excellent agreement with Baumjohann et al. (1981). In Opgenoorth et al. (1982) conductivity could also be checked due to rocket observations in the wake of the surge.

10. DISCUSSION

Some discussion has already been presented in the previous sections; here the aim is to relate our work to some recently published articles and to discuss the new views on substorm mechanisms. From our own work we shall also point out some interesting details that are still speculative and need further supporting observations in order to be confirmed. The presentation follows the sequence of the sections in the paper.

Are the substorm phases internally or externally controlled?

In Sections 4 and 5 we gave the impression that purely internal controlling mechanisms operating in the magnetotail lead to substorm onset. However, several studies give evidence that both discontinuities in the solar wind pressure (SSC triggering, see e.g. Kokubun et al., 1977) and changes in the direction of the interplanetary magnetic field (IMF) (see

e.g. Caan et al., 1977) may cause substorm triggering. In a series of articles Akasofu (e.g. Akasofu, 1981) claims that the properties of the solar wind (IMF and speed) are mainly responsible for substorm development by a driven process. Hence, according to Akasofu there should be no significant energy storage in the magnetotail prior to substorm onset. In order to study this question in more detail Pellinen et al. (1982) made an event study where the growth and trigger phase signatures were clearly distinguished, and where the solar wind data were available. Details of the trigger phase of this event were given in Sections 2 and 5. Here we will mainly concentrate on the IMF related aspects.

A sudden southward turning of the IMF immediately led to a worldwide convection enhancement (growth phase) which was observed to start almost simultaneously at stations within the auroral zone and polar cap. After 35 minutes from the southward turning a localized substorm onset took place in the midnight sector. The onset was preceded by a 8 minutes long trigger phase.

The energy coupling between solar wind and magnetosphere during the pre-substorm phases was studied by utilizing the energy coupling function $\epsilon = V E^2 \sin^4(\phi/2) 10^2$ defined by Perreault and Akasofu (1978). Some other parameters may yield equally good correlations (such as $V B_z$, see Baker et al., 1981), but here we will concentrate on ϵ . In this particular event the ϵ values appeared to be above the substorm level ($> 10^{11}$ W) during the growth phase (Fig. 23). A good correlation between ϵ and the growth of the Joule heating rate (estimated from the AE data) was found in the beginning, but during the last 20 minutes before substorm triggering ϵ was high while the Joule heating rate (magnetic disturbance) showed a slight decrease. However, this decrease was so small that we can take the view that both ϵ and the Joule dissipation were approximately constant for half an hour before the onset of the expansion phase.

Energy going into the plasma in the plasma sheet must have been at least 10^{12} watts that was given by Heikkila et al. (1979) for average conditions. Since the Joule dissipation was about two orders of magnitude less we must conclude that most of the extra energy was stored in the magnetotail. In view of observations that during the period before onset the magnetosphere becomes more tail-like (Camidge and Rostoker, 1970; Fairfield and Ness, 1971), we are led to the conclusion that conditions approached thermodynamic equilibrium, with some of the energy appearing as energized particles, and some as magnetic energy associated with the tail-like field. This argues against a driven process, and for the existence of a growth phase of half an hour. Similar arguments have been presented by Mishin (1978) and Fairfield et al. (1981)

Nevertheless, the IMF seemed to control many of the phase changes that were observed in this event. The growth phase began within minutes of the southward turning of the IMF. It should be obvious that this event was initiated by the changed IMF; in our view, the southward turning is like throwing a switch to turn on the voltage to an unstable electronic circuit like an oscillator, or a flip-flop. In fact, we believe that the first part of the trigger phase was dependent on internal processes only, and a substorm onset would have occurred soon after.

However, during the trigger phase there was a decided change in the IMF, with a northward turning (Fig. 23). At the same time there was a change in auroral conditions within the trigger phase; this is shown most clearly by Figure 7 of Pellinen et al. (1982), by Figure 3 in this paper as a complete stopping of the electrojet and the auroral arc, and also Figure 6 as an abrupt reduction of x-rays, especially in the lower curve. Thus, we feel that the approaching onset was preempted by the IMF, and the onset of the expansion phase began immediately. Such an effect has been noticed before, and was given theoretical justification by Galeev (1979).

An entirely different sequence of events was observed by Sauvaud & Treilhou (private communication) for the event of 4 March 1979 at 22 to 23 UT with a similar variation in the IMF. In their case the IMF also had a brief northward excursion, but only a minor perturbation in the plasma sheet was observed. The IMF then returned to southward for 30 minutes, and the onset was observed during this interval, 20 minutes after the northward turning. Apparently in that case the conditions in the plasma sheet were not ready for a breakup.

One should not make too far-reaching conclusions from the data of a few events; one needs better statistics. However, we cannot avoid the fact that even a single event, if it is well enough treated, may provide essential information about some more universal mechanisms. Hence, in order to recognize these mechanisms and to get a final answer to the question of internal or external triggering the problem has to be studied more extensively in the future.

Substorm Triggering

The theory by Pellinen and Heikkila described in this paper does not present analytical details of the triggering mechanism itself. Only the asymptotic behavior of cross-tail current during growth and trigger phases is described after which the treatment jumps directly to the onset phenomena. Tailward flow of plasma is taken as an initial observation; the causal relation to the triggering moment is not given. All theoretical arguments are supported by observations as can be seen in the previous Sections. The existence of an induced electric field at all stages of substorm development is emphasized in the theory.

The so-called tearing mode instability (e.g. Schindler, 1974; Galeev, 1979) appears to be a promising candidate to explain the substorm triggering. Recently the studies of explosive tearing mode instability (Birn and Hones, 1981; Terasawa, 1981) have been developed to the point

that a comparison between our work and the MHD-based tearing mode studies can be made; these show some interesting common features, even if the basic philosophies between these two theories are quite different.

The main shortcoming of some earlier tearing mode instability studies

was their two-dimensional treatment. Since the nature of the substorm phenomena is basically three-dimensional, many of the well-known substorm features were not reproduced in two-dimensional studies. Here we will compare and contrast the work by Birn and Hones (1981) with our results.

They assumed plasma sheet thickening towards the flanks of the tail, and found that the reconnection region is limited in the y direction. Increased plasma flows are observed before the neutral lines form because of the enhanced resistivity they assumed in their model. The neutral X-line is found to be a dividing line between the regions with oppositely directed strong flow. Also they found that the X-line is the only neutral line where the cross-tail electric field increases to large values. However, Birn and Hones did obtain localized inductive electric fields in their calculations, and tailward $\underline{E} \times \underline{B}$ drift in regions of northward B_z . This puts our model on a firm basis, since we assumed such flow at the outset. We also assumed that the flowing plasma would carry the cross-tail current with it, to form a strengthening meander. With these assumptions the properties of the induction electric field are clearly elucidated. We take the view that the induction electric field is the driving force for the plasma, drawing its energy from the magnetic field (this is obvious since $\partial(B^2/2\mu_0)/\partial t$ is $\underline{H} \cdot \partial \underline{B}/\partial t$ and $\partial \underline{B}/\partial t$ is the source of the induction electric field by equation 3.7).

Birn and Hones (1981) also found field-aligned currents with the same sense as region 2 currents (Tajima and Potemra, 1976) as an output of their calculations. The source region of these currents differ from our model since their currents originate on the earthward side of the X-line while our currents are located in the regions mapping to the tailward side. Thus, their calculations do not lead to a disruption of the tail current into field-aligned currents. This feature in their model is quite distinct from ours; the action of E_{\parallel}^{ind} in our model gives the correct sense of the field aligned currents, with the closure current being a Cowling-type chan-

nel formed in the ionosphere.

According to Birn and Hones (1981) the regions around neutral lines form magnetic islands (plasmoids) (see also Terasawa, 1981) that move tailwards with high speeds. We have not studied this aspect in detail since our model is valid only for the very few seconds following the onset. However, our magnetic bubble does grow in size, because $\underline{E} \times \underline{B}$ drift is explosive (Heikkila and Pellinen, 1977, p. 1612). In addition, the net force on the plasmoid is outward due to a repulsive force $\underline{F} = -\mu \nabla B$ away from the earth (see p. 1613).

Particle acceleration near magnetic neutral lines

In our model a continuous neutral line of both X and O-type is formed in the neutral sheet region. A similar type of geometry was suggested by Vasyliunas (1976). In both models the area surrounded by neutral line is growing as the substorm disturbance proceeds. In our model all neutral lines play an important role in the particle energization mechanism. Local E-fields are especially strong along the X and O-type neutral lines in the cross-tail direction. The E-field is directed from dawn to dusk along the X-line while along the O-line the direction is opposite. This leads to some asymmetries in the production of high-energy particles.

In the literature (mainly in connection with the different reconnection theories) X-type neutral line is referred as the main accelerator of charged particles. However, it may seem reasonable that an O-type neutral line region is even more effective as a particle accelerator (Stern, 1979); magnetic field lines around an O-line are closed, hence particles may remain trapped in the bubble for longer times. O-line, according to Stern (1979), keeps particles better contained than the X-type line. Like many other authors he assumes that the inductive E-field is a large-scale one extending over the magnetotail from dawn to dusk. He considers only linear acceleration along O-line which means that unreasonably high E-field values

have to exist along the line to produce particles in the MeV range. This problem was pointed out by Vasyliunas (1960) who showed that the integral of the electric field along the full length of the O-line cannot exceed a value equal to the cross-tail potential derived by Alfvén (1968). Hence the maximum energy which can be gained by a charged particle that drifts along the full length of the O-line is not much larger than the energy of particles drifting through the magnetic field reversal in the neutral sheet.

In fact, Stern (1979) assumed an electric field in the same sense as the current; when the induction electric field is taken into account that sense is not correct. Instead of being a load, the current now becomes a generator. The sense of the $\underline{V} \times \underline{B}$ forces on runaway particles is such as to disperse the particles away from the O-line, rather than to focus them as stated by Stern. Thus, it appears that a moving O-line is not an efficient accelerator, unlike an X-line where a few particles are accelerated to very high energies, in agreement with Birn and Hones (1981).

Terasawa and Nishida (1976) reported that bursts of relativistic electrons are nearly centered at the focus of the magnetic loop structure where the polarity of B_z turns from northward to southward. They inferred that these bursts of relativistic electrons are accelerated on the neutral line (O-type or X-type) connected to the magnetic loop structure. These authors accept the view that inductive E-fields are involved, but as Nishida (1976) reported electric field values of 80 mV/m are required to accelerate electrons up to 0.5 MeV along a $1 R_E$ long straight line. As shown earlier, such values are unphysical and lack experimental evidence. Quite a few theoretical and experimental papers have been written on

induced E-fields (see e.g. review by Kim et al., 1979) but they all predict or report E-fields that are only a few mV/m (less than 10 mV/m).

Combination of linear and betatron acceleration as the main mechanism for high-energy particle production in solar flares has been proposed by Bulanov and Sasorov (1975). Their mechanism is quite the same as ours: localized induced E-fields appear close to magnetic neutral lines where the non-adiabatic linear acceleration is followed by magnetic drift away from the line. The high magnetic moment value, induction field geometry and rotational property of the E-field leads to powerful adiabatic acceleration of the particle. No high E-field values are required, the geometry is as (or even more) important.

Substorm current system

As the last topic in the Discussion section we return back to the substorm current circuit. As shown in Sections 8 and 9 the understanding of the substorm current wedge has developed considerably since the start of the IMS in 1976. In the recent COSPAR meeting report Baumjohann (1982) summarized the present status on this field and gave an impression that current systems related to substorm auroras are well known today. However, there still seems to be at least one gap in knowledge, a gap that is important for the Pellinen and Heikkila substorm mechanism, and that is: What are the carriers of the downward field-aligned current above the ionosphere during the first few minutes after substorm onset? As stated by Pellinen and Heikkila (1978) protons are much slower than electrons, and hence protons cannot contribute to the downward field-aligned current immediately after the onset. However, the counterclockwise and clockwise DEC loops (related to upward and downward field-aligned currents respectively,

Section 2) start to develop simultaneously which means that there must be additional current carriers involved in order to maintain current balance.

Opgencorth et al. (1980) threw some light to the above dilemma. They studied the development of the 486.1 (H_{β}) and 630.0 nm emission lines (Fig. 24) in the region of clockwise DEC-vector rotation. The excitation moments of the two emissions became approximately comparable by shifting the 630.0 nm curve 110 sec towards earlier times according to the average delay in the emission of this particular wavelength. Fig. 24 shows that the rise in the H_{β} -emissions is preceded by a shortlived peak of red auroral emission which certainly is related to the substorm onset. The entire photometric data set (not shown here) reveals that, in contrast to the H_{β} -emissions this peak is at the observing site (Kiruna) only seen from 40° to 90° N elevation. If one compares this observation with DEC vector rotations (Section 2) it seems as if the red emissions are restricted to the initial area of downward FAC while the later observed proton-emissions correspond in time and location to the final area of downward FAC which has clearly widened and spread out further to the south.

According to Klumpar et al. (1976), Kamide and Rostoker (1977), and Klumpar (1978), the downward equivalent current is carried to a large extent by upward going ionospheric electrons of lower energy. Hence, the photometer observations together with the ground signatures of localized downward FAC give rise to some questions. It may be possible that the red auroral emission that usually come from heights greater than 200 km (Vallance Jones, 1976) have in this case been excited by upward going electrons. If this happens to be the case, it would suggest that the necessary upward directed field-aligned acceleration mechanism for

ionospheric thermal electrons is related to the positive charge of the cloud of energized protons arriving from the magnetotail, for the red auroral peak is observed to decrease when the protons arrive at the ionosphere. In some cases the downward current may be due to runaway electrons, implying a voltage drop of several tens of volts along ionospheric field lines (Klumppar and Heikkila, 1982). However, the answer to these questions has to be postponed until some better observations are available.

In summary, we believe that a substorm is caused by the escape (or attempted escape) of plasma that is being strongly energized in the plasma sheet, plasma on closed field lines contained by a magnetic bottle. That such an escape is likely to occur follows directly from the virial theorem of plasma physics, which shows that no self-containment is possible (Schmidt, 1976). A reversal of the electric field must be involved for reversed $\underline{E} \times \underline{B}$ drift, and that reversal can be accomplished by an outward meander of a cross-tail current filament. Such a meander can be caused by an ion-tearing mode instability. It certainly is not reconnection, since there is initially no magnetic neutral line. The action of the induction electric field is explosive, and does lead to formation of a neutral line, a natural accelerator for cosmic plasmas, and an escaping plasmoid. The various features of the auroral breakup follow immediately (at least in principle) from the changing electromagnetic field. The complication is only a quantitative one. We present one final figure (Fig. 25) which shows an ISIS photograph above compared to ground based observations below, in complete agreement with our simple ideas.

Acknowledgements

WJH acknowledges support by NSF grant ATM80-25/94 and a grant from the Swedish Natural Science Research Council.

References

- Akasofu, S.-I.: 1964, Planet. Space Sci. 12, 273.
- Akasofu, S.-I., Kimball, D. S., and Meng, C.-I.: 1965, J. Atmospheric Terrest. Phys. 27, 173.
- Akasofu, S.-I.: 1968, Polar and Magnetospheric Substorms, D. Reidel Publ. Comp., Dordrecht.
- Akasofu, S.-I., Eather, R. H., and Bradbury, J. N.: 1969, Planet. Space Sci. 17, 1409.
- Akasofu, S.-I. and Meng, C.-I.: 1969, J. Geophys. Res. 74, 293.
- Akasofu, S.-I.: 1974, Space Sci. Rev. 16, 617.
- Akasofu, S.-I.: 1980, Planet. Space Sci. 28, 933.
- Akasofu, S.-I.: 1981, Space Sci. Rev. 28, 121.
- Akasofu, S.-I. and Kan, J. R. (editors): 1981, Physics of Auroral Arc Formation, American Geophysical Union, Washington, D. C.
- Alfvén, H. and Fälthammar, C.-G.: 1963, Cosmical Electrodynamics, Fundamental Principles, 2nd Edition. Clarendon Press, Oxford.
- Alfvén, H.: 1968, J. Geophys. Res. 73, 4379.
- Alfvén, H.: 1976, J. Geophys. Res. 81, 4019.
- Alfvén, H.: 1977, Rev. Geophys. Space Phys. 15, 271.
- Alfvén, H.: 1981, Cosmic Plasma, D. Reidel Publ. Comp., Dordrecht, 37.
- Anderson, K. A.: 1965, J. Geophys. Res. 70, 4741.
- Axford, W. I and Hines, C. O.: 1961, Can. J. Phys. 39, 1433.
- Axford, W. I.: 1969, Rev. Geophys. 7, 421.
- Baker, D. N., Hones, E. W., Jr., Payne, J. B., and Feldman, W. C.: 1981, Geophys. Res. Lett. 8, 179.
- Baumjohann, W. and Kamide, Y.: 1981, J. Geomag. Geoelectr. 33, 297.
- Baumjohann, W., Pellinen, R. J., Opgenoorth, H. J., and Nielsen, E.: 1981, Planet. Space Sci. 29, 431.

- Baumjohann, W.: 1982, Ionospheric and field-aligned current systems in the auroral zone: a concise review, Invited paper (C.2.3.1) COSPAR XXIV, OTTAWA
- Beard, D. E., Bird, M., and Huang, T. H.: 1970, Planet. Space Sci. 18, 1349.
- Belian, R. D., Baker, D. N., Hones, E. W. Jr., Higbie, P. R., Bame, S. J., and Asbridge, J. R.: 1981, J. Geophys. Res. 86, 1415.
- Birn, J. and Hones, E. W., Jr.: 1981, J. Geophys. Res. 86, 6802.
- Boström, R.: 1964, J. Geophys. Res. 69, 4983.
- Brice, N. M.: 1967, J. Geophys. Res. 72, 5193.
- Bryant, D. S., Hall, D. S., Lepine, D. R., and Mason, R. W.: 1977, Nature 266, 148.
- Bryant, D. S.: 1981, Rocket studies of particle structure associated with auroral arcs, in Physics of Auroral Arc Formation, S.-I. Akasofu and J. R. Kan (ed.), Geophysical Monograph 25, 103, American Geophysical Union, Washington, D.C.
- Bulanov, S. V. and Sasorov, P. V.: 1975, Astronomical Journal 52:4, 763, (in Russian).
- Caan, M. N., McPherron, R. L., and Russell, C. T.: 1973, J. Geophys. Res. 78, 808.
- Caan, M. N., McPherron, R. L., and Russell, C. T.: 1977, J. Geophys. Res. 82, 4837.
- Camidge, F. P. and Rostoker, G.: 1970, Can. J. Phys. 48, 2002.
- Carbary, J. R. and Krimigis, S. M.: 1979, J. Geophys. Res. 84, 7123.
- Chapman, S. and Ferraro, V. C. A.: 1931, Terr. Mag. Atmosph. Elec. 36, 77.
- Clauer, C. R. and McPherron, R. L.: 1974, J. Geophys. Res. 79, 2811.
- Coroniti, F. V. and Kennel, C. F.: 1972, J. Geophys. Res. 77, 3361.
- Cowley, S. W. H.: 1978, Planet. Space Sci. 26, 539.
- Cragin, B. L. and Heikkila, W. J.: 1981, Rev. Geoph. Space Phys. 19, 223.
- DeForest, S. E. and McIlwain, C. E.: 1971, J. Geophys. Res. 76, 3587.
- Dungey, J. W.: 1961, Phys. Rev. Letters 6, 47.
- Dungey, J. W.: 1963, J. Geophys. Res. 68, 3540.

- Fairfield, D. H. and Ness, N. F.: 1970, J. Geophys. Res. 75, 7032.
- Fairfield, D. H., Lepping, R. P., Hones E. W., Jr., Bame, S. J., and
Asbridge, J. R.: 1981, J. Geophys. Res. 86, 1396.
- Fennell, J. F.: 1970, J. Geophys. Res. 75, 7048.
- Fukunishi, H.: 1975, J. Geophys. Res. 80, 533.
- Galeev, A. A. and Zelenyi, L. M.: 1976, Sov. Phys. JETP 43, 1113.
- Galeev, A. A., Coroniti, F.V., and Ashour-Abdalla, M.: 1978, Geophys.
Res. Lett. 5, 707.
- Galeev, A. A.: 1979, Space Sci. Rev. 23, 411.
- Greenwald, R. A., Weiss, W., Nielsen, E., and Thomson, N. R.: 1978,
Radio Sci. 13, 1021.
- Heikkila, W. J.: 1973, Astrophys. Space Sci. 23, 261.
- Heikkila, W. J.: 1974, J. Geophys. Res. 79, 2496.
- Heikkila, W. J. and Pellinen, R. J.: 1977, J. Geophys. Res. 82, 1610.
- Heikkila, W. J.: 1978, Planet. Space Sci. 26, 121.
- Heikkila, W. J., Pellinen, R. J., Fälthammar, C.-G., and Block, L. P.: 1979,
Planet. Space Sci. 27, 1383.
- Heikkila, W. J.: 1981, Formation of auroral arcs by plasma sheet processes,
in Physics of Auroral Arc Formation, S.-I. Akasofu and J. R. Kan
(ed.), Geophysical Monograph 25, 266, American Geophysical Union,
Washington, D. C.
- Heikkila, W. J.: 1982, Geophys. Res. Lett. 9, 159.
- Hill, T. W.: 1974, Rev. Geoph. Space Phys. 12, 379.
- Hines, C. O.: 1963, Planet. Space Sci. 10, 239.
- Hones, E. W., Jr., Lui, A. T. Y., Bame, S. J. and Singer, S.: 1974, J. Geophys.
Res. 79, 1385.
- Hones, E. W., Jr., Palmer, I. D., and Higbie, P. R.: 1976, J. Geophys. Res.
81, 3366.

- Hultqvist, B., Borg, H., Riedler, W., and Christophersen, P.: 1971, Planet. Space Sci. 19, 279.
- Iijima, T. and Potemra, T. A.: 1976, J. Geophys. Res. 81, 5971.
- Kamide, Y. and Rostoker, G.: 1977, J. Geophys. Res. 82, 5589.
- Kan, J. R.: 1982, Space Sci. Rev. 31, 71.
- Kim, J. S., Graham, D. A., and Wang, C. S.: 1979, Rev. Geoph. Space Phys. 17, 2049.
- Kirsch, E., Krimigis, S. M., Sarris, E. T., Lepping, R. P., and Armstrong, T. P.: 1977, Geophys. Res. Lett. 4, 137.
- Kirsch, E., Krimigis, S. M., Sarris, E. T., and Lepping, R. P.: 1981, J. Geophys. Res. 86, 6727.
- Kisabeth, J. L. and Rostoker, G.: 1973, J. Geophys. Res. 78, 5573.
- Klumpar, D. M., Burrows, J. R., and Wilson, M. D.: 1976, Geophys. Res. Lett. 3, 395.
- Klumpar, D. M.: 1979, J. Geophys. Res. 84, 6524.
- Klumpar, D. M. and Heikkila, W. J.: 1982, Geophys. Res. Lett. 9, 873.
- Kokubun, S., McPherron, R. L., and Russel, C. T.: 1977, J. Geophys. Res. 82, 74.
- Krall, N. A. and Trivelpiece, A. W.: 1973, Principles of Plasma Physics, McGraw Hill, New York.
- Krimigis, S. M. and Sarris, E. T.: 1979, Energetic particle bursts in the earth's magnetotail, in Dynamics of the Magnetosphere (Ed. S.-I. Akasofu), 599. D. Reidel, Hingham, Mass.
- McIlwain, C.: 1974, Substorm injection boundaries, in Magnetospheric Physics (Ed. B. M. McCormac), 143, Reidel, Dordrecht.
- McPherron, R. L.: 1970, J. Geophys. Res. 75, 5592.
- McPherron, R. L., Russel, C. T., and Aubry, M. P.: 1973, J. Geophys. Res. 78, 3131.
- McPherron, R. L.: 1979, Rev. Geoph. Space Phys. 17, 657.
- Meng, C.-I.: 1971, J. Geophys. Res. 76, 862.

- Meng, C.-I.: 1981, J. Geophys. Res. 86, 4607.
- Mishin, V. M.: 1978, Aeron. 18, 961.
- Montbriand, L. E.: 1971, The proton aurora and auroral substorm, in The Radiating Atmosphere, edited by B.M. McCormac, p. 366, D. Reidel, Hingham, Mass.
- Montgomery, M. D.: 1968, J. Geophys. Res. 73, 871.
- Mozer, F. S., Torbett, R. B., Fahlsson, U. V., Fälthammar, C.-G., Gonfalone, A., and Pedersen, A.: 1978, Electric field measurements in the solar wind, bowshock, magnetosheath, magnetopause and magnetosphere. Proc. ESTEC Symposium, Innsbruck, May 1978.
- Nishida, A. and Nagayama, N.: 1973, J. Geophys. Res. 78, 3782.
- Nishida, A.: 1976, in Proceedings of the International Symposium on Solar-Terrestrial Physics June 7-18, 1976, Boulder, Colorado, 572, AGU, Washington D.C., 572.
- Northop, T. G.: 1963, Adiabatic Motion of Charged Particles, Interscience Publishers, New York.
- Oguti, T.: 1973, J. Geophys. Res. 78, 7543.
- Opgenoorth, H. J., Pellinen, R. J., Maurer, H., Küppers, F., Heikkila, W. J., Kaila, K. U. and Tanskanen, P.: 1980, J. Geophys. 48, 101.
- Opgenoorth, H. J., Pellinen, R. J., Baumjohann, W., Nielsen, E., Marklund, G., Holmgren, G., and Eliasson, L.: 1982, accepted for publication in J. Geophys. Res.
- Parker, E. N.: 1967, in Physics of Geomagnetic Phenomena, Ed. by S. Matsushita and Wallace H. Campbell, Academic Press New York and London, 1153.
- Pedersen, A. and Grand, R.: 1978, Report ESLAB No. 81, ESA.
- Pellinen, R. J.: 1978, Geophysica 15, 42.

- Pellinen, R. J. and Heikkila, W. J.: 1978a, J. Geophys. Res. 83, 1544.
- Pellinen, R. J. and Heikkila, W. J.: 1978b, J. Geophys. Res. 83, 4207.
- Pellinen, R. J.: 1979a, Planet. Space Sci. 27, 19.
- Pellinen, R. J.: 1979b: Induction model and observations of onset of magnetospheric substorms. PhD Thesis, University of Helsinki, Finland
- Pellinen, R. J., Baumohann, W., Heikkila, W. J., Sergeev, V. A., Yahnin, A. G., Marklund, G., and Melnikov, A. O.: 1982, Planet. Space Sci. 30, 371.
- Perreault, P. and Akasofu, S.-I.: 1978, Geophys. J. R. Astr. Soc. 54, 547.
- Potemra, T. A.: 1979, Rev. Geoph. and Space Phys. 17, 640.
- Pytte, T., Trefall, H., Kremser, G., Jalonen, L., and Riedler, W.: 1976a: J. Atmos. Terr. Phys. 38, 739.
- Pytte, T., McPherron, R. L., and Kokubun, S.: 1976b: Planet. Space Sci. 24, 1115.
- Pytte, T.: 1976. Scientific/Technical Rep. No. 96, Dep. of Physics, Univ. of Bergen, Norway.
- Robert, P., Gendrin, R., Ferraut, S., Roux, A., and Pedersen, A.: 1982, Geos-2 identification of fast moving current tubes in the equatorial region of the magnetosphere during substorms. Submitted in J. Geophys. Res.
- Roederer, J. G.: 1970, Dynamics of Geomagnetically Trapped Radiation, Springer-Verlag Berlin Heidelberg New York.
- Rostoker, G. and Camidge, F. P.: 1971, J. Geophys. Res. 76, 6944.
- Sarris, E. T., Krimigis, S. M., and Armstrong, T. P.: 1976a, J. Geophys. Res. 81, 2341.
- Sarris, E. T., Krimigis, S. M., Iijima, T., Bostrom, C. G., and Armstrong, T. P.: 1976b, Geophys. Res. Lett. 3, 437.
- Schmidt, G.: 1966, Physics of High Temperature Plasmas: an Introduction. Academic Press, New York, USA.
- Schindler, K.: 1974, J. Geophys. Res. 79, 2803.
- Semenov, V. S. and Sergeev, V. A.: 1981, Planet. Space Sci. 29, 271.

- Shawhan, S. D.: 1979, Rev. Geophys. Space Phys. 17, 705.
- Snyder, A. L. and Akasofu, S.-I.: 1972, J. Geophys. Res. 77, 3419.
- Sonnerup, B. U. O.,: 1979, Magnetic field reconnection, in Space Plasma Physics: The Study of Solar-System Plasmas, p. 879-972, C. F. Kennel et al., eds., North Holland Pub.
- Starkov, G. V., Raspopov, O. M., and Uspensky, M. V.: 1979, Report PGI 79-6 Polar Geophysical Institute, Apatity, USSR.
- Stern, D. P. and Palmadesso, P.: 1975, J. Geophys. Res. 80, 4244.
- Stern, D. P.: 1979, J. Geophys. Res. 84, 63.
- Sulzbacher, H., Baumjohann, W., and Fofemra, T. A.: 1980, J. Geophys. Res. 48, 7.
- Swift, D.: 1981, Rev. Geophys. Space Phys. 19, 185.
- Terasawa, T. and Nishida, A.: 1976, Planet. Space Sci. 24, 855.
- Terasawa, T.: 1981, J. Geophys. Res. 86, 9007.
- Ullaland, S., Ejordal, J., Block, L.P., Bronstad, K., Iversen, I. B., Kangas, J., Korth, A., Kremser, G., Madsen, M. M., Moe, T., Riedler, W., Stadsnas, J., Tanskanen, P., and Torkar, K. M.: 1981, Adv. Space Res. 1, 273.
- Untiedt, J., Pellinen, R., Küppers, F., Opgenoorth, H. J., Pelster, W. D., Baumjohann, W., Ranta, H., Kangas, J., Czechowsky, P., and Heikkila, W. J.: 1978, J. Geophys. 45, 41.
- Uspensky, M. V., Pellinen, R. J., Baumjohann, W., Starkov, G. V., Nielsen, E., Sofko, G., and Kaila, K. U.: Accepted for publication in J. Geophys. 1982.
- Vallance Jones, A.: 1976, Aurora, Dordrecht, Boston: D. Reidel Publ. Comp.
- Vallance Jones, A., Creutzberg, F., Gattinger, R. L., and Harris, F. R.: 1982, J. Geophys. Res. 87, 4489.
- Vasyliunas, V. M.: 1975, Rev. Geophys. Space Phys. 13, 303.
- Vasyliunas, V. M.: 1976, in B. M. McCormac (ed.), Magnetospheric Particles and Fields, D. Reidel Publishing Company, Dordrecht-Holland, 99.

Vasyliunas, V. M.: 1980, J. Geophys. Res. 85, 4616.

Whalen, B. A. and Daly, P. W.: 1979, J. Geophys. Res. 84, 4175.

Yahnin, A. G., Sergeev, V. A., Pellinen, R. J., Baumjohann, W., Kaila, K. U.,

Ranta H., Kangas, J. and Raspopov, O. M.: Submitted for publication

in J. Geophys. 1982.

FIGURE CAPTIONS

- Fig. 1. Schematic diagram to illustrate the development of the auroral substorm. The center of the geocentric circles (80 and 60°) is the geomagnetic pole and the Sun is towards the top of the diagram. The directions of movement of the different auroral structures are indicated by arrows. (Montbriand, 1971)
- Fig. 2. Typical development in auroral absorption during substorm growth phase. Absorption decreases at Kevo while it increases at Ivalo indicating southward movement of the region of high-energy precipitation, which is mainly located on the equatorward side of auroral arc. The three vertical broken lines indicate different stages of the substorm trigger phase.
- Fig. 3. Southward movement of auroral arc, peak high-energy precipitation and westward electrojet center prior to substorm onset at 2102 UT. Variations in the IMF polarity recorded by the IMP-8 spacecraft are given in the upper right corner. Vertical broken lines indicate the trigger phase.
- Fig. 4. Total equivalent current vectors at stations within Scandinavia before, during and after the enhanced convection interval (2030-2100 UT). The equivalent current vectors originate where the corresponding magnetic disturbance was observed; squares and crosses denote negative and positive Z perturbations, respectively. The discrete auroral forms are indicated by solid lines (Pellinen et al., 1982).

- Fig. 5 A sequence of all-sky photographs illustrating the optical auroral fading prior to activation. This is the series of figures in which we identified this phenomenon. (The photographs were taken on the Airborne Ionospheric Observatory; courtesy of J. Whalen of the U.S. Air Force Geophysics Laboratory.) (Pellinen and Heikkila, 1978b)
- Fig. 6 Changes of X-ray counting rates around auroral break-up. The data were recorded by three balloons (1, 2 and 3) located in the region of substorm onset (Pellinen, 1979b).
- Fig. 7 Time sequence of equivalent current vectors (in nT) on the Earth's surface for stations at a meridional profile in the Kiruna System. The y_{KI} axis is parallel to the time axis, and the x_{KI} axis is positive upwards. The origins of the current vectors for one instant of time are spaced relative to their x_{KI} coordinates. Also shown are photographs taken by the all-sky camera at Muonio at the relevant times. (Baumjohann et al., 1981)
- Fig. 8a Differential equivalent current vectors for selected intervals during the early time of the substorm development. The vertical components are shown separately in the lower panels by isolines computed from the values recorded at the stations. The aurorae at 2223:00 UT in the central and 2226:00 UT in the right panel are indicated by solid curves and shaded areas with intensity scaling. The approximate centres of cable-type field-aligned currents are given in the panel to the left. (Opgenoorth et al., 1980)
- Fig. 8b DEC vectors 90 s and 210 s after substorm onset at 2118:30 UT. The development of the counterclockwise loop lasted 90 s while most of the clockwise loop development occurred between 90 s and 210 s. The approximate centres of cable-type field-aligned currents are given in the panel to the right.

- Fig. 9 Irregularity drift velocity vectors recorded by the STARE-system in the region of substorm onset. (Opgenoorth et al., 1980)
- Fig. 10 Energization by curvature drift is proportional to cross-tail current density times the total electric field. This can explain inverted V events, and several other features of auroral arcs. The sheet-type structure of a quiet arc can be explained by a current sheet pinch. With rapidly changing current there will be an induction electric field as well, but for quiescent arcs this can be ignored. (Heikkila, 1981)
- Fig. 11 Neutral sheet current with rectangular disturbance. The current density is depicted by the spacing of the current-flow lines. The disturbance increases linearly in amplitude and size. (Pellinen, 1979a)
- Fig. 12a Meridional components B_x and B_z of the magnetic field produced by and b the disturbed J_y current. (Pellinen, 1979a)
- Fig. 13 Changes in the magnetic field structure at $y = 0R_e$. The individual field lines have been tracked by computer. The dotted lines indicate the growth of the disturbance. The development of the X- and O-type neutral points is clearly shown on the tailward side of the disturbance. (Pellinen, 1979a)
- Fig. 14 Shapes of X-type and O-type neutral lines in the equatorial plane 15 seconds after substorm onset. (Pellinen, 1979b)
- Fig. 15 E_y and E_x depicted when $Z = 1 R_E$. The outward shifts of the field a and b maxima are due to the expansion of the disturbance. (Pellinen, 1979a)
- Fig. 16 Polarization currents J^P due to changing electric fields in the neutral sheet and due to E_n along magnetic field lines maintain the magnetospheric part of the three-dimensional current circuit associated with the substorm expansive phase.

- Fig. 17 Paths of two protons and two electrons, starting with typical plasma sheet energies near the 0- and X-type neutral lines (shown as a continuous heavy line). The solid curves are normalized to the size of the growing disturbance. The straight line path (dotted line) for one electron would involve an energy gain of only 5 keV, as compared with the actual gain of 75 keV for the tortuous path; the difference is due to the electromotive force of the induced electric field. (Pellinen and Heikkila, 1978a)
- Fig. 18 Kinetic energy and the first relativistic invariant for an electron starting near the 0 line, for a much faster rate of change of the magnetic field of 2.5 nT/s. Linear acceleration to a point A results in a large magnetic moment, after which drift and gyrobetatron acceleration can boost the energy by 1 or 2 orders of magnitude. (Pellinen and Heikkila, 1978a)
- Fig. 19a Energy contours for electrons and protons heading toward the earth.
19b The energized electron flux at high latitudes would produce the pure electron excited aurora in the westward traveling surge in an auroral break-up. A cyclic pattern of precipitation could result, as is observed during substorms. (Pellinen and Heikkila, 1978a)
- Fig. 20 Spatial distribution of equivalent current vectors on the ground (upper panel), ionospheric electric field vectors (middle panel) and auroral structures (lower panel) before, at the start of, and during the peak development of the auroral activation. The equivalent current vectors originate where the corresponding magnetic disturbance was observed; squares and crosses denote negative and positive Z perturbations, respectively. (Baumjohann et al., 1981)

- Fig. 21 Parameters of the model current system and resultant equivalent currents on the ground for the initial brightening of the aurora at 2119:00 UT: a. height-integrated Hall (square) and Pedersen (cross) conductivities; b. ionospheric electric fields; c. height-integrated ionospheric currents; d. upward (square) and downward (cross) directed field-aligned currents; e. equivalent current vectors on the ground caused by the model field-aligned currents; f. equivalent current vectors on the ground caused by the total model three-dimensional current system (squares and crosses denote positive and negative Z components). (Baumjohann et al., 1981)
- Fig. 22 Model distributions of ionospheric parameters in the vicinity of a westward travelling surge: A: Distribution of field-aligned columns of positive (cross) and negative (square) charges. B: Ionospheric electric field vectors produced by this charge distribution. C: Ionospheric height-integrated Pedersen (cross) and Hall (square) conductivities. D: Height-integrated ionospheric horizontal currents. E: Upward (square) and downward (cross) field-aligned current densities. F: Equivalent current pattern as would be detected by ground-based magnetometers from the field-aligned currents only. G: Same as F, but for the horizontal currents only. H: Total equivalent current pattern of the three-dimensional current system. (Opgenoorth et al., 1982)
- Fig. 23 Comparison of the polarity θ of the interplanetary magnetic field B_z component and the solar wind energy coupling function ϵ with variations in the worldwide electrojet development and the ionospheric Joule heating rate. (Pellinen et al., 1982)

Fig. 24 Photometric recordings of the photometer in the region of downward field-aligned current for the wavelengths 486.1 nm (H_{β}) and 630.0 nm (red O_1), with background subtracted, for a representative elevation angle of 75° N. The original curve for the 630.0 nm line has been shifted 110 s back in time to correspond to the excitation of the aurora rather than its emission. The peak in red emission is followed by enhancement in H_{β} . (Opgenoorth et al., 1980)

Fig. 25 ISIS-2 photograph of an auroral breakup on 22 December, 1971 and a schematic drawing produced by Fukunishi (see Fig. 19b) on the basis of ground-based observations. (Courtesy of C. Anger, University of Calgary)

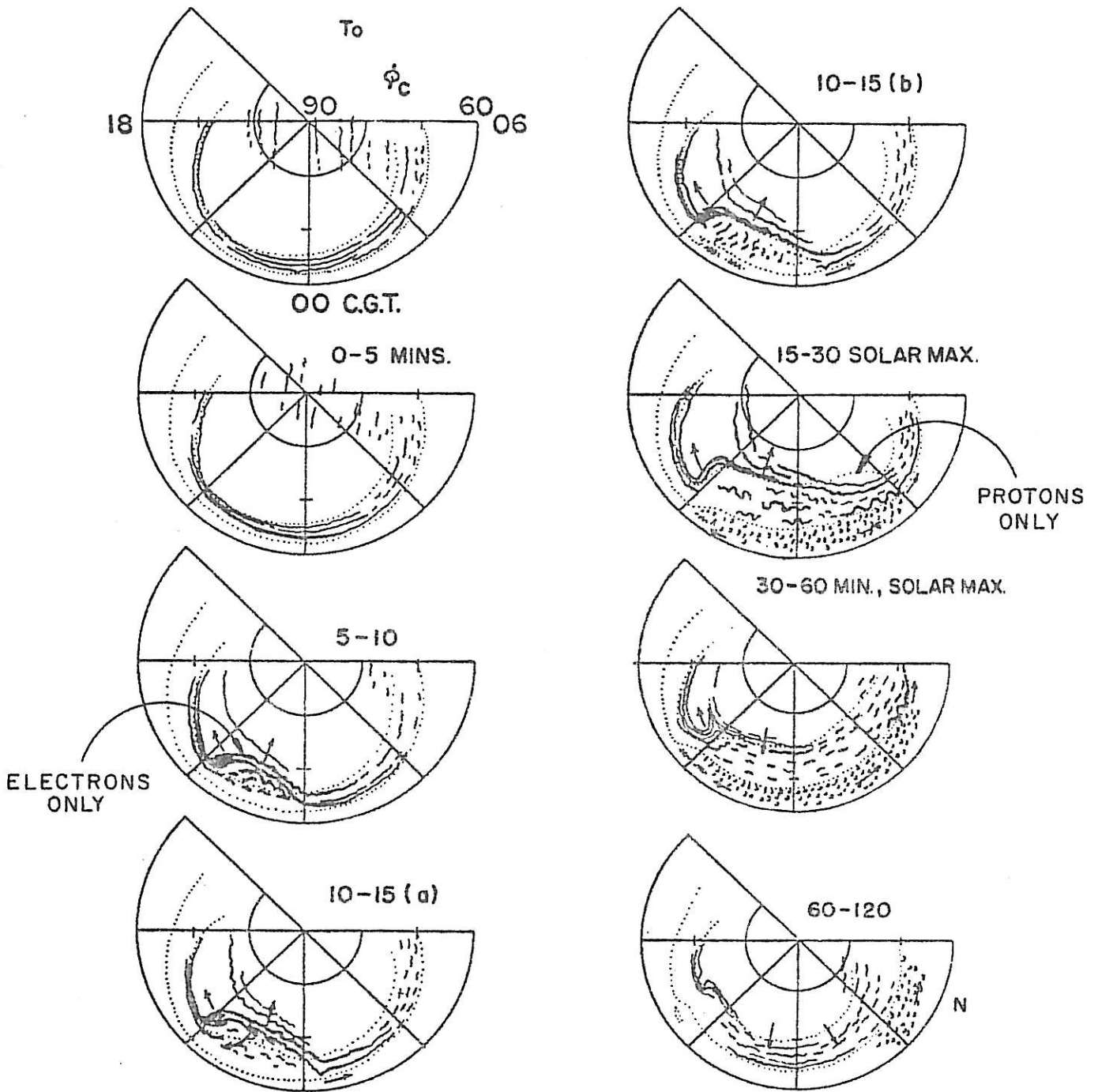


FIG 1

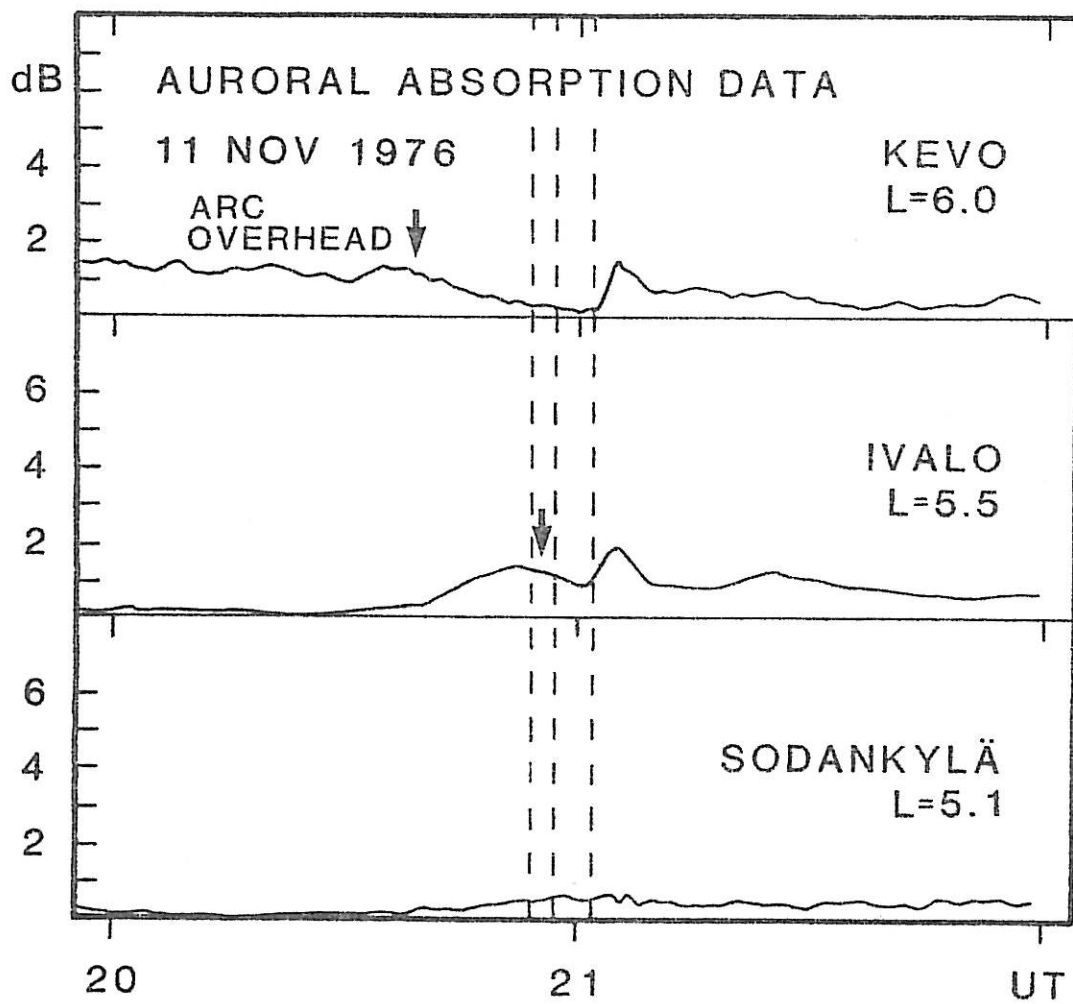
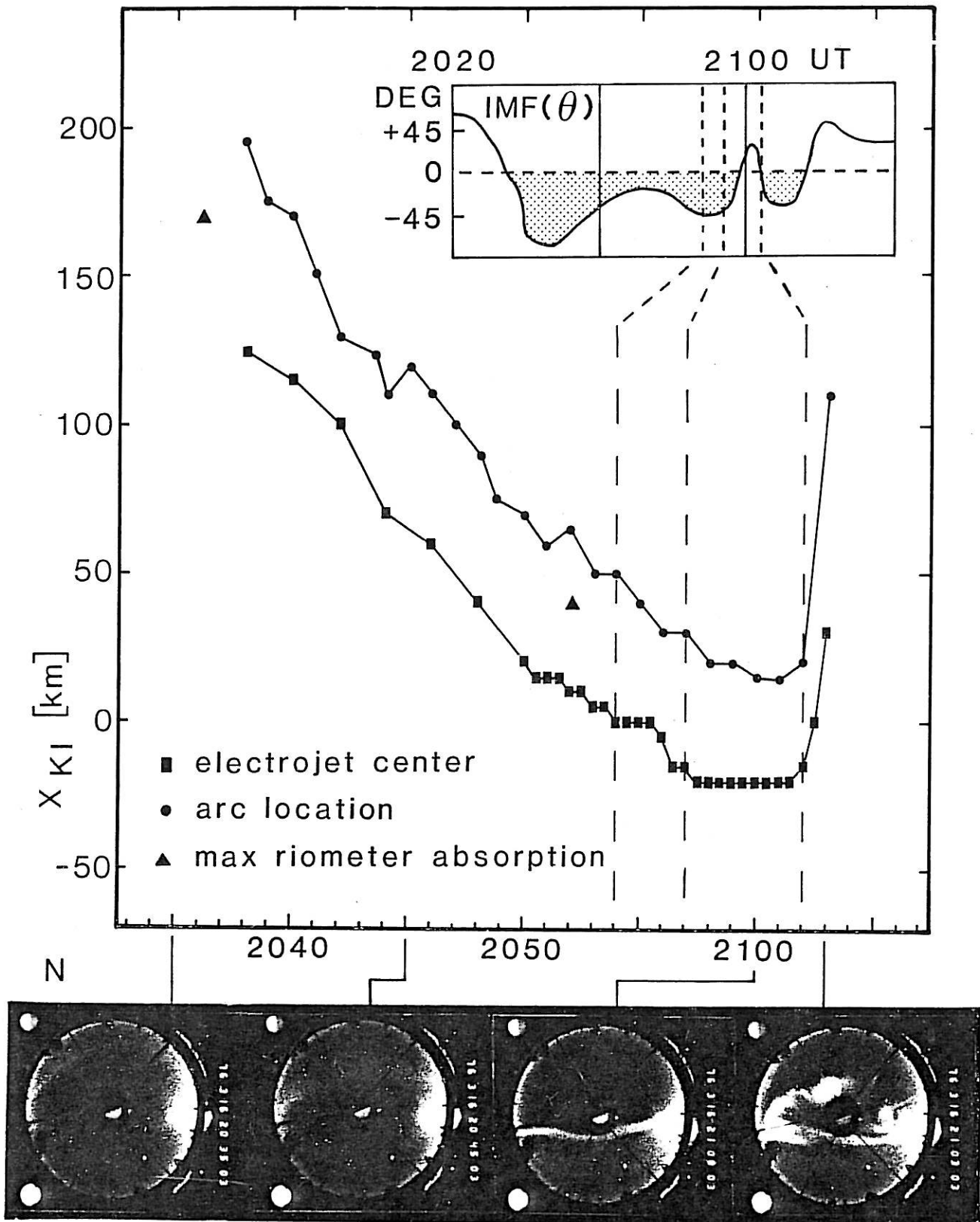


FIG 2

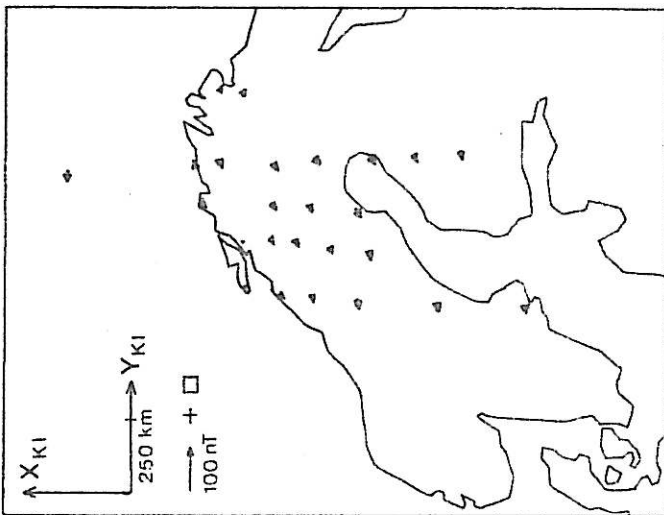
11 NOV 1976



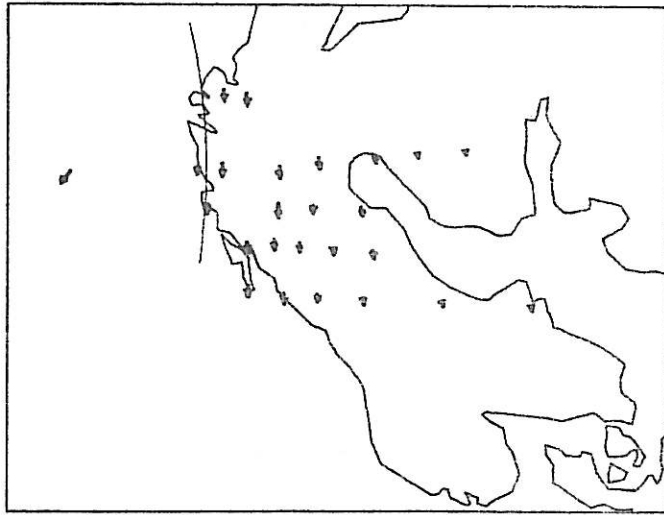
IVALO

FIG 3

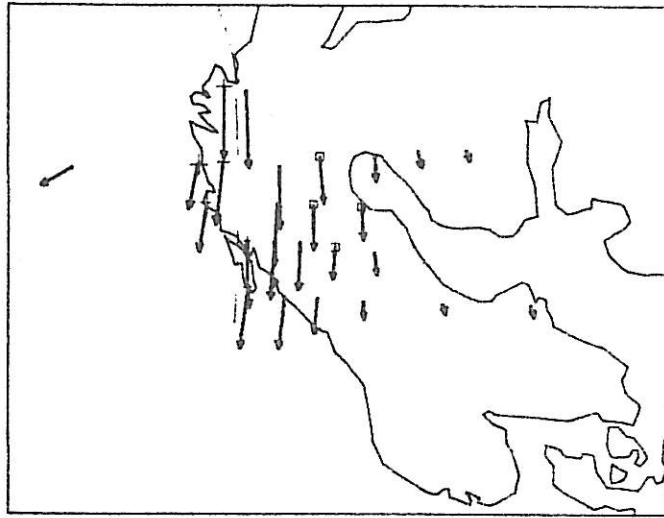
76-11-11 20.20 UT TEC



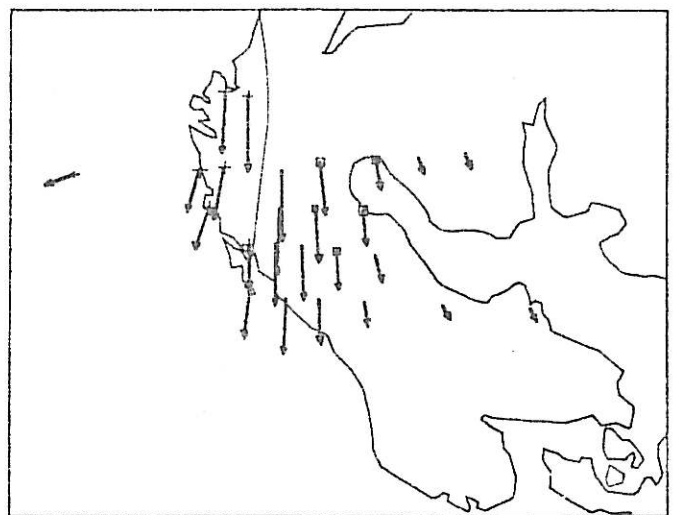
20.30



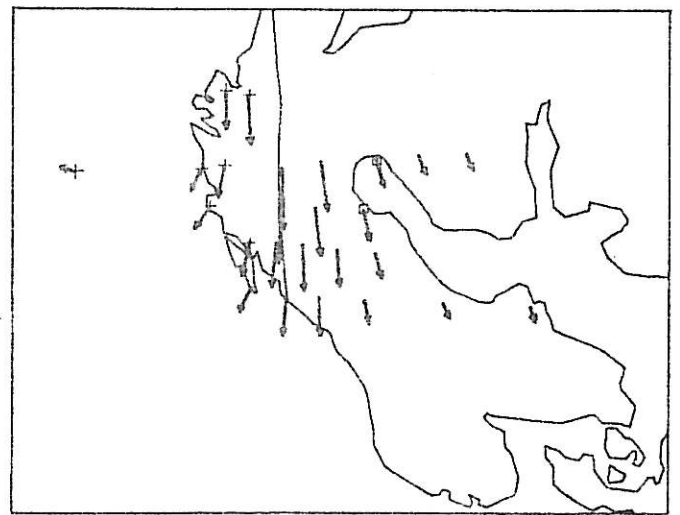
20.40



20.50



21.00



21.10

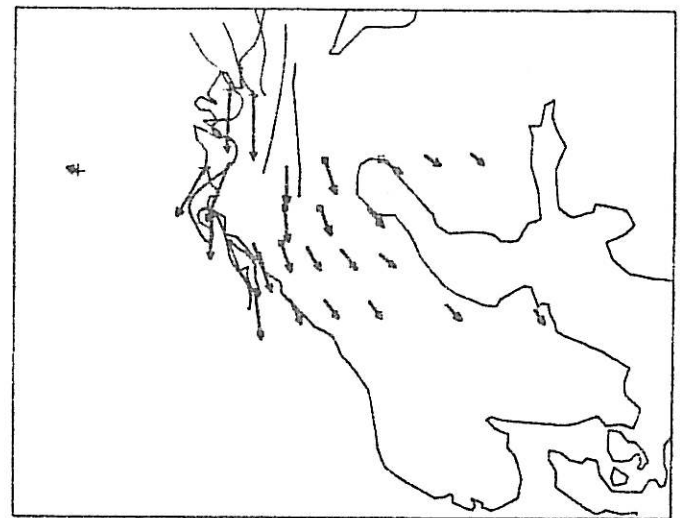


FIG 4

FEBRUARY 24 1974

QHA

QHA

FADING

BREAKUP



21:32 UT

21:33

21:34

21:35

21:36

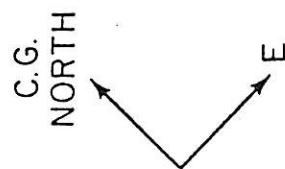


FIG 5

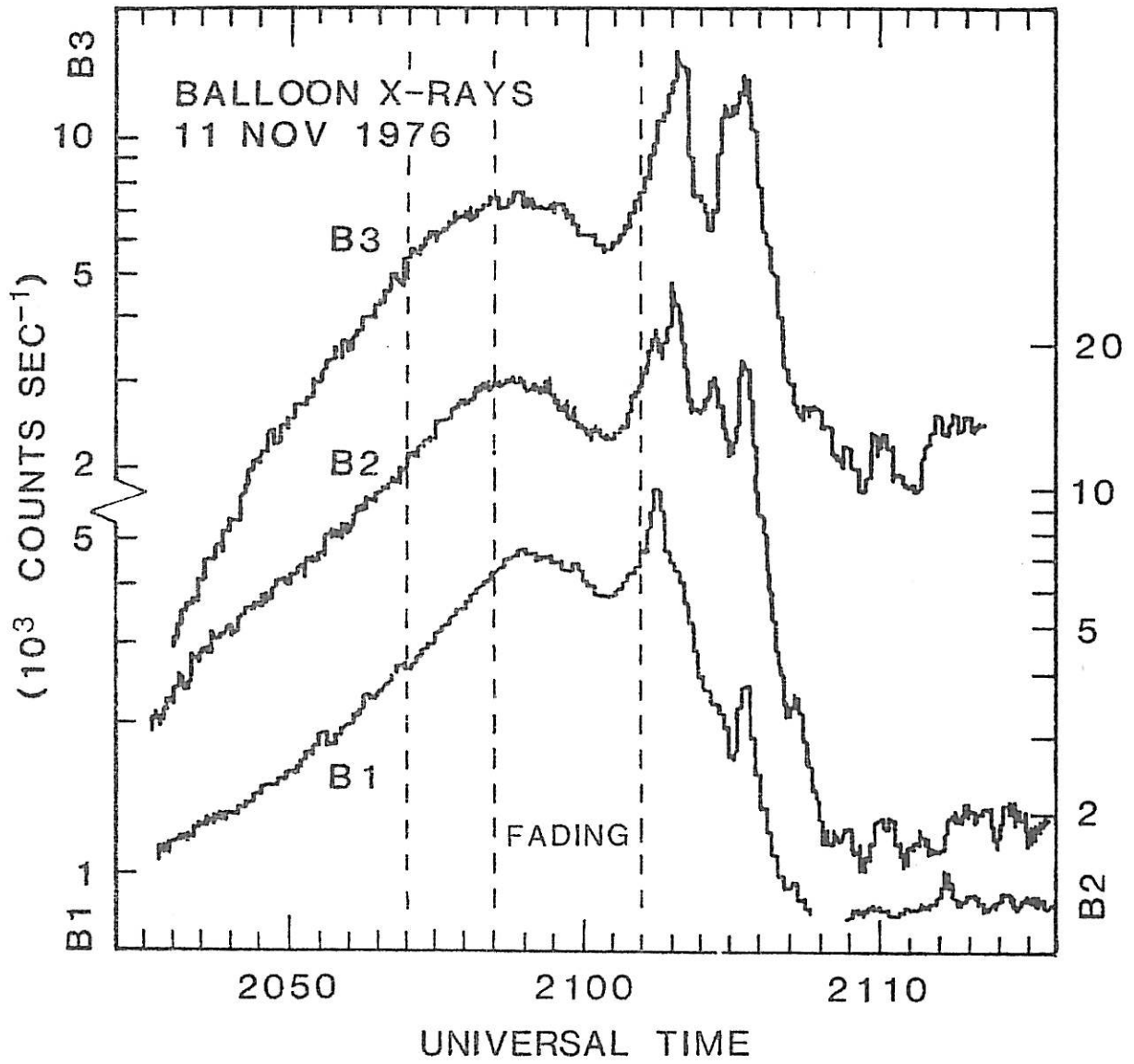


FIG 6

77 - 02 - 15 EQUIVALENT CURRENT VECTORS ON A LATITUDINAL PROFILE

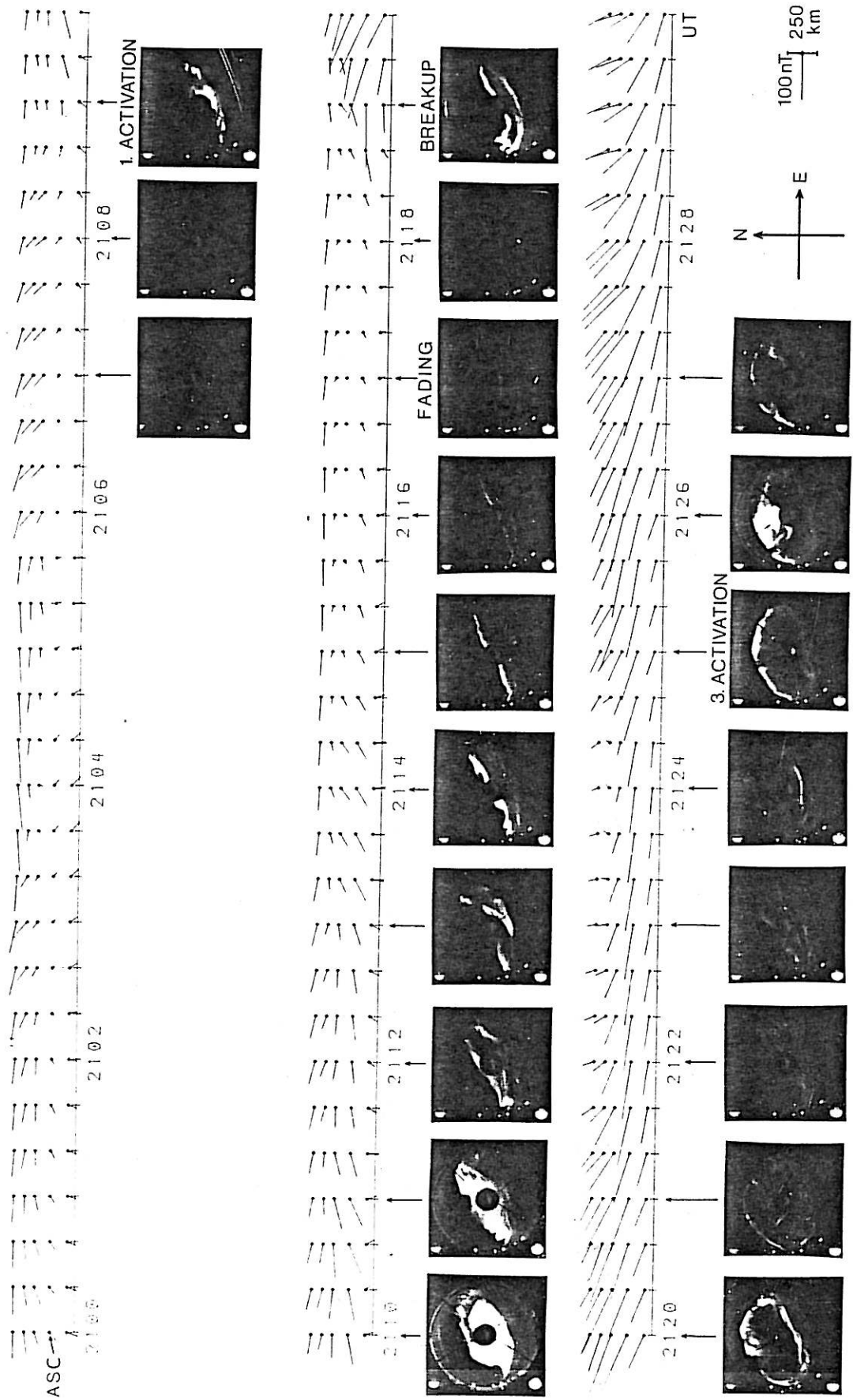


FIG 7

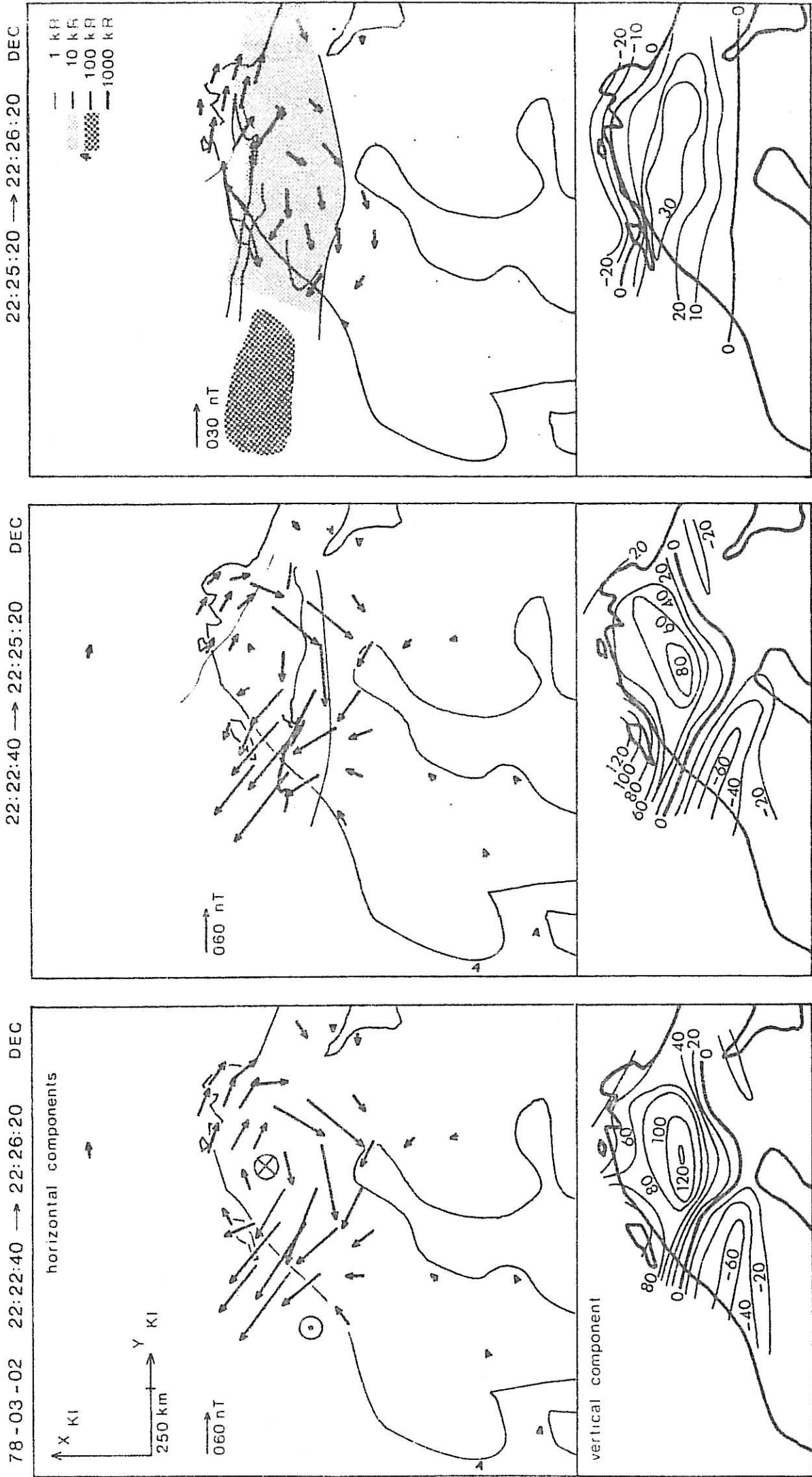
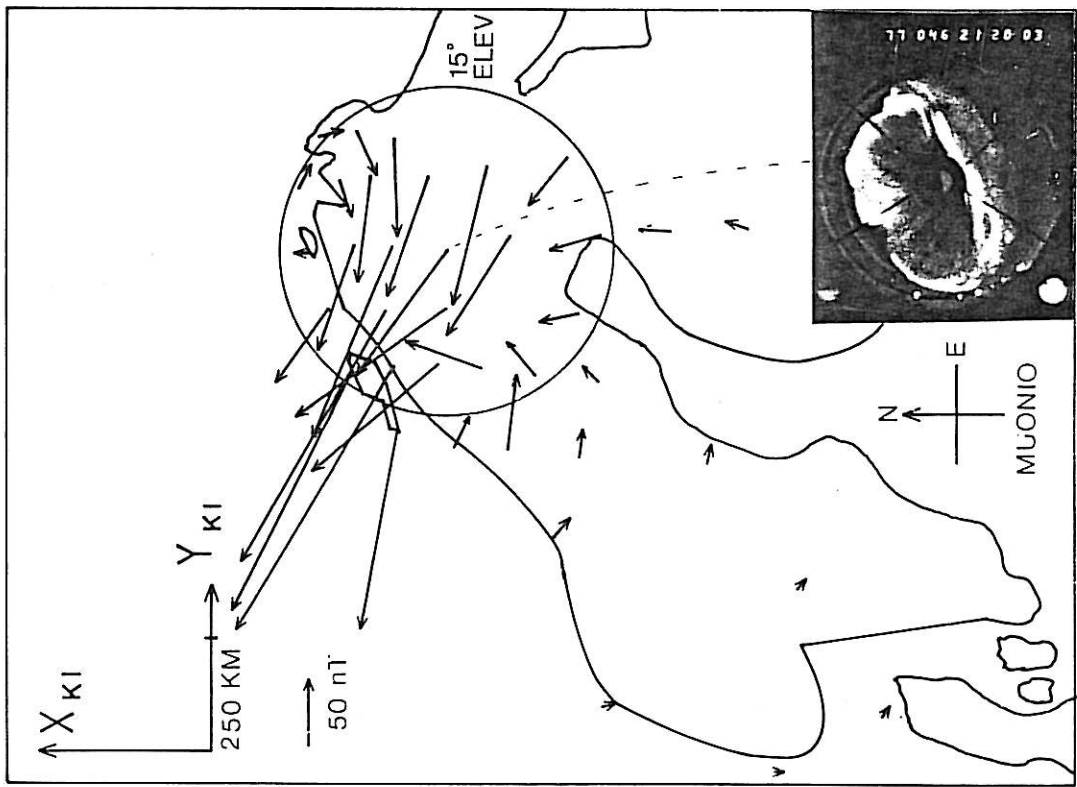


FIG 8a

DIFFERENTIAL HORIZONTAL EQUIVALENT CURRENT VECTORS

FEB 15, 1977

21.20:00 - 21.18:30 UT



21.22:00 - 21.18:30

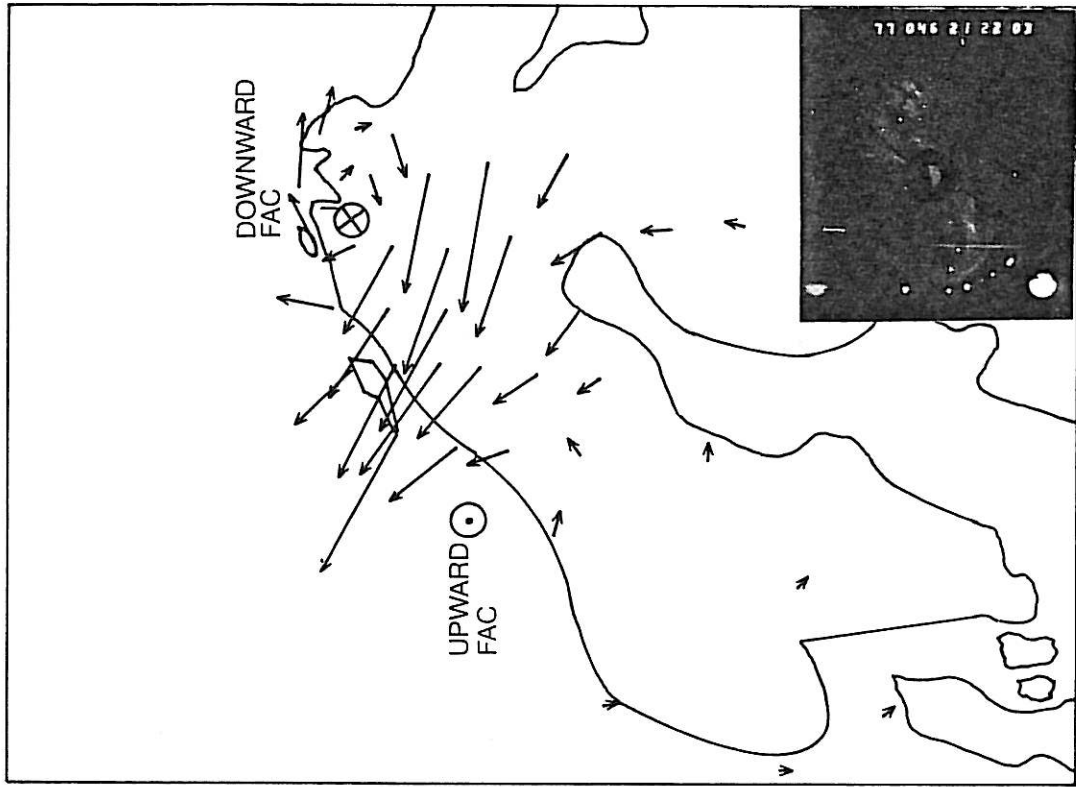
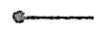


FIG 8b

IRREGULARITY DRIFT VELOCITY

1000 m/s = 

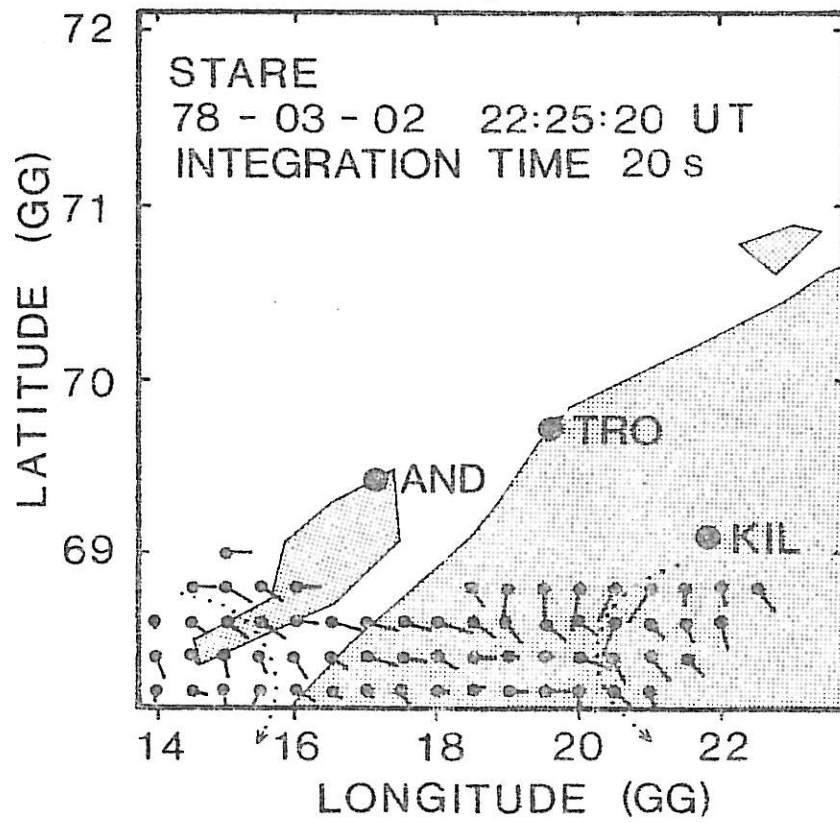


FIG 9

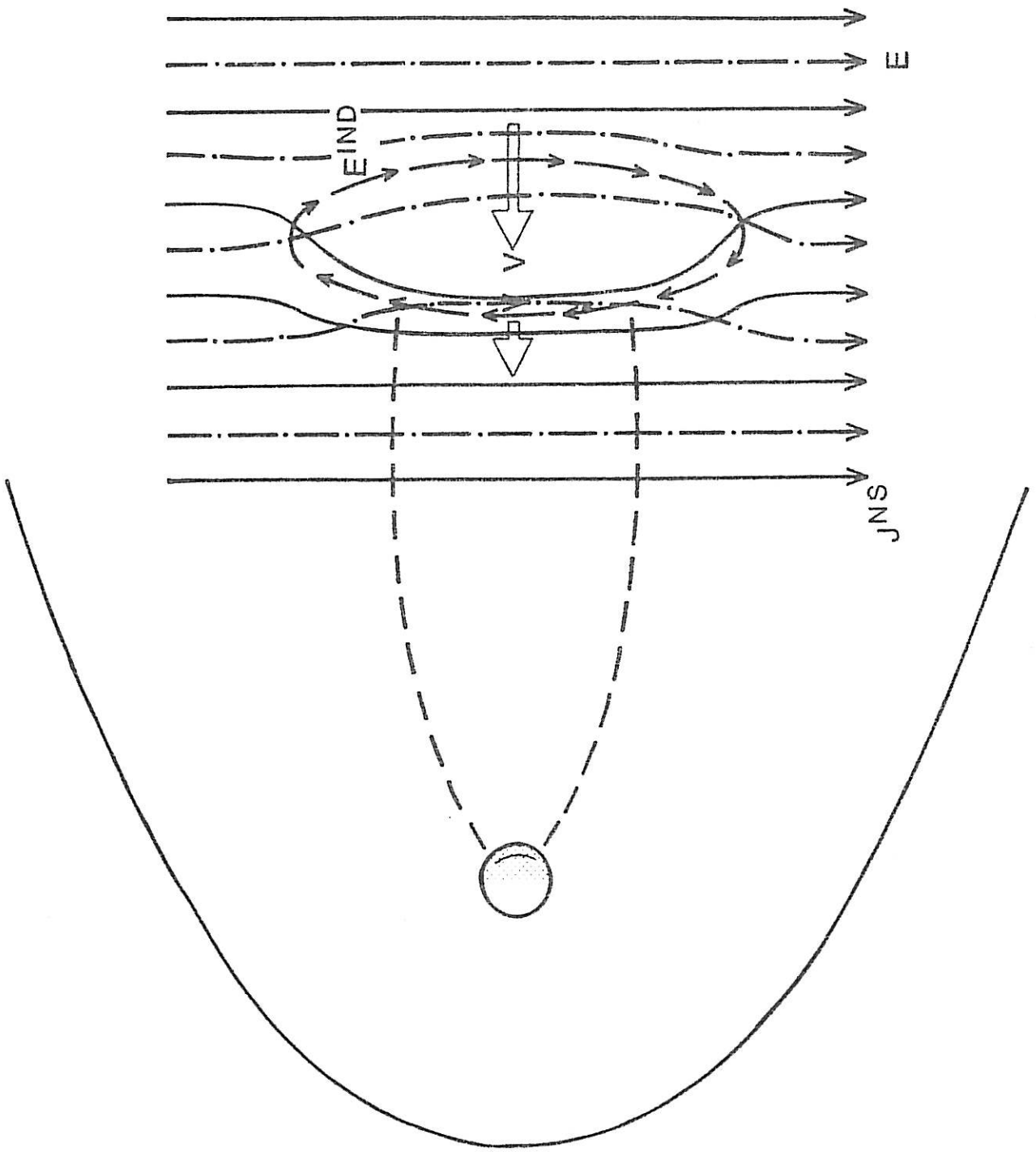


FIG 10

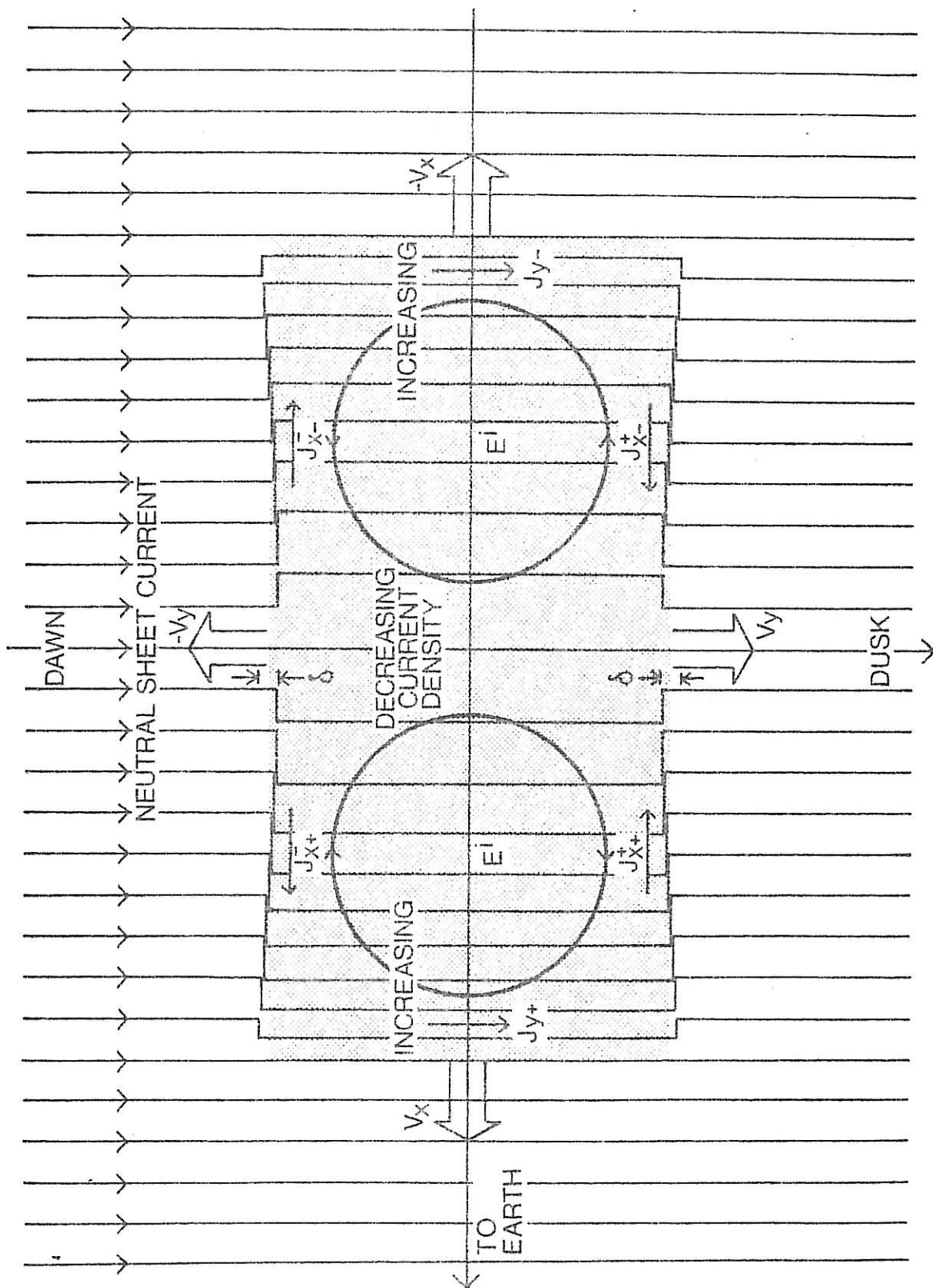


FIG 11

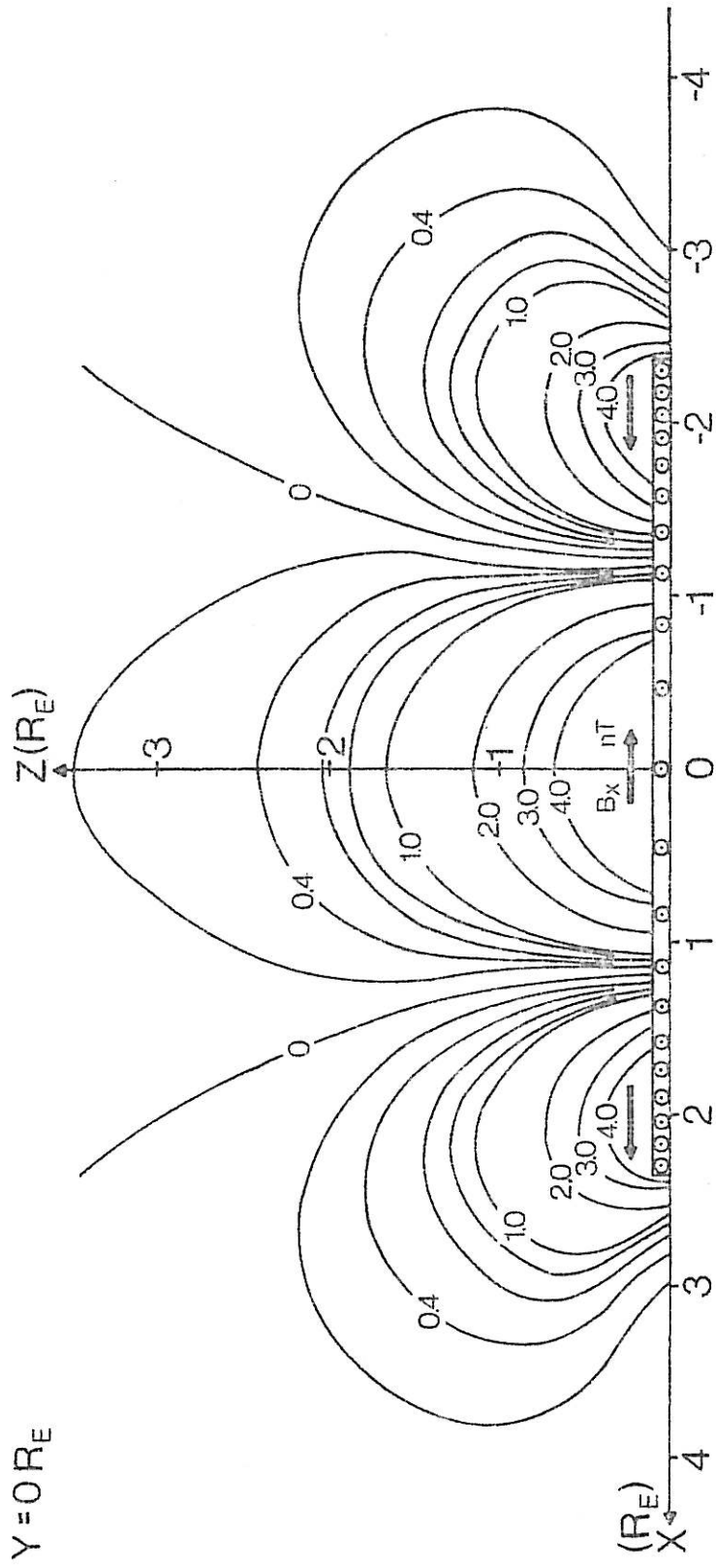


FIG 12 a

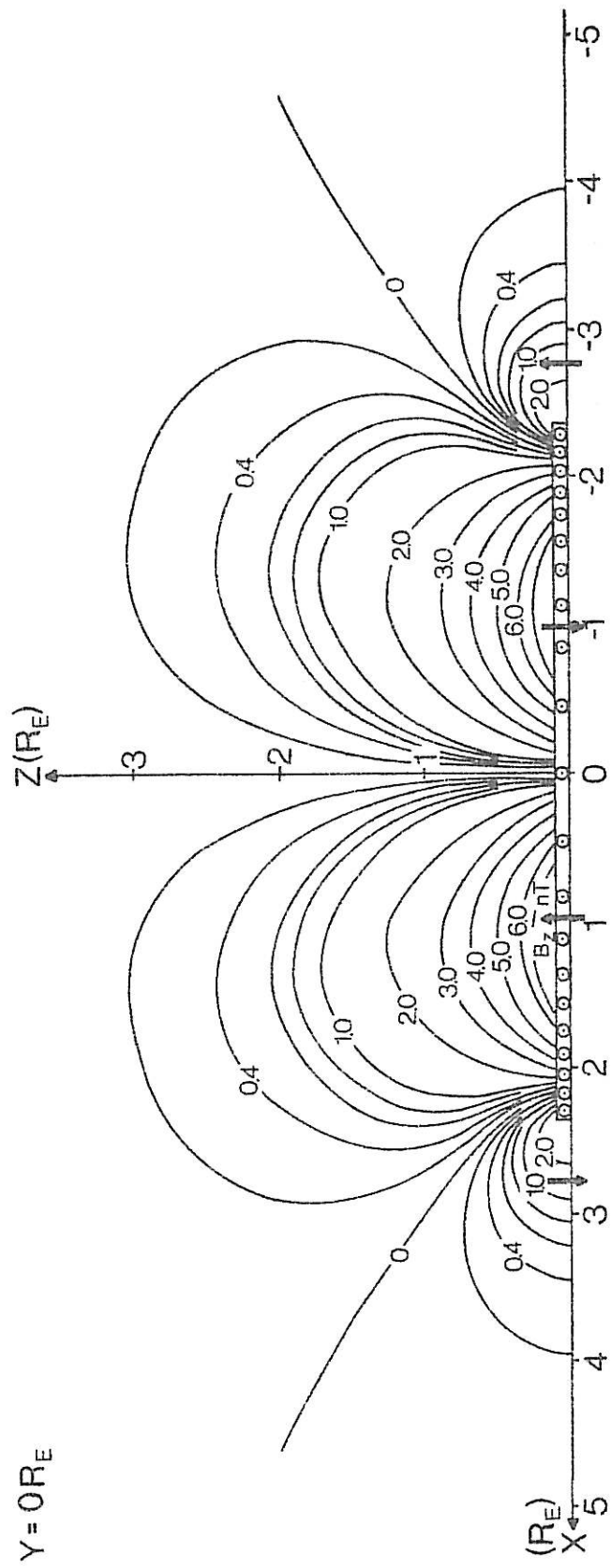


FIG 12b

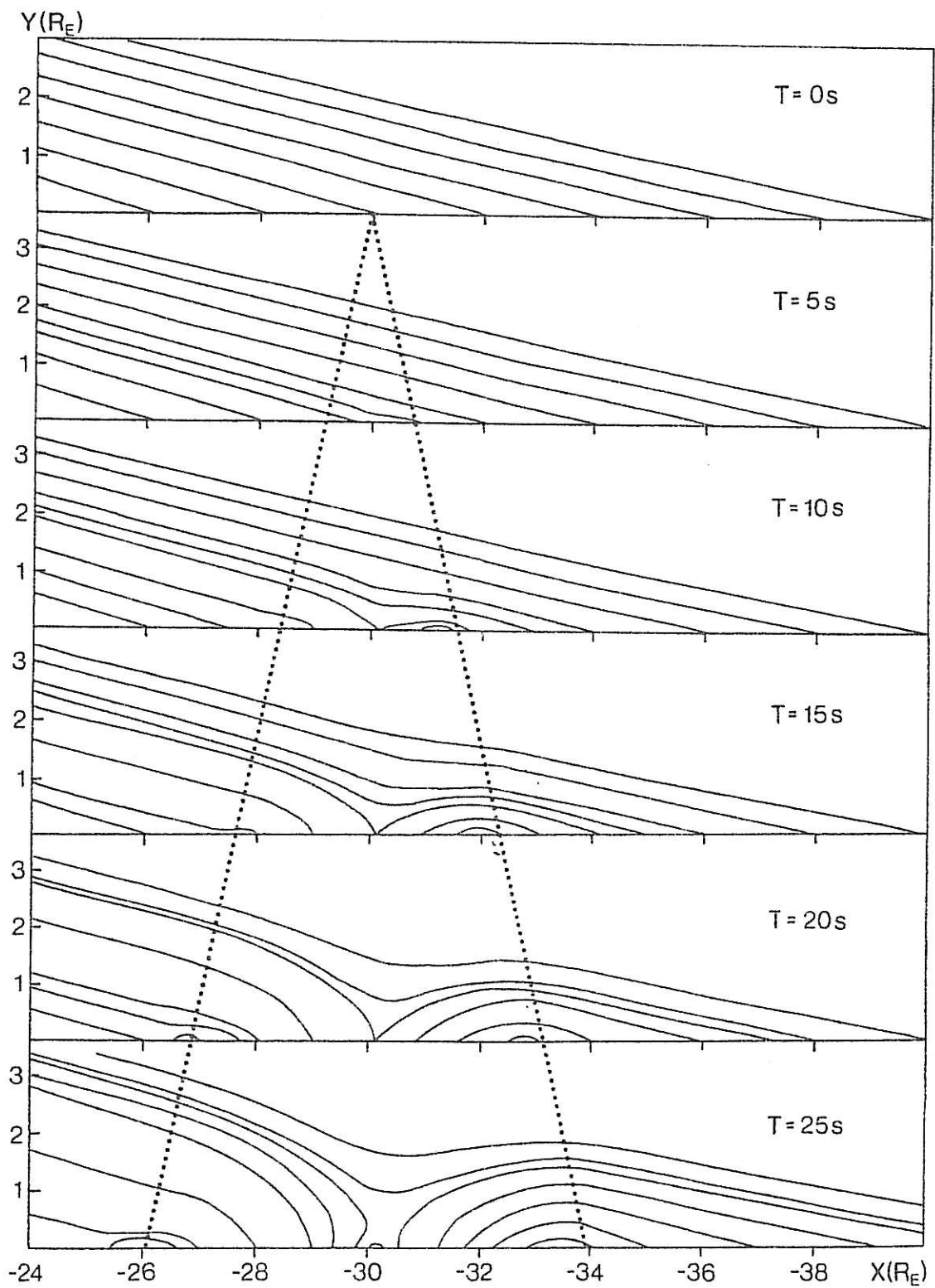


FIG 13

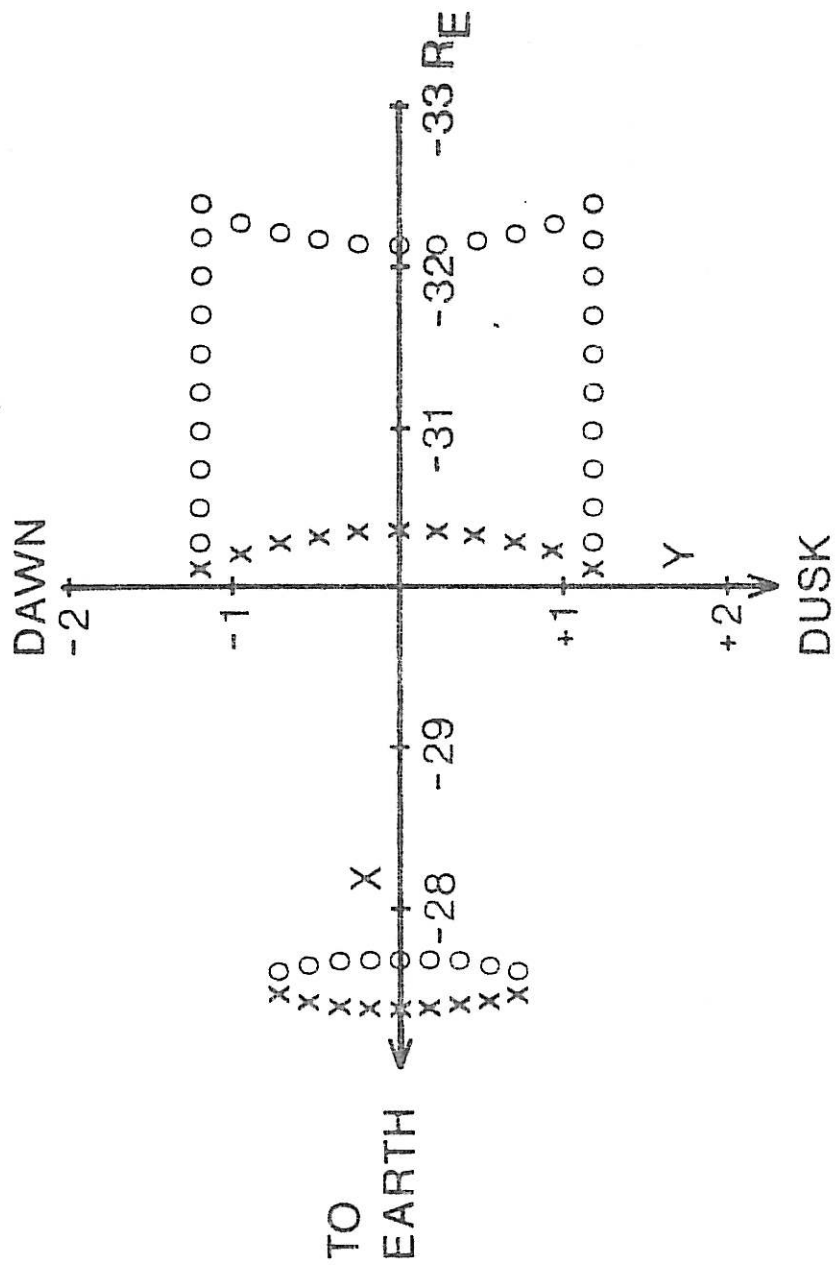


FIG 14

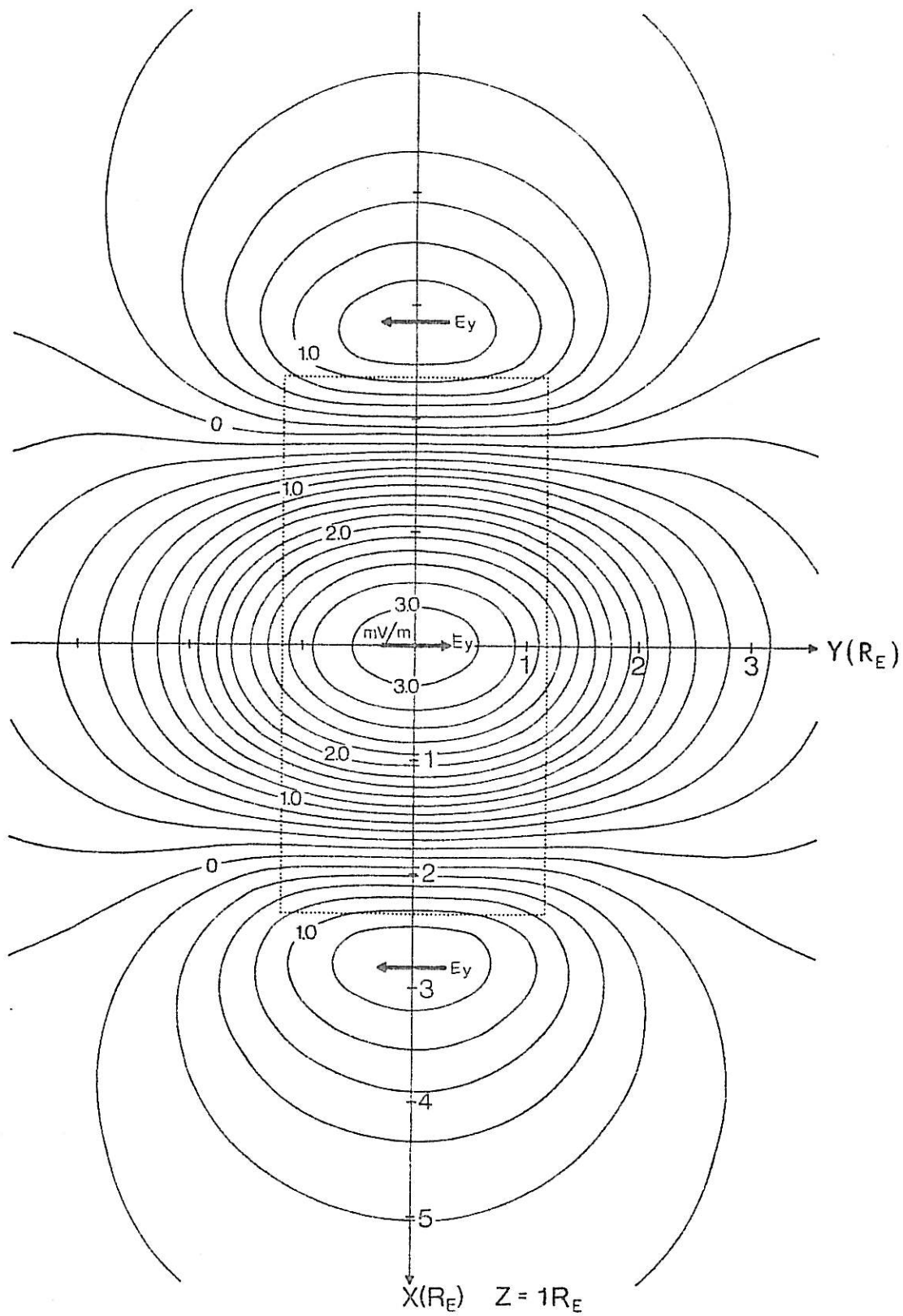


FIG 15a

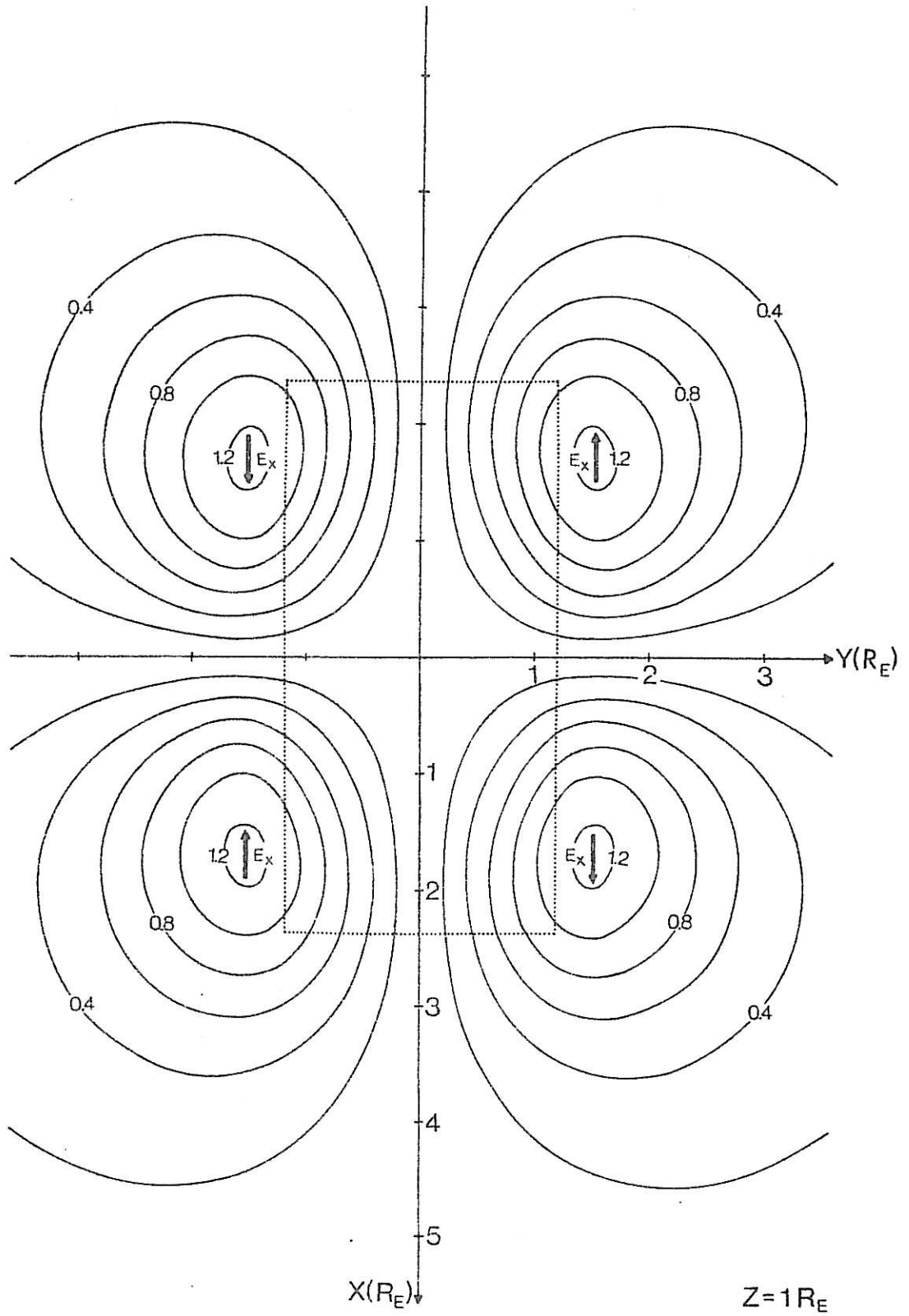


FIG 15 b

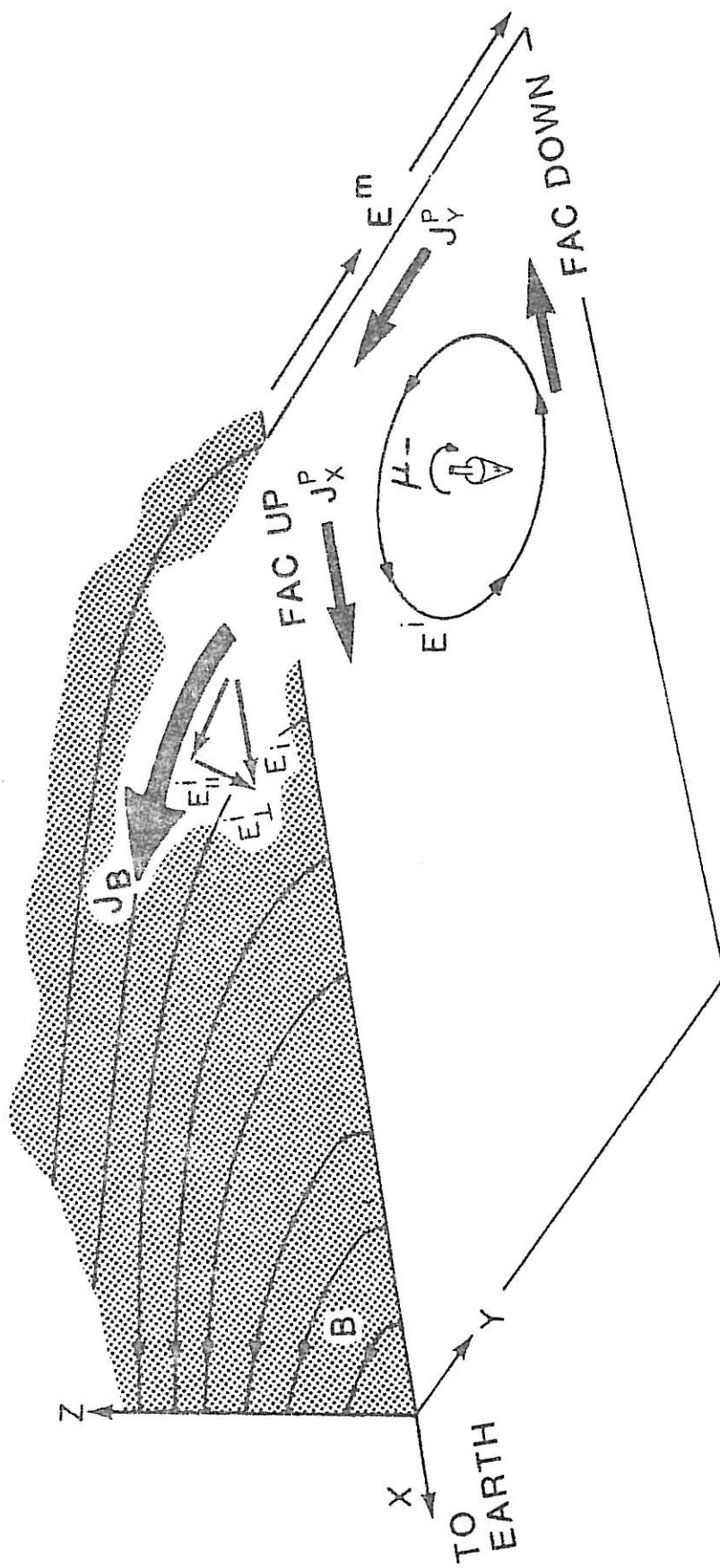


FIG 16

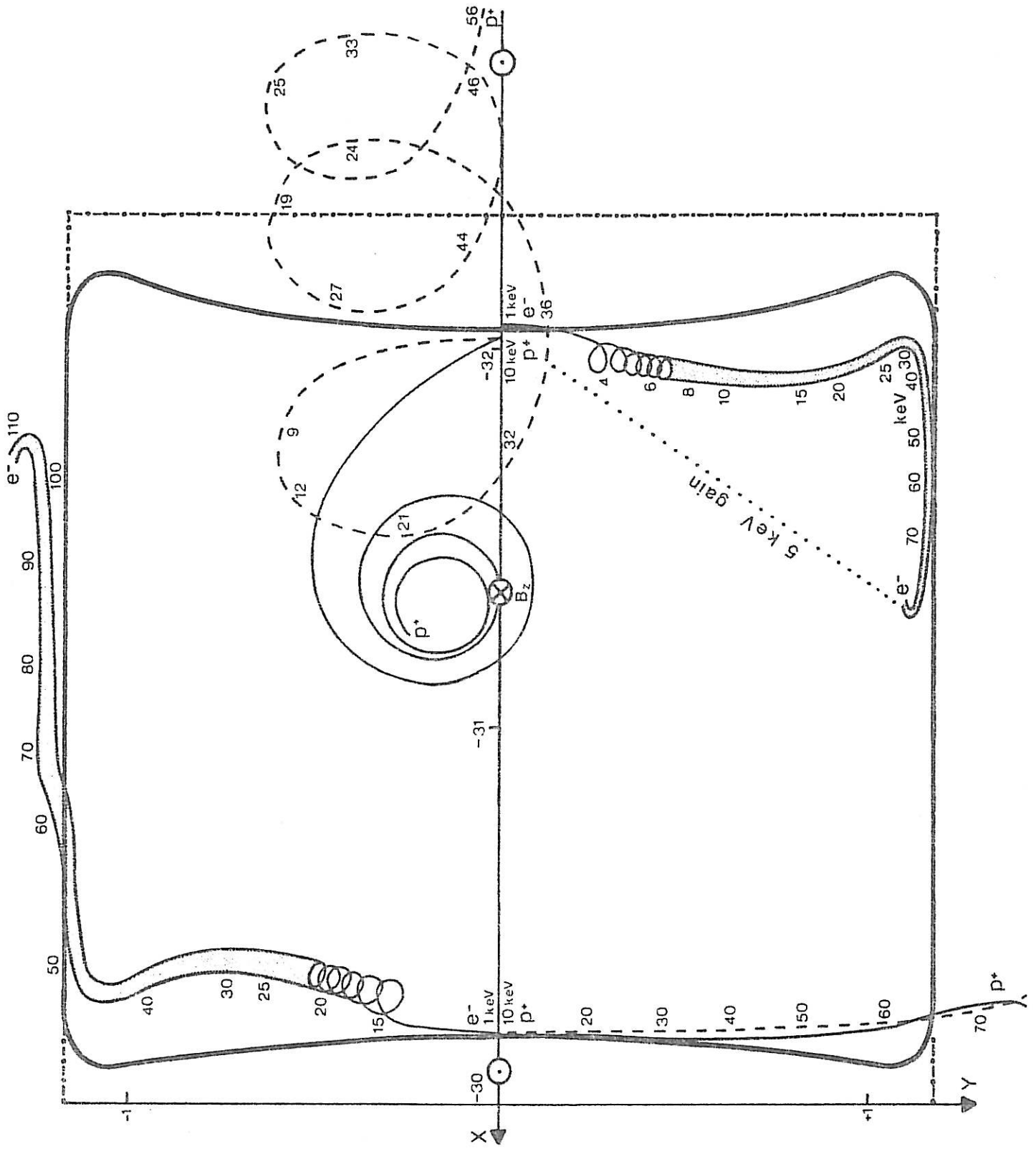


FIG 17

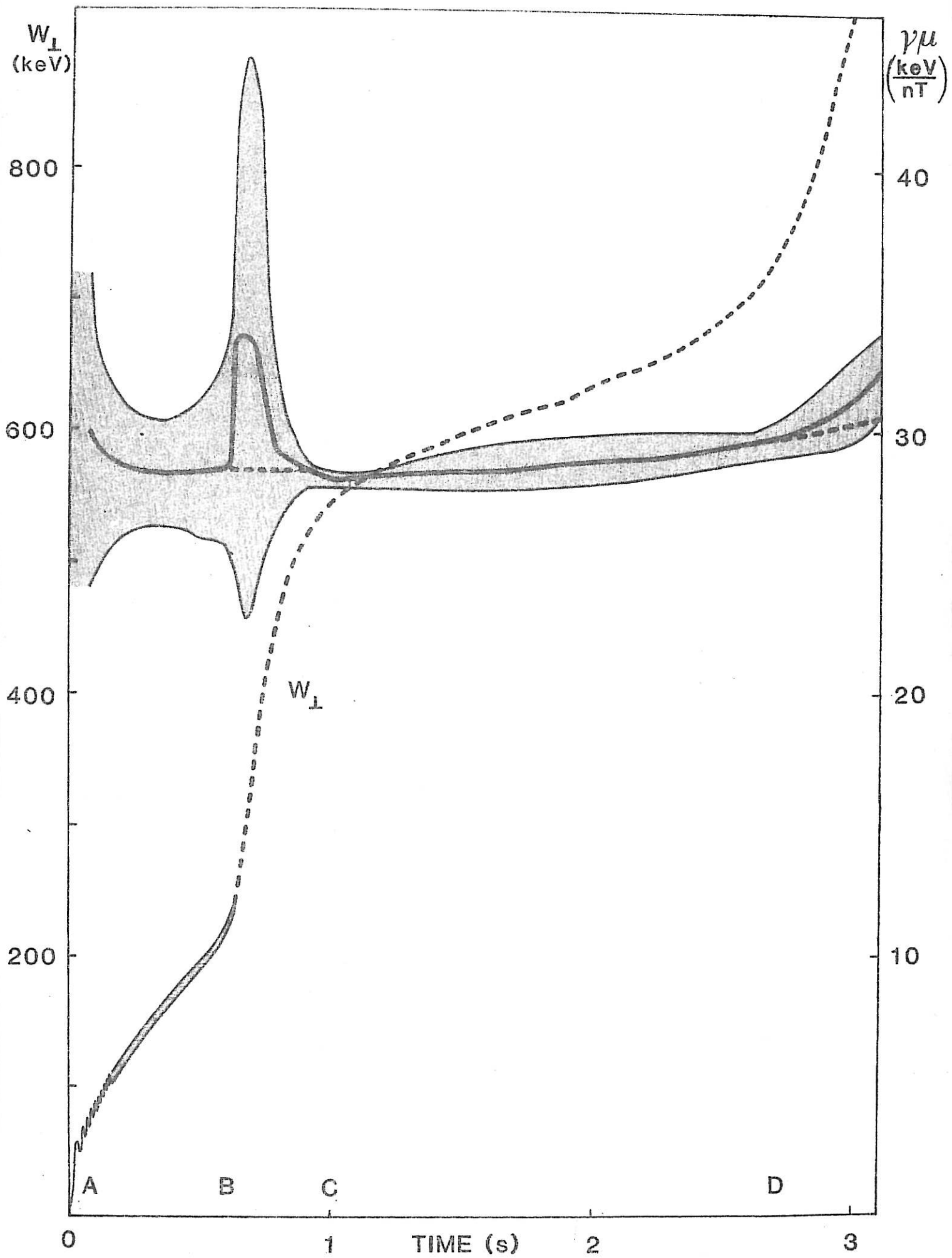


FIG 18

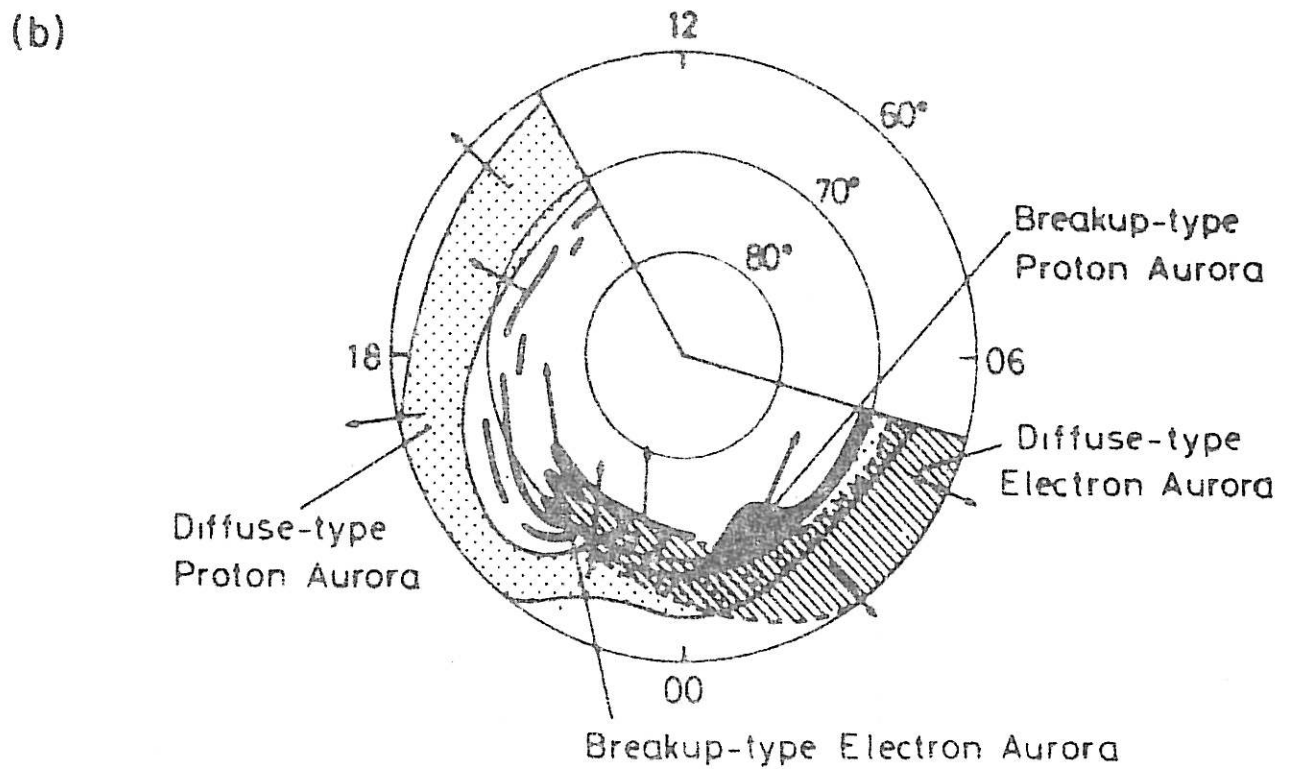
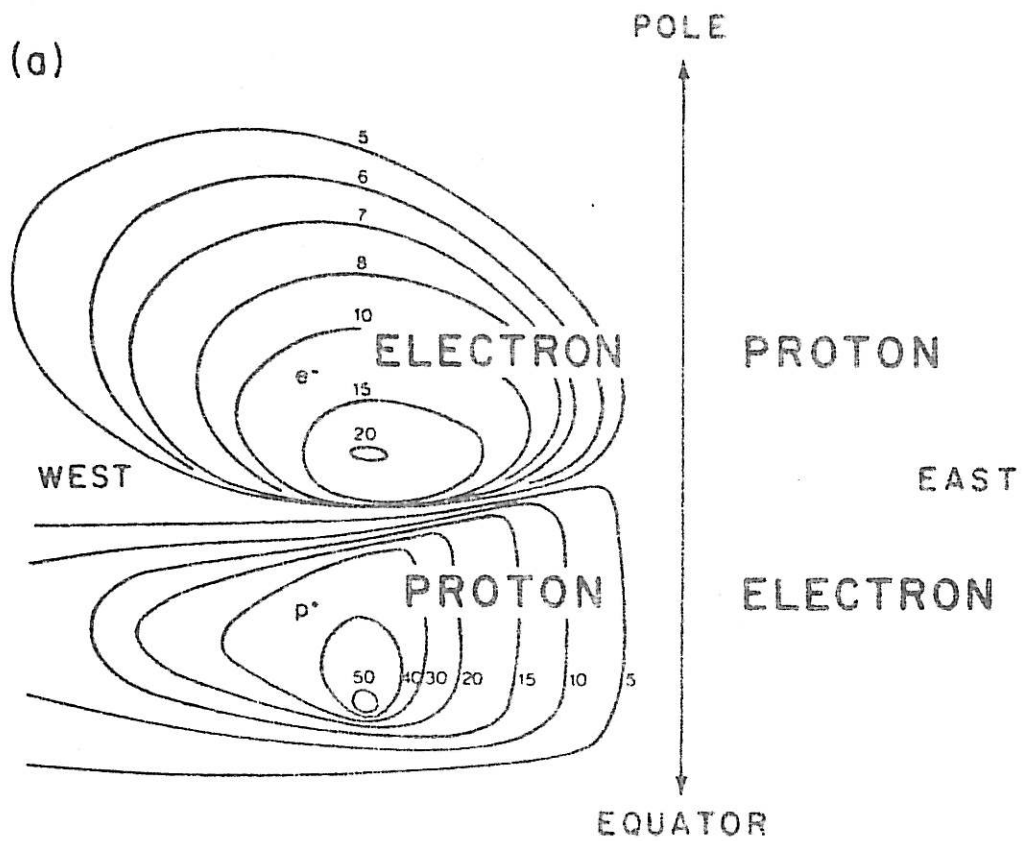
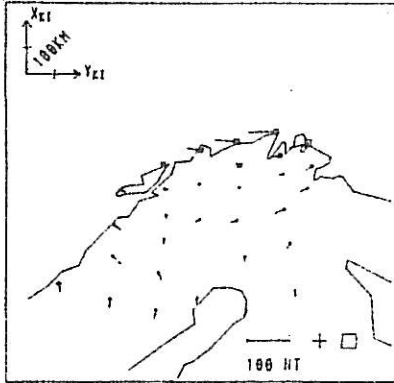
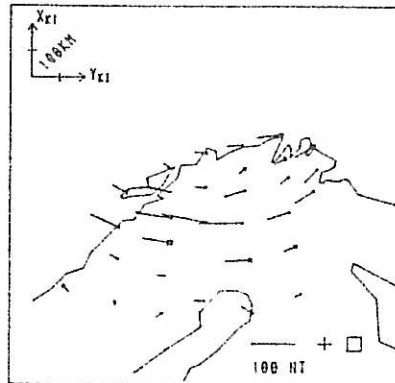


FIG 19

77-02-15 21:10:00



77-02-15 21:19:00



77-02-15 21:20:30

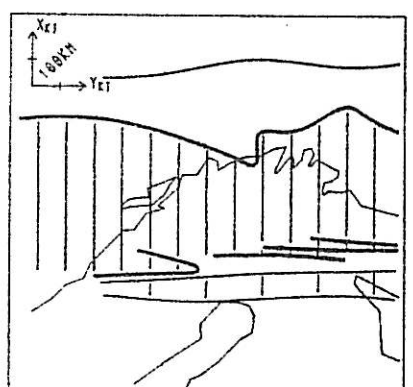
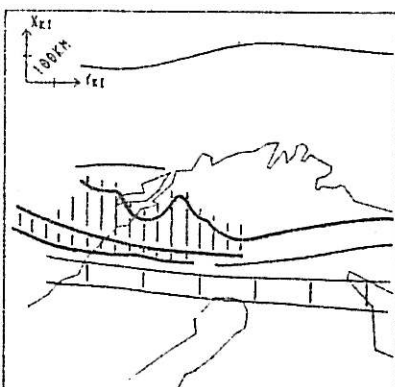
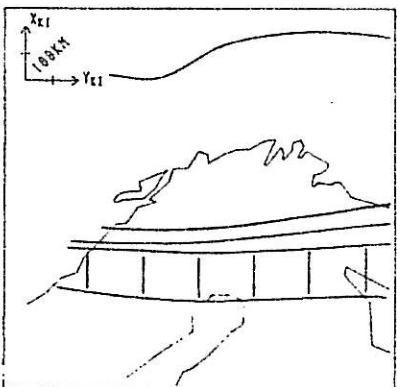
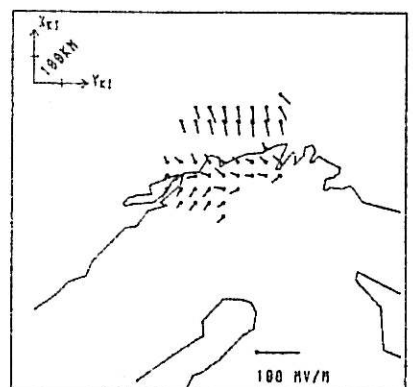
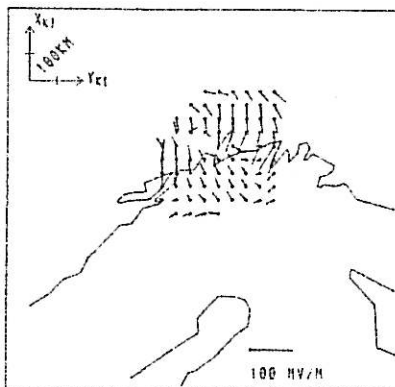
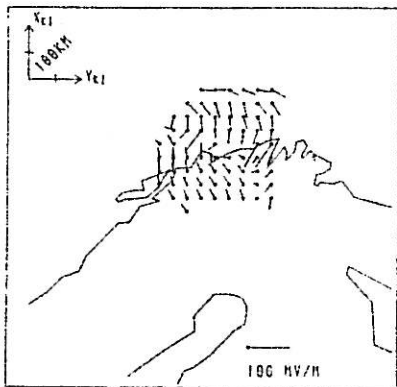
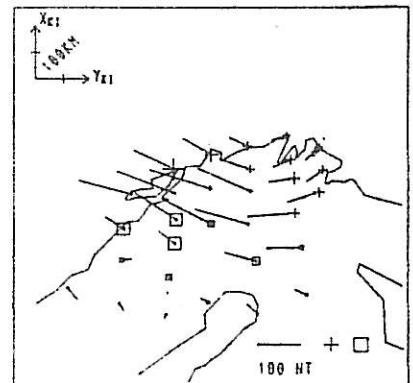
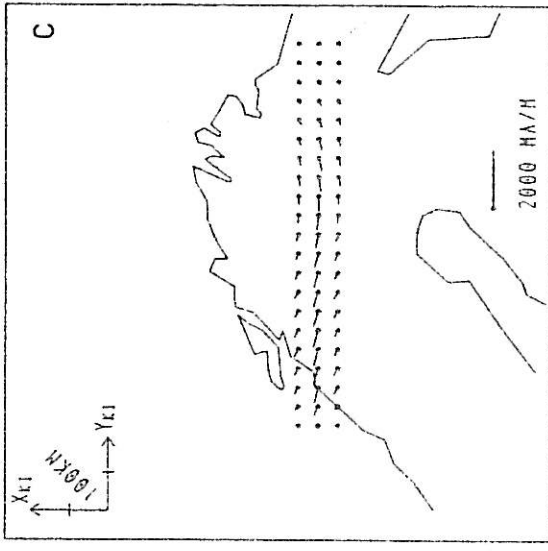
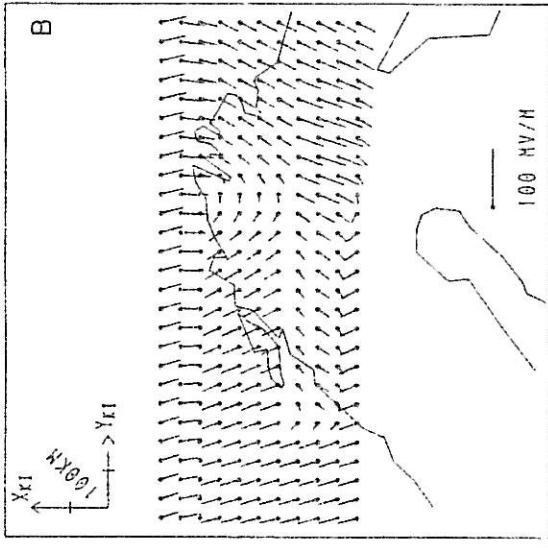


FIG 20

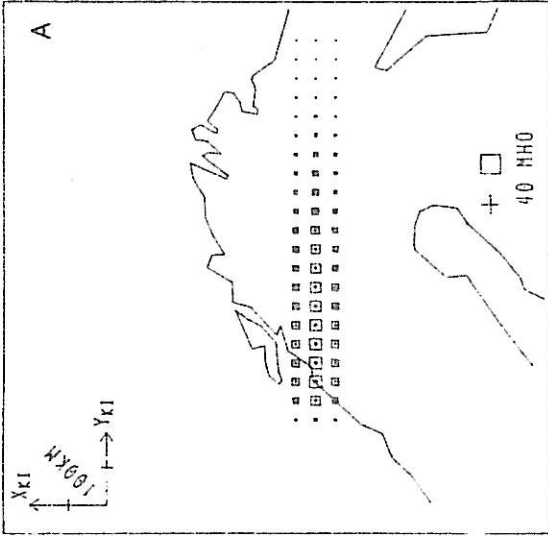
IONOSPHERIC CURRENTS 2119:00



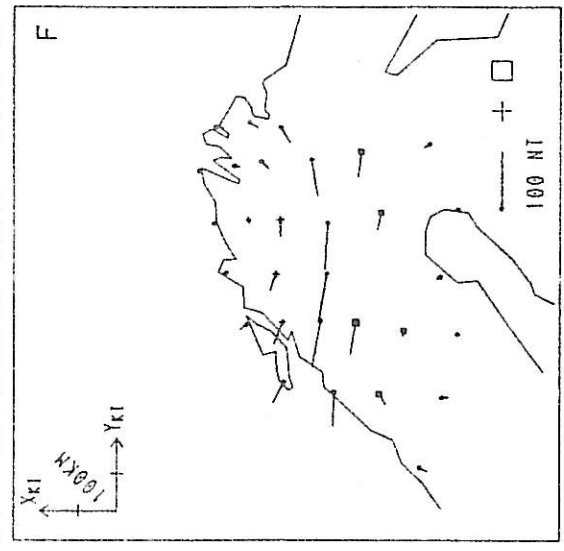
IONOSPHERIC ELECTRIC FIELD 2119:00



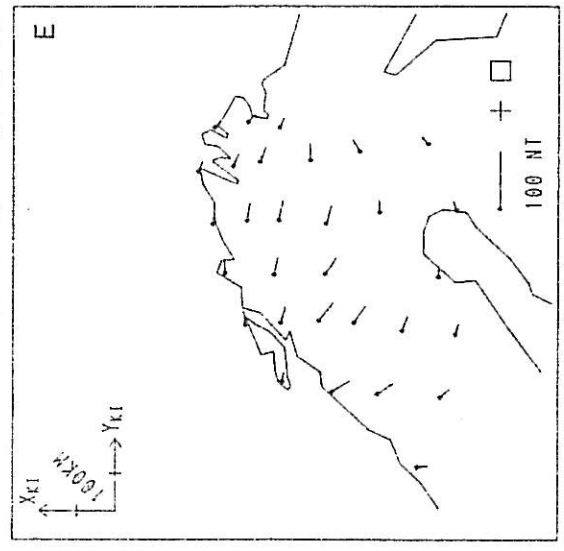
IONOSPHERIC CONDUCTIVITY 2119:00



E0 CURR GROUND (TOT) 2119:00



E0 CURR GROUND (FAC) 2119:00



FIELD-ALIGN CURRENTS 2119:00

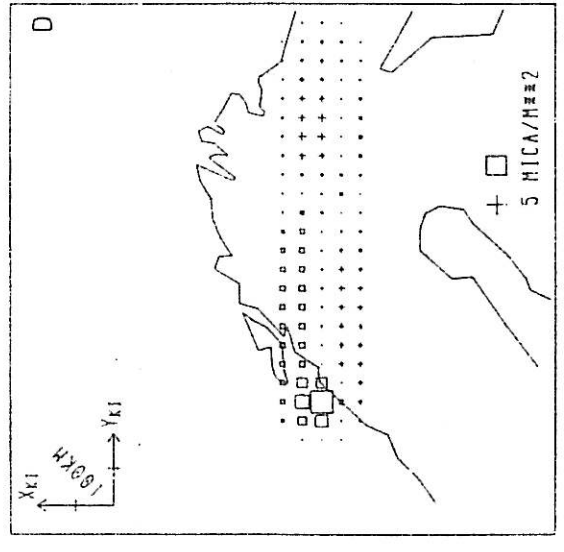
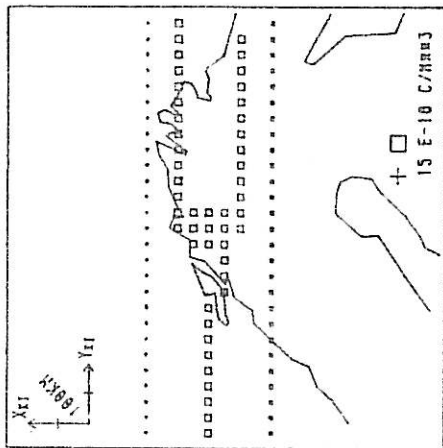
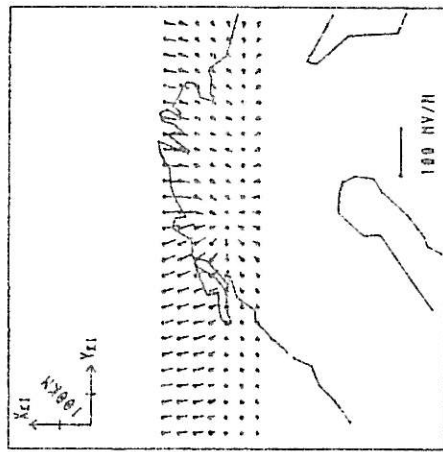


FIG 21

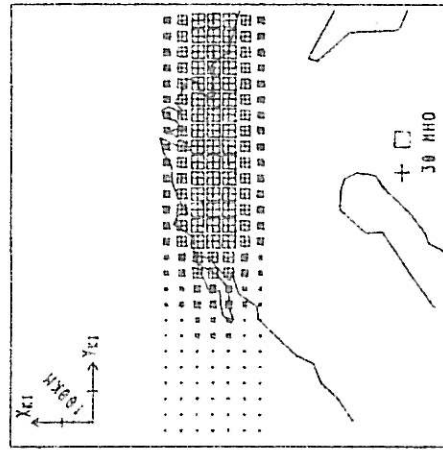
COLUMN CHARGES A



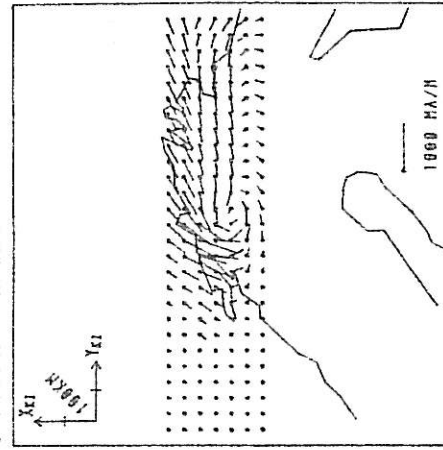
IONOSPHERIC ELECTRIC FIELD B



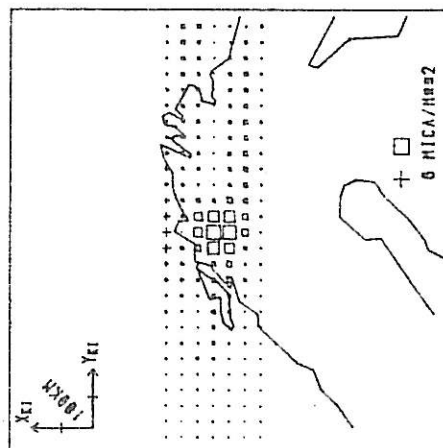
IONOSPHERIC CONDUCTIVITY C



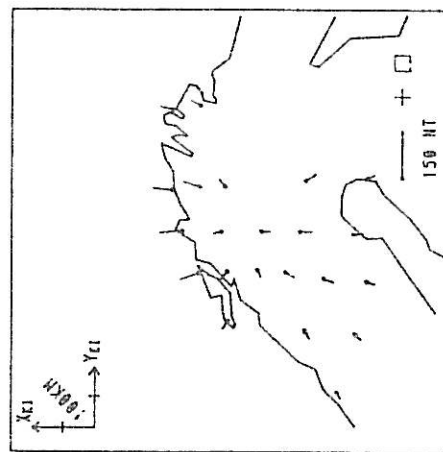
IONOSPHERIC CURRENTS D



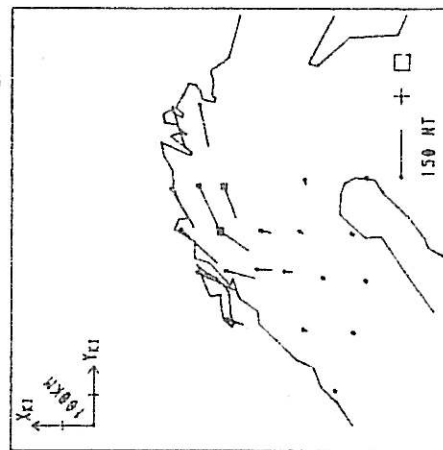
FIELD-ALIGN CURRENTS E



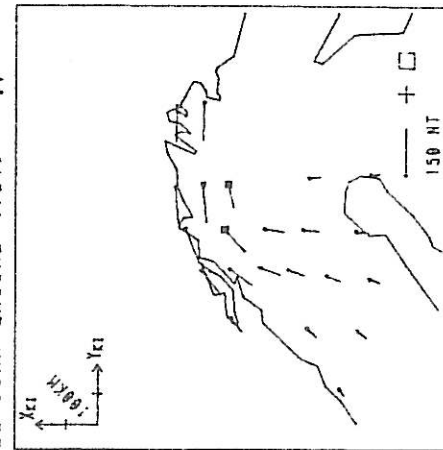
EQ CURR GROUND (FAC) F



EQ CURR GROUND (ION) G



EQ CURR GROUND (TOT) H



1976 NOV 11

COMPARISON OF IMF AND POLAR ELECTROJET VARIATIONS

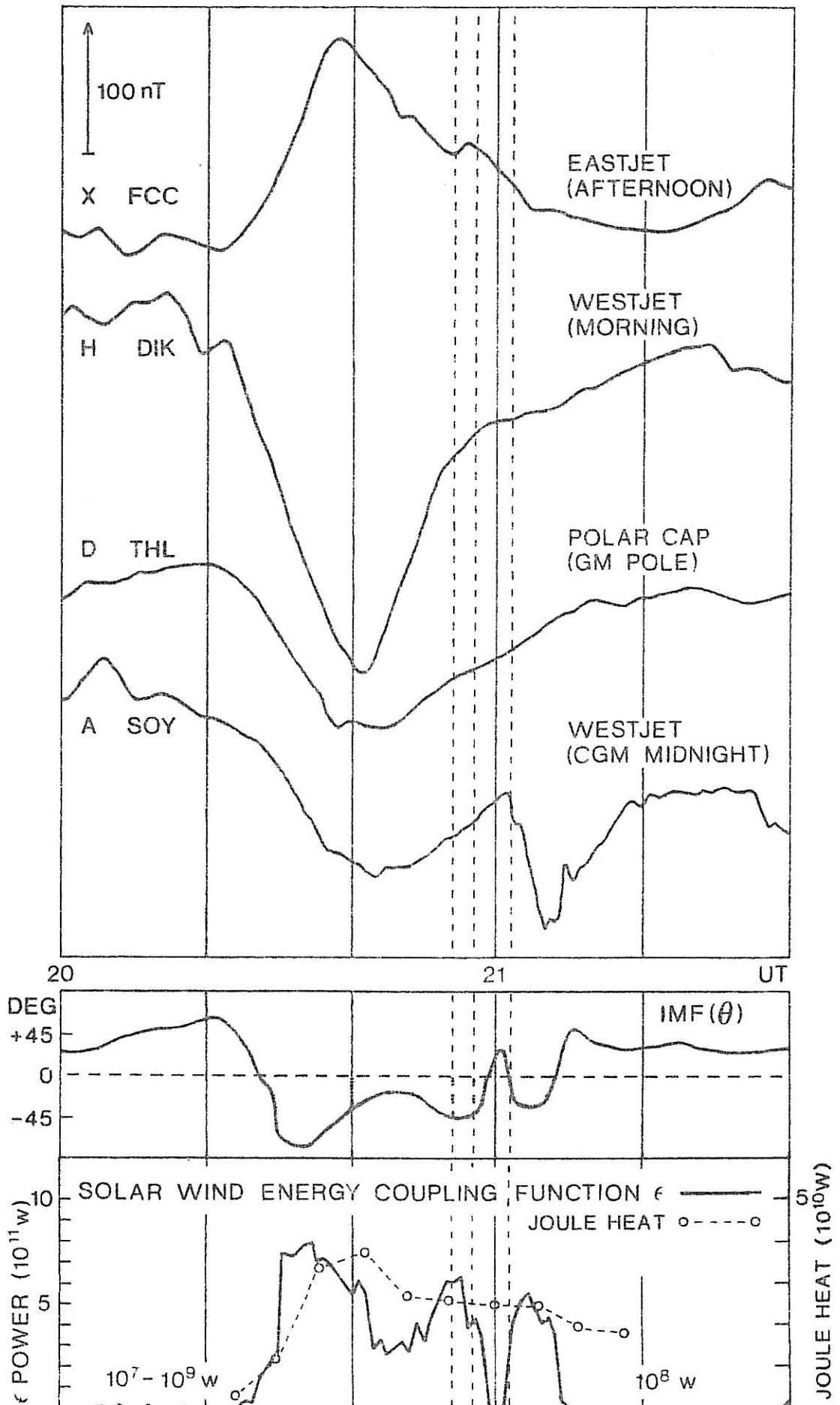


FIG 23

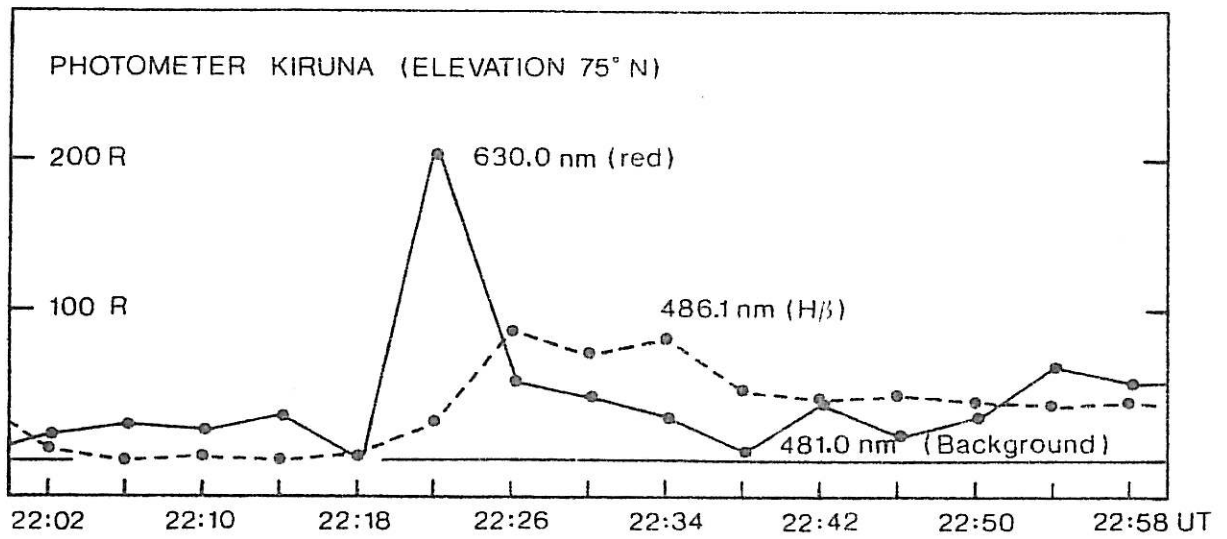


FIG 24

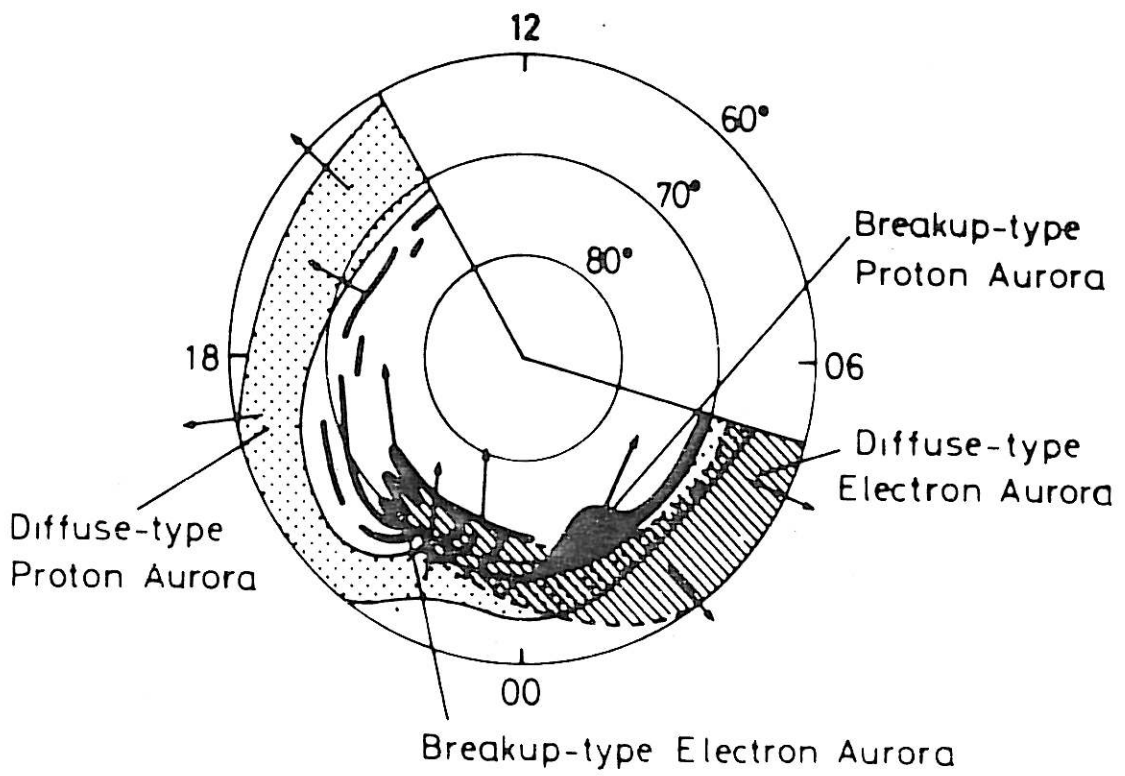
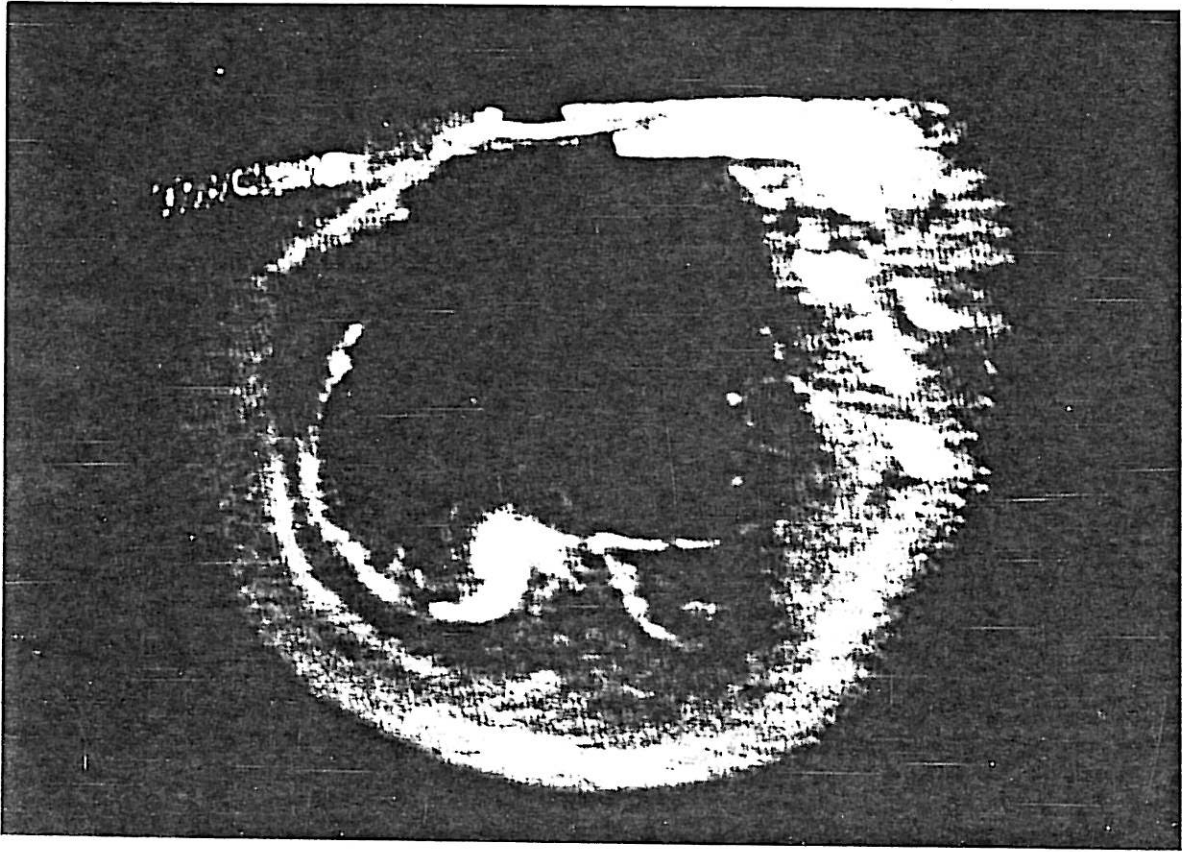


FIG 25

Royal Institute of Technology, Department of Plasma Physics,
S-100 44 Stockholm, Sweden

INDUCTIVE ELECTRIC FIELDS IN THE MAGNETOTAIL AND THEIR RELATION TO
AURORAL AND SUBSTORM PHENOMENA

R. J. Pellinen and W. J. Heikkila

November 1982, 111 pp. incl. ill., in English

The paper reviews the importance of inductive electric fields in explaining different magnetospheric and auroral phenomena during moderately and highly disturbed conditions. Quiet-time particle energization and temporal development of the tail structure during the substorm growth phase are explained by the presence of a large-scale electrostatic field directed from dawn to dusk over the magnetotail. Conservation of the first adiabatic invariant in the neutral sheet with a small value of the gradient in the magnetic field implies that the longitudinal energy increases at each crossing of the neutral sheet. At a certain moment, this may result in a rapid local growth of the current and in an instability that triggers the onset. During the growth phase energy is stored mainly in the magnetic field, since the energy density in the electric field is negligible compared to that of the magnetic field (ratio $1:10^7$). An analytical model is described in which the characteristic observations of a substorm onset are taken into account. One major feature is that the triggering is confined to a small local time sector. During moderate disturbances, the induction fields in the magnetotail are stronger by at least one order of magnitude than the average cross-tail field. Temporal development of the disturbed area results in X- and O-type neutral lines. Particles near to these neutral lines are energized to over 1 MeV energies within a few seconds, due to an effective combination of linear and betatron acceleration. The rotational property of the induction field promotes energization in a restricted area with dimensions equivalent to a few Earth's radii. The model also predicts the existence of highly localized cable-type field-aligned currents appearing on the eastern and western edges of the expanding auroral bulge. It is shown that the predictions agree with satellite observations and with the data obtained from the two-dimensional instrument networks operated in Northern Europe during the International Magnetospheric Study (IMS, 1976-79).

Key words: Aurora, C parameter, Field-aligned currents, Inductive electric field, Magnetospheric substorm, Particle energization, Substorm current system, Substorm triggering, X- and O-type neutral lines